MAGNETIC COOLING AND PHASE TRANSITION IN SPIN PAIR SYSTEM

Naohiko YAMASHITA

OSAKA UNIVERSITY
GRADUATE SCHOOL OF ENGINEERING SCIENCE
DEPARTMENT OF MATERIAL PHYSICS
TOYONAKA OSAKA

報告番号 甲第

論文目録

大阪大学

報告番号	甲第1845号	氏名	山下直彦

主論文

Magnetic Cooling and Phase Transition in Spin Pair System

（スピンペア系の磁気冷却と相転移）

参考論文

(その1) Pulsed Adiabatic-Magnetization in $Cu(NO_3)_2 2.5H_2O$

($Cu(NO_3)_2 2.5H_2O$ における断熱磁化冷却)

J.Phys.Soc.Japan昭和49年37巻4号 1173頁~1173頁

長谷田泰一郎他2名と共著

(その2) Notes on Paramagnetic Relaxation in Cobaltous Salts

(Co常磁性塩における緩和現象)

Physica昭和48年69巻1号 273頁~285頁

長谷田泰一郎他3名と共著

(その3) Field Induced Phase Transitions in Uniaxial Antiferromagnets

(一軸性反強磁性体における磁場による相転移)

J.Phys.Soc.Japan昭和47年32巻3号 610頁~615頁

単名

(その4) Magnetic Field Dependence of the Spin Lattice Relaxation of Co^{60} in Very Dilute Co-Fe Alloys at Very Low Temperature

(極低温における Co-Fe 希薄合金中の Co^{60} 原子核の核スピン－格子緩和時間の磁場依存性)

J.Phys.Soc.Japan昭和47年32巻6号 1678頁~1678頁

伊藤順吉他2名と共著

MAGNETIC COOLING AND PHASE TRANSITION IN SPIN PAIR SYSTEM

Naohiko YAMASHITA

PART I MAGNETIC COOLING AND PHASE TRANSITION IN $CeCl_3.7H_2O$

PART II PULSED ADIABATIC MAGNETIZATION IN $Cu(NO_3)_2.2.5H_2O$

1975

ABSTRACT

The magnetic cooling and phase transition are studied experimentally in the spin pair systems with the singlet ground state, $CeCl_3.7H_2O$ and $Cu(NO_3)_2.2.5H_2O$.

In Part I, the results of the successful adiabatic demagnetization of $CeCl_3.7H_2O$ with the initial condition, H_i = 48 kOe and T_i = 1.2 K, are reported. The cooling curve is obtained with the minimum temperature of 68 mK around the energy level crossing field of 4.7 kOe. The susceptibility at the crossing field is represented by the Curie-Weiss law with the ferromagnetic Curie-Weiss temperature of 68 mK in sufficiently low temperature region. This is consistent with the temperature dependence of the zero field susceptibility. It is found that the bottom of the cooling curve becomes flat around the crossing field at the temperature below 72 mK. From this fact, it is concluded that the spin ordering occurs around the crossing field at the temperatures lower than the critical temperature of 72 mK.

In Part II, the adiabatic magnetization experiment in $Cu(NO_3)_2.2.5H_2O$ is performed below 4K using a pulsed magnetic field. The cooling of the spin system is assured by the induced signal $\partial M/\partial t$, which is found to be proportional to the adiabatic susceptibility $(\partial M/\partial H)_S$ under the adiabatic magnetization process. The results in the present "transient" experiments are consistent with those in the "static" case. The spin ordering around the crossing field is confirmed with the appearance of the double peaks of $\partial M/\partial t$ signal there. The theoretical analyses of the double peaks, as well as their asymmetry, are given in quantitative agreement with the experiments.

TABLE OF CONTENTS

GENERAL INTRODUCTION

In order to reach lower and lower temperatures, various kinds of methods have been proposed and actually tried. Above all, adiabatic cooling methods are well known examples. For such a method, a working substance is needed, whose entropy depends both on the temperature and on an externally variable parameter. Following the method of the adiabatic expansion of gases, the adiabatic demagnetization of paramagnetic salts was proposed by Debye[1] and Giauque[2] in 1926, and the first experimental results were reported in 1933 from Leiden,[3] Berkley[4] and Oxford.[5] The fact that the adiabatic demagnetization of paramagnetic salt produces a cooling effect follows from the next equation

$$\left(\frac{\partial T}{\partial H}\right)_S = - \frac{T}{C_H}\left(\frac{\partial M}{\partial T}\right)_H . \qquad (1)$$

Since in ordinary paramagnet $(\partial M/\partial T)_H$ is negative, a negative dH entails a negative dT.

Equation (1) also says that if there exists a system in which $(\partial M/\partial T)_H$ is positive then one can produce cooling by adiabatic magnetization. Among such classes of systems, antiferromagnet is the first example. Schelleng and Friedberg[6] have carried out adiabatic magnetizations on powdered $MnBr_2 \cdot 4H_2O$, an antiferromagnet below 2.13 K. They obtained $\Delta T = - 0.125$ K by the adiabatic magnetization starting from $T_i = 1.75$ K up to the magnetic field of 10 kOe.

Kittel[7] and Wolf[8] proposed that ions or molecules

having a singlet ground state of the order of 1 to 10 cm^{-1} below a magnetic first excited state may be used for adiabatic magnetization cooling. The principle is simple. We consider, for example, salts containing Ni^{2+} ions (spin S = 1), in which an axial crystalline field brings the $S_z = 0$ state below the $S_z = \pm 1$ states (see Fig. 1). At temperatures such that $kT \ll D$, the entropy of such a salt will tend to zero. If a magnetic field is now applied isothermally along the direction parallel to the crystalline D axis, the entropy will increase because the lower of the excited states approaches to the ground state. Just at the crossing field, the entropy will be nearly $R \cdot \ln 2$. For higher fields the entropy again decreases towards zero. If, on the other hand, the field is applied adiabatically so that the entropy remains constant, the temperature will fall initially, reaching a minimum when the field is again such that the two energy levels cross. Another example is a system of coupled pairs of ions with $S = \frac{1}{2}$ which have a singlet ground state.

Such cooling has been observed experimentally in $Cu(NO_3)_2.2.5H_2O$ by Haseda et al.[9] In this system, Cu^{2+} ions ($S = \frac{1}{2}$) are coupled in pairs by nearly isotropic antiferromagnetic exchange interaction giving the excited state of interest being a spin triplet with the energy gap of $\Delta = 5.2$ K above the ground state S = 0. In their experiment, they have found an anomaly that the bottom of the cooling curve becomes flat when the initial temperature T_i at H = 0 is reduced and then becomes to give double minimum around the crossing field

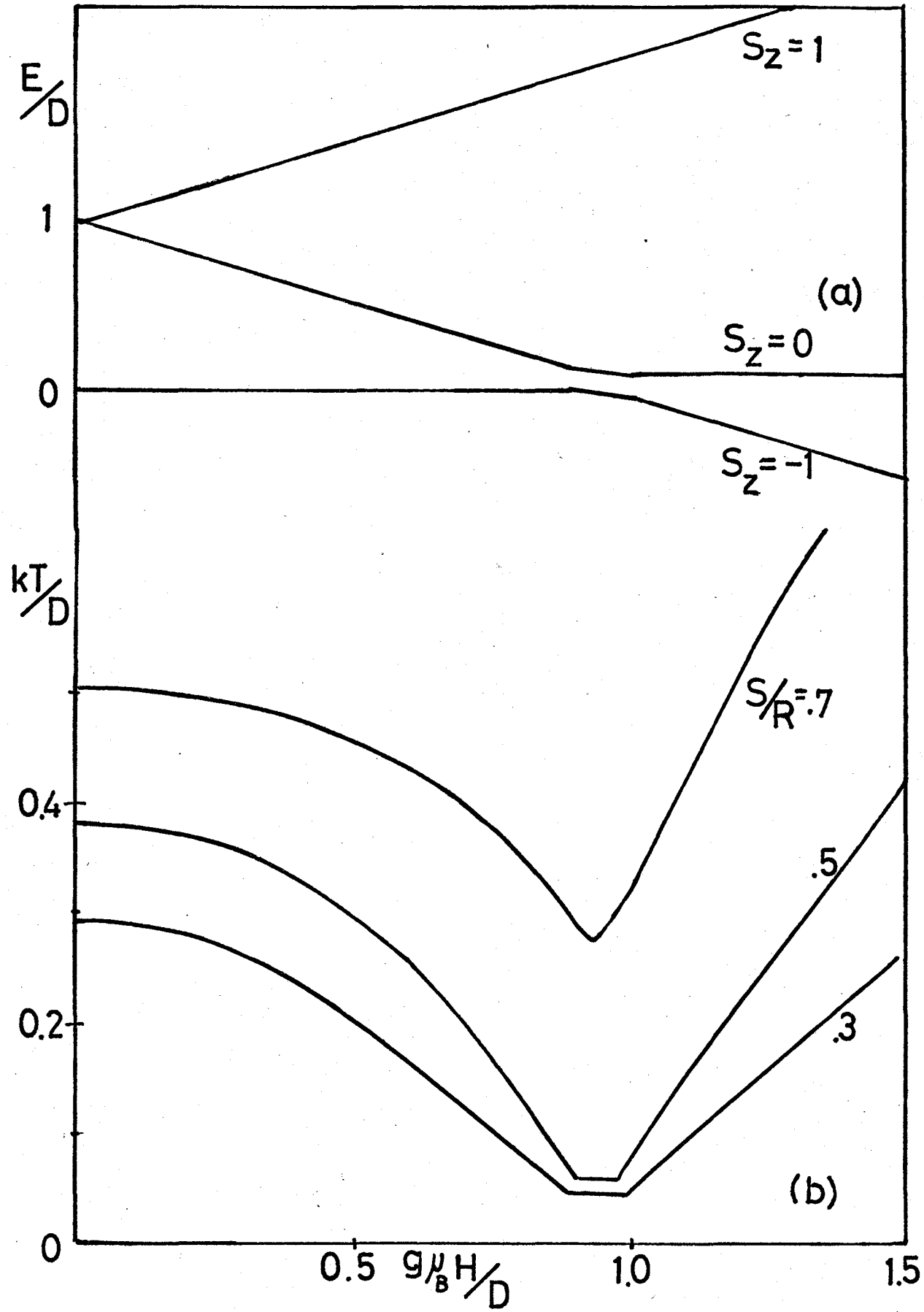

Fig. 1 (a) Variation of energy levels with magnetic field.

(b) Isentropic curves with ferromagnetic interaction.

when T_i is lower than about 0.7 K. This anomaly indicates that some kind of spin ordering occurs around the point of the level crossing when the sample is cooled lower than a critical temperature.

The magnetism of the system having a singlet ground state has been discussed at zero field by Moriya.[10] He considered Ni^{2+} ions, having spin S = 1, in an orthorhombic crystalline field. He showed that, when the crystalline field splitting between the lowest two spin levels is more than two times larger than the exchange energy, there is no long range ordering at zero field, at least within the framework of molecular field theory.*

Stimulated by the success in adiabatic cooling experiment by Haseda et al., the spin ordering of the system having the singlet ground state was theoretically investigated by Tsuneto and Muro,[11] and Tachiki et al.[12] For this spin ordering of the spin pair system, Tachiki et al. proposed the following mechanism. The inter-pair exchange interaction has non-vanishing matrix elements between the siglet and the triplet state, in other words, the interaction causes a mixing between them. If the isotropic inter-pair exchange is projected onto the subspace, spanned by the singlet and the lowest component of the triplet, the component of the exchange interaction perpendicular to the field becomes larger than the component parallel to the field. Furthermore, the effective magnetic field in this subspace becomes very small near the point of the level crossing. As the result, we can expect an ordering of the spin component perpendicular to the field in the vicinity

* See the footnote at the end of this introduction.

of the point of the level crossing at sufficiently low temperatures.

They applied this model to an explanation for Haseda et al.'s experiment of cooling by adiabatic magnetization of $Cu(NO_3)_2.2.5H_2O$. Furthermore, they consider various types of spin ordering for general cases of the inter-pair exchange interaction. Therefore, much more varieties of spin ordering in other samples are expected to be found experimentally. Especially, the ferromagnetic case would be very interesting for the comparison with the antiferromagnetic case of $Cu(NO_3)_2.2.5H_2O$. But few experimental studies have been reported up to now for lack of the materials favourable to the use.

One of the serious difficulties to proceed the experiments have been pointed out for the system having the singlet ground state originating from crystalline field splitting. The misalignment of the magnetic field from the principal axis of the crystalline field will easily introduce serious anti-crossing among two levels of interest. Therefore, it is very important to have the crystalline field axes of all magnetic ions in a unit cell parallel to each other.

On the other hand, for a spin pair system whose intra-pair exchange interaction has symmetrical anisotropy, the energy level crossing occurs, as far as the field direction is chosen such that the two ions have the equal effective g-value, even if the principal axes of the g-tensors of the two ions in pairs are not parallel to each other. Further, when the two

ions have the same g-tensor, the energy level crossing occurs independently of the field direction.

$CeCl_3.7H_2O$ is one of the rare examples known as an exchange-pair system like as $Cu(NO_3)_2.2.5H_2O$. Several experimental studies by Weber et al.[13] suggested that Ce^{3+} ions in this salt are coupled in pairs by isotropic antiferromagnetic exchange interaction such that the energy levels consist of a snglet ground state and an excited triplet separated by 1.16 K. For the purpose to obtain low temperature, it is necessary that each pair should be magnetically dilute in the crystal. From the AC susceptibility measurement,[13] the inter-pair interaction of $CeCl_3.7H_2O$ is expected to be very small.

We start the investigation of this salt, expecting to get another example of the appearance of the ordered state under the external magnetic field, hopefully of ferromagnetic one. The results are described in Part I in this article.

The difficulties for the experiments depend also on the experimental conditions. Usually magnetic cooling is performed by means of a static magnetic field. The level separation should be limited by the available static magnetic field. However, for the adiabatic magnetization cooling, we may use a pulsed magnetic field. The method is attractive from several points of view. First, it will be possible to investigate such substances having excited states of much higher than usual static magnetic field. Furthermore, from the experimental point of view, the metnod has the advantage to be free from the

external heat leak problem, because the adiabatic condition holds even on the sample which is directly immersed in liquid helium, in some experimental conditions, such that the duration of the pulsed magnetic field is shorter than either spin-lattice or lattice-bath relaxation time. Beside, the pulsed magnetic field methods may deduce some new problems as follows. First, problem is whether such transient method may be applied to the studies of the phase transition. Second, problem is whether the ordering would occur just in the same way as occurs in the spin system which is in the equilibrium with the lattice system, even if it may do in the condition isolated from the lattice system. For the system having the siglet ground state originating from crystalline field splitting, the condition that all magnetic ions in a unit cell have the crystalline field axes parallel to each other, however, would not be necessary if we use the pulsed magnetic method. In these system, the possibility of occurrence of ordering among the ions of only one site would be also another attractive problem.

We check the validity of the pulsed magnetic field method experimentally in the case of $Cu(NO_3)_2.2.5H_2O$ whose nature of adiabatic cooling and phase transition have been well known in equilibrium condition. The results are described in Part II in this article.

---

* The similar situation exists also in spin pair system, which will be described in §1.2 of Part I.

REFERENCES

1) P.Debye : Ann. Phys. 81(1926)1154.

2) W.F.Giauque : J. Amer. Chem. Soc. 49(1927)1864,1870.

3) W.J.de Haas, E.C.Wiersma and H.A.Kramers : Leiden Comm. No.229a; Physica's-Grav. 1(1933/34)1.

4) W.F.Giauque and D.P.McDougall : Phys. Rev. 43(1933)768.

5) N.Kurti and F.Simon : Nature, London 133(1934)907.

6) J.H.Schelleng and S.A.Friedberg : J. appl. Phys. 34(1963) 1087.

7) C.Kittel : Physica 24(1958)Suppl. p88.

8) W.P.Wolf : Phys. Rev. 115(1959)1196.

9) K.Amaya, Y.Tokunaga, R.Yamada, Y.Ajiro and T.Haseda : Phys. Letters A 28(1969)732; T.Haseda, Y.Tokunaga, R.Yamada, Y.Kuramitsu, S.Sakatsume and K.Amaya : Proc. 12th Intern. Conf. on Low Temp. Phys., Kyoto, p685(1970).

10) T.Moriya : Phys. Rev. 117(1960)635.

11) T.Tsuneto and T.Murao : Physica 51(1971)186.

12) M.Tachiki and T.Yamada : J. Phys. Soc. Japan 28(1970)1413; M.Tachiki and T.Yamada : Progr. theor. Phys. 46(1970) Suppl. p291; M.Tachiki, T.Yamada and S.Maekawa : J. Phys. Soc. Japan 29(1970)656,663; M.Tachiki, T.Yamada and S. Maekawa : Proc. 12th Intern. Conf. on Low Temp. Phys., Kyoto, 1970 p687.

13) S.Hüfner, R.v.Klot, F.Küch and G.Weber : Z. Naturforsch. A 22(1967)1999; R.von Klot and G.Weber : Z. Phys. 209 (1968)380.

Part I Magnetic Cooling and Phase Transition in $CeCl_3.7H_2O$

Chapter I INTRODUCTION

§1.1 A Spin Pair System : $CeCl_3.7H_2O$

Several experimental studies of $CeCl_3.7H_2O$ have been performed by Weber et al.[1~3] They have shown that Ce^{3+} ions in this salt are coupled in pairs by the isotropic antiferromagnetic exchange interaction, giving the singlet ground state and triplet excited state. The spin pair Hamiltonian is described as follows:

$$\mathcal{H}_o = J\mathcal{S}_1\cdot\mathcal{S}_2 + \mu_B \mathbf{H}\cdot\mathbf{g}\cdot(\mathcal{S}_1 + \mathcal{S}_2) \qquad (1)$$

where the isotropic exchange parameter J/k is 1.16 K, g-tensor is very anisotropic and the greatest principal g-value is 3.60, which is at least one order of magnitude greater than the values of other axes. Their typical results of the AC susceptibility measurements and the energy level scheme proposed, are shown in Fig. 1. If the field is applied parallel to the axis with the greatest g-value, the singlet and the lowest component of the triplet cross at the field value H = 4.71 kOe.

In order to understand the AC susceptibility behaviors, it is covenient to introduce the three types of susceptibilities, that is, the isothermal, the adiabatic and the isolated susceptibility. For the paramagnetic substance, they are obtained in the following way,

$$M = -\left\langle \frac{\partial E_j}{\partial H} \right\rangle = \frac{\sum_j -\left(\frac{\partial E_j}{\partial H}\right) e^{-\frac{E_j}{kT}}}{\sum_j e^{\frac{-E_j}{kT}}} \qquad (2)$$

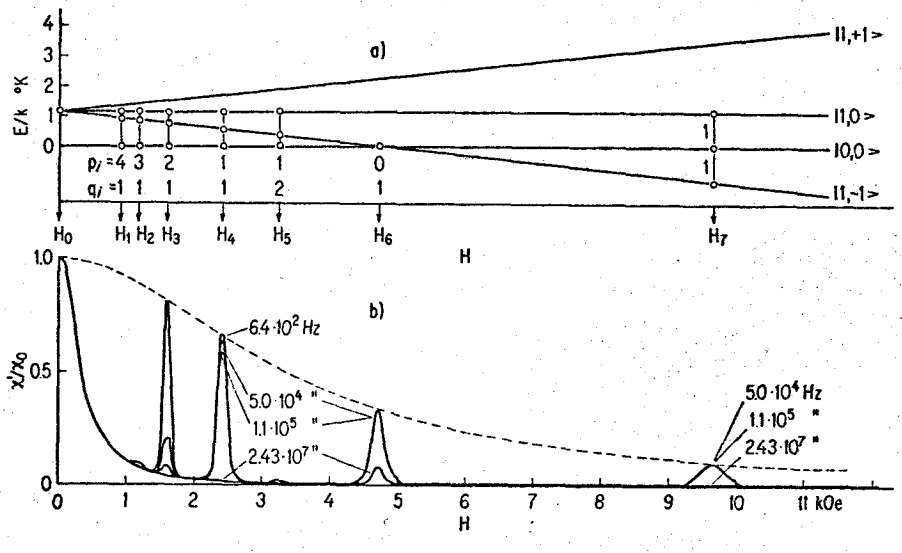

Weber et al.

Fig. 1 a) Energy level scheme of spin pair.

b) Normalized AC susceptibility χ'/χ_o as function of magnetic field H at T = 4.21 K. Dotted line represents the adiabatic susceptibility.

$$\chi_T = \left(\frac{\partial M}{\partial H}\right)_T = \chi_{iso} + \frac{1}{kT}\left\{\left\langle\left(\frac{\partial E_j}{\partial H}\right)^2\right\rangle - \left\langle\frac{\partial E_j}{\partial H}\right\rangle^2\right\}, \tag{3}$$

$$\chi_{iso} = \lim_{\Delta H \to 0} \frac{1}{\Delta H} \frac{\sum_j -\left[E_j'(H+\Delta H) - E_j'(H)\right] e^{-\frac{E_j}{kT}}}{\sum_j e^{-\frac{E_j}{kT}}} = \left\langle -\frac{\partial^2 E_j}{\partial H^2}\right\rangle \tag{4}$$

$$\chi_S = \chi_T - \frac{\left(\frac{\partial M}{\partial T}\right)_H^2}{\left(\frac{\partial S}{\partial T}\right)_H} = \chi_T - \frac{1}{kT} \frac{\left\{\left\langle E_j \frac{\partial E_j}{\partial H}\right\rangle - \left\langle E_j\right\rangle\left\langle\frac{\partial E_j}{\partial H}\right\rangle\right\}^2}{\left\langle E_j^2\right\rangle - \left\langle E_j\right\rangle^2}, \tag{5}$$

where the bracket $\langle\ \rangle$ expresses the thermal average. Their physical meaning may be mentioned in the following way. If we look at the individual energy levels under the external field, the magnetic moment of each level is expressed by the $-\partial E_j/\partial H$. Thus, when the frequency of the AC magnetic field is so high as the population of the individual level can not be changed, the response of the system is expressed by the isolated susceptibility χ_{iso}. On the other hand, when the frequency is low enough so that the spin system is always in the equilibrium with the thermal bath, the response is expressed by the isothermal susceptibility χ_T. If the spin system is in the internal equilibrium in itself, a spin temperature T_S can be defined although it is isolated from the lattice system. The spin temperature will change following with the instantaneous value of the AC magnetic field, keeping the entropy of spin system constant. In this case, the response is expressed by the adiabatic susceptibility χ_S.

The magnetic field dependence of the AC susceptibility in Fig. 1 are now interpreted to express a relaxation phenomena of a spin system having unequal energy level spacings in general and then, three kinds of static susceptibility χ_S, χ_{iso} and χ_T will be appeared corresponding to each different equili-

brium condition.

In fact, susceptibility peaks at several harmonic field show apparently a recovery of magnetization, or, in other words, a recovery of a certain kind of equilibrium state for which the response will be given by χ_S at each peak, and by χ_{iso} between these peaks.

If the energy level scheme is assumed as in Fig.1, these harmonic fields are found to be corresponding to the point where the intervals between energy levels make the simple integer ratio, where the internal thermal equilibrium within spin system is attained quickly. The susceptibility, there, is expressed by χ_S.

Investigated study of the dynamic susceptibility, its dependence on magnetic field, temperature and frequency has given a further evidence for the supposed energy level scheme, that is, evidence for the spin pair model as described by Eq.(1).

Before the description of our experimental results about the magnetic cooling and the phase transition in $CeCl_3.7H_2O$, we consider several characteristics of a spin pair system.

§1.2 Absence of Ordering at Zero Field

Absence of the long range order at zero field is one of the characteristics of the spin pair systems concerned in this article. Therefore, we consider the matter in the begining. We consider the pairs coupled by the isotropic antiferromagnetic exchange interaction, whose Hamiltonian can be written as follows,

$$\mathcal{H}_0 = J \sum_i \mathbf{S}_{i1} \cdot \mathbf{S}_{i2} \quad , \tag{6}$$

where $\mathcal{S}_{i1}$ and $\mathcal{S}_{i2}$ are the spins of the i-th pair and their magnitude are $\frac{1}{2}$. Further, we consider the weak inter-pair exchange interaction as follows:

$$\mathcal{H}' = -|J'| \sum_{<ij>} (\mathcal{S}_{i1} \cdot \mathcal{S}_{j1} + \mathcal{S}_{i2} \cdot \mathcal{S}_{j2}) . \tag{7}$$

For simplicity, we consider here only the case, where J' is ferromagnetic. Noting the isotropic antiferromagnetic intra-pair interaction and using a molecular field approximation for the inter-pair interaction, we obtain the following effective Hamiltonian,

$$\mathcal{H}_{eff} = J \mathcal{S}_1 \cdot \mathcal{S}_2 - \frac{1}{2} z |J'| n (\mathcal{S}_{z1} - \mathcal{S}_{z2}) , \tag{8}$$

where z gives the number of interacting neighbours, and

$$n = \langle \mathcal{S}_{z1} - \mathcal{S}_{z2} \rangle = 2 \langle \mathcal{S}_{z1} \rangle = -2 \langle \mathcal{S}_{z2} \rangle . \tag{9}$$

At the absolute zero temperature, the solution is written as follows

$$n = \sqrt{1 - \left(\frac{J}{zJ'}\right)^2} . \tag{10}$$

Therefore, there is no long range order if the inequality $z|J'| < J$ holds.

§1.3 Ordering in the Magnetic Field

Next, following Tachiki et al.,[4] we consider the ordering in the magnetic field, which is another characteristic of the spin pair systems. In this case, the Hamiltonian for the isolated pairs would read

$$\mathcal{H}_0 = J \sum_i \mathcal{S}_{i1} \cdot \mathcal{S}_{i2} + g_{/\!/} \mu_B H \sum_i (\mathcal{S}_{zi1} + \mathcal{S}_{zi2}) . \tag{11}$$

For the inter-pair interaction, again we assume the form

$$\mathcal{H}' = J' \sum_{\langle ij \rangle} (\mathbf{\Delta}_{i1} \cdot \mathbf{\Delta}_{j1} + \mathbf{\Delta}_{i2} \cdot \mathbf{\Delta}_{j2}) \tag{12}$$

Introducing operators $\mathbf{S}_i$ and $\mathbf{t}_i$ defined by

$$\mathbf{S}_i = \mathbf{\Delta}_{i1} + \mathbf{\Delta}_{i2} \quad \text{and} \quad \mathbf{t}_i = \mathbf{\Delta}_{i1} - \mathbf{\Delta}_{i2}, \tag{13}$$

we write the Hamiltonian as

$$\mathcal{H}_0 = \frac{1}{2} J \sum_i \mathbf{S}_i^2 + g_{/\!/} \mu_B H \sum_i S_{zi}, \tag{14}$$

and

$$\mathcal{H}' = \frac{1}{2} J' \sum_{\langle ij \rangle} (\mathbf{S}_i \cdot \mathbf{S}_j + \mathbf{t}_i \cdot \mathbf{t}_j) \ . \tag{15}$$

In the case, $z|J'| \ll J$, we may neglet the highest two levels of the triplet and confine ourselves to the subspace spanned by $|0,0\rangle$ and $|1,-1\rangle$. In this case, noting the relations

$$S_{xi} = S_{yi} = 0, \quad t_{zi} = 0,$$

$$S_{zi}|1,-1\rangle = -|1,-1\rangle, \quad S_{zi}|0,0\rangle = 0, \tag{16}$$

$$t_{xi}|1,-1\rangle = \frac{1}{\sqrt{2}}|1,-1\rangle \quad \text{and} \quad t_{yi}|1,-1\rangle = \frac{1}{\sqrt{2}}|0,0\rangle$$

we may introduce the following Pauli spin operators σ_i,

$$S_{zi} = \frac{1}{2}(\sigma_{zi} - 1), \quad t_{xi} = \frac{1}{\sqrt{2}}\sigma_{xi}, \quad t_{yi} = \frac{1}{\sqrt{2}}\sigma_{yi} \tag{17}$$

By use of these relations, the total Hamiltonian is written as

$$\mathcal{H} = \frac{N}{2}(J + \frac{\alpha}{4} - h) - \frac{1}{2}(J + \frac{\alpha}{2} - h) \sum_i \sigma_{zi} + \frac{J'}{8} \sum_{\langle ij \rangle} \{2(\sigma_{xi}\sigma_{xj} + \sigma_{yi}\sigma_{yj}) + \sigma_{zi}\sigma_{zj}\}, \tag{18}$$

where $h = g_{//}\mu_B H$ and $\alpha = z J'/2$.

Now, it is easy to expect the natures of the ordering in this system. For example, again using molecular field theory, the magnetization at absolute zero is described as follows,

$$m = \frac{h - (J - |\alpha|)}{2|\alpha| + \alpha} , \quad (h_{c1} < h < h_{c2}) \tag{19}$$

where $h_{c1} = J - |\alpha|$, $h_{c2} = J + |\alpha| + \alpha$.

The critical temperature is given by

$$k T_c = \frac{|\alpha|}{2} , \quad (h = J + \frac{\alpha}{2}) \tag{20}$$

It is possible to apply the method for the more general inter-pair interaction as follows

$$\mathcal{H}' = \sum_{\langle i,j \rangle} \left\{ J_{11} \epsilon_{ij}^{11} \Delta_{i1} \cdot \Delta_{j1} + J_{22} \epsilon_{ij}^{22} \Delta_{i2} \cdot \Delta_{j2} + J_{12} \epsilon_{ij}^{12} (\Delta_{i1} \cdot \Delta_{j2} + \Delta_{i2} \cdot \Delta_{j1}) \right\}, \tag{21}$$

where $\epsilon_{i,j}^{m,n} = 1$ for the i-j pair interacting with the exchange constant J_{mn}, and $\epsilon_{ij}^{m,n} = 0$ for the other pairs. In this case, the total Hamiltonian is written as

$$\begin{aligned} \mathcal{H} = {} & \frac{N}{2}(J + \frac{\alpha}{2} - h) - \frac{1}{2}(J + \frac{\alpha}{2} - h) \sum_i \sigma_{zi} \\ & + \frac{1}{4} \sum_{\langle ij \rangle} \left\{ \frac{1}{2}(J_{11}\epsilon_{ij}^{11} + J_{22}\epsilon_{ij}^{22} - 2J_{12}\epsilon_{ij}^{12})(\sigma_{xi}\sigma_{xj} + \sigma_{yi}\sigma_{yj}) \right. \\ & \left. + \frac{1}{4}(J_{11}\epsilon_{ij}^{11} + J_{22}\epsilon_{ij}^{22} + 2J_{12}\epsilon_{ij}^{12})\sigma_{zi}\sigma_{zj} \right\} , \end{aligned} \tag{22}$$

where $\alpha = \frac{1}{4}(J_{11}Z_{11} + J_{22}Z_{22} + 2J_{12}Z_{12})$. (23)

Now, we take the two sublattice model and consider the spin ordering at absolute zero temperature in the molecular field approximation. For the purpose of the classification of the various types of the ordered states, we introduce another parameter β as follows,

$$\beta = \frac{1}{2}(J_{11}z_{11} + J_{22}z_{22} - 2J_{12}z_{12}) \ . \qquad (24)$$

These two parameters, α and β , are the measures of the parallel and the perpendicular exchange interaction, respectively. The classification of the values of α and β in eight cases is shown in Fig. 2. In each of the cases, the configuration of the spin $\langle\sigma_i\rangle$ varies with the change of the magnetic field as shown in Fig. 3. Furthermore, the $\langle\Delta_i\rangle$-configurations corresponding to the $\langle\sigma_i\rangle$-configurations are illustrated in Fig. 4.

In this section, we have reviewed several points from Tachiki et al.'s work about the magnetism in spin pair system. Although the keen insight is gained by using the two level approximation, this approximation confines our to the case where the next two conditions hold at the same time. One is the condition $zJ' \ll J$. Another is the condition $kT \ll J$. As the result of this approximation, theory predicts some symmetric behavior, with respect to the crossing point, for the thermodynamical and the magnetical properties in spin pair system. Including the effect of the upper two levels, we will discuss the molecular field theory for the comparison with our experiments in Chap. IV of Part I (and also in §4.2 of Part II).

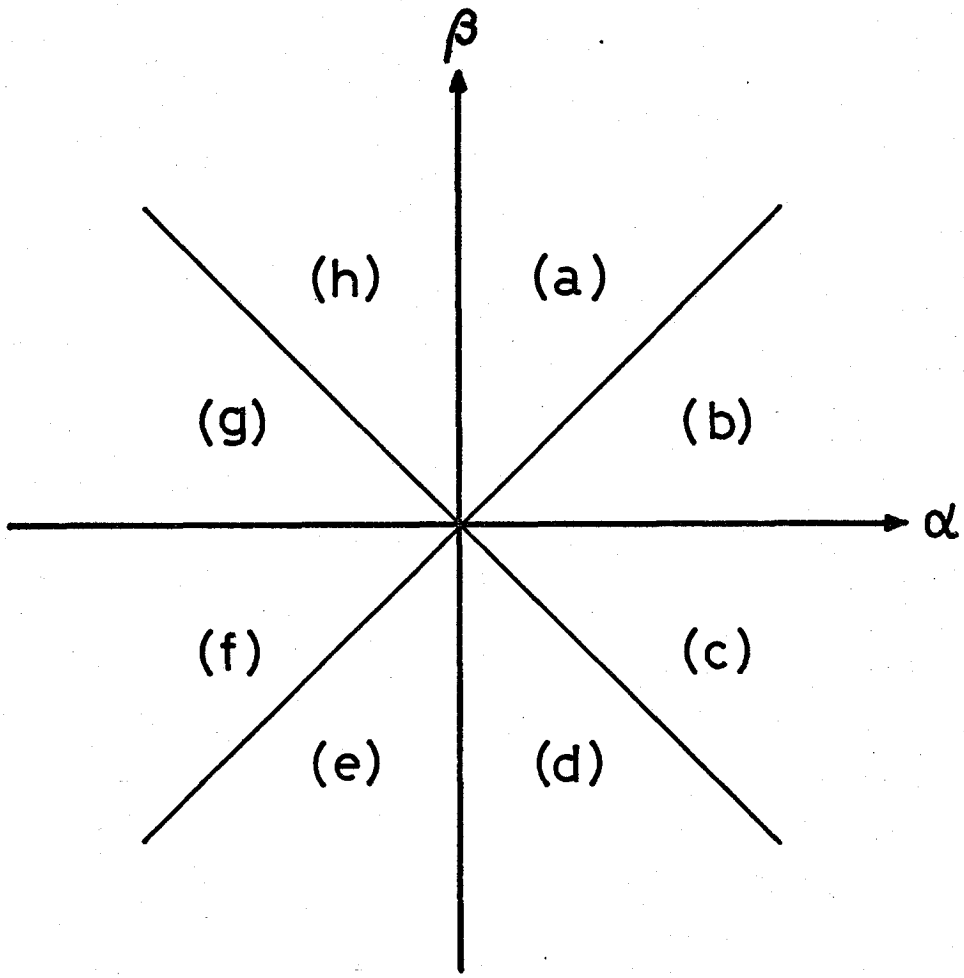

Fig. 2 The classification of the values of α and β.

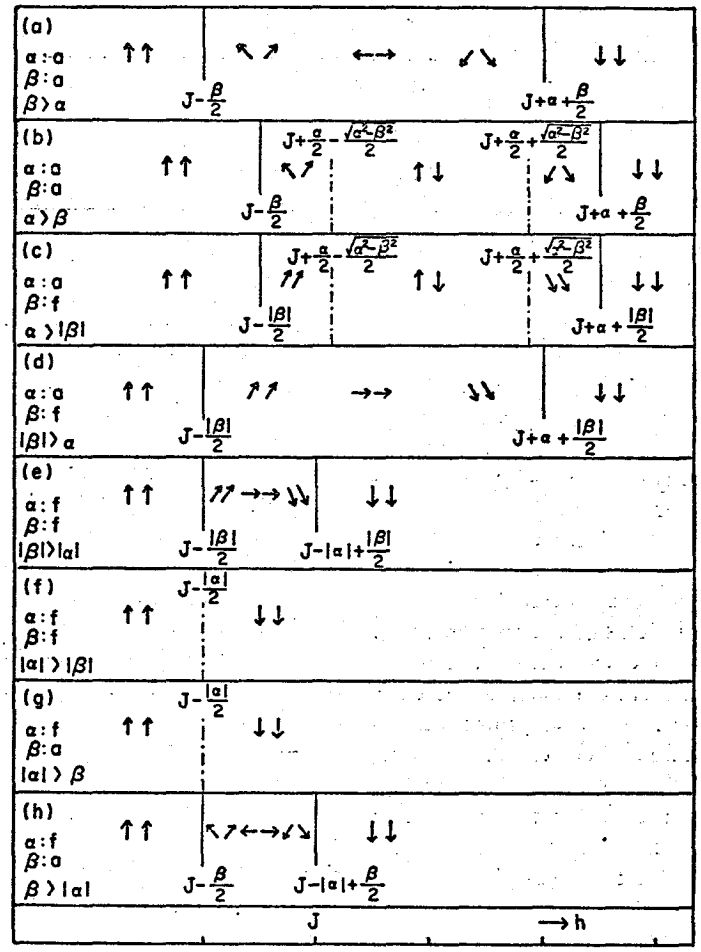

Fig. 3 Variation of the configuration of the spins $\langle\sigma\rangle$ and $\langle\sigma'\rangle$ with change of the magnetic field for each of the cases (a), (b) etc. defined in Fig. 2.

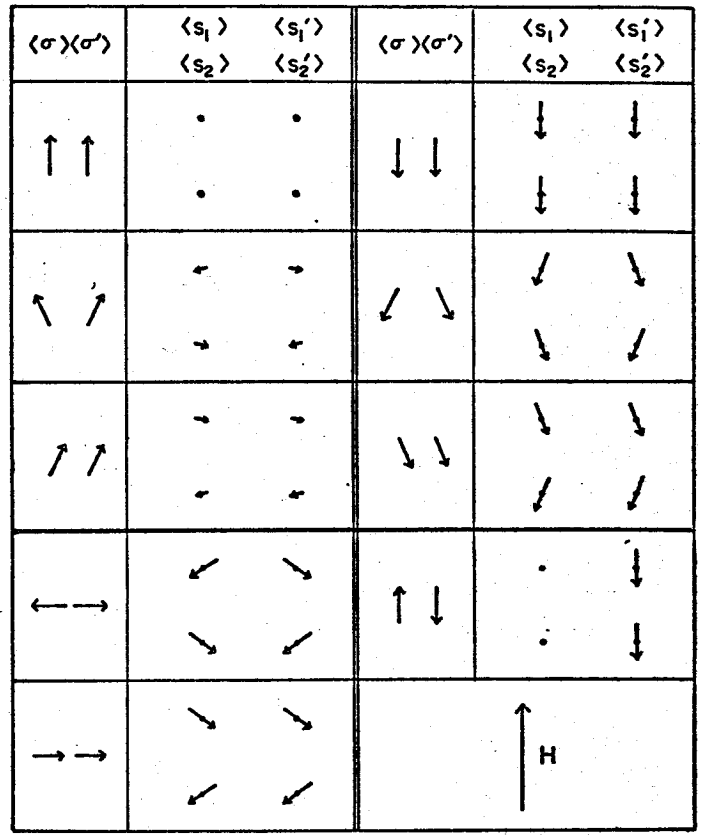

Fig. 4 Configurations of the spins $\langle \mathcal{O}_1 \rangle$, $\langle \mathcal{O}_2 \rangle$, $\langle \mathcal{O}_1' \rangle$, and $\langle \mathcal{O}_2' \rangle$. These configurations correspond to the $\langle \sigma \rangle$- and $\langle \sigma' \rangle$-configurations at their left-hand sides.

Chapter II EXPERIMENTALS

§2.1 Sample

The X-ray structure analysis of $CeCl_3.7H_2O$ was performed by Weitz.[5] The crystal structure is monoclinic ($\beta = 137°$). The lattice constants are determined to be a = 12.2 Å, b = 10.4 Å and c = 12.0 Å. The unit cell contains four formula units. The specimens used in this work were grown from a saturated aqueous solution below about 5°C in the electric refrigerator. By this method, we could easily obtain the large transparent single crystals. The crystal habit is shown in Fig. 5. This is the cross section perpendicular to monoclinic b-axis. The principal axis χ_2 makes an angle about 6° from a-axis. The susceptibility is the greatest in this direction. In most of our experiments, the external field H was applied parallel to this direction. By free suspension in the magnetic field, the axis χ_2 is found easily at room temperature. Fast cooling down to liq. N_2 temperature makes many cracks in the sample, therefore the slow precooling has to be cared. To prevent deliquescence, single crystals were preserved in Carbon Tetrachloride. The crystals have a tendency to form frequently twin structure.

§2.2 Check of Twin Crystals and Setting of Samples

To check the twin samples and the orientation of the specimen, the cross relaxation measurements are utilized. For the simplicity of the experimental apparatus, the measurements

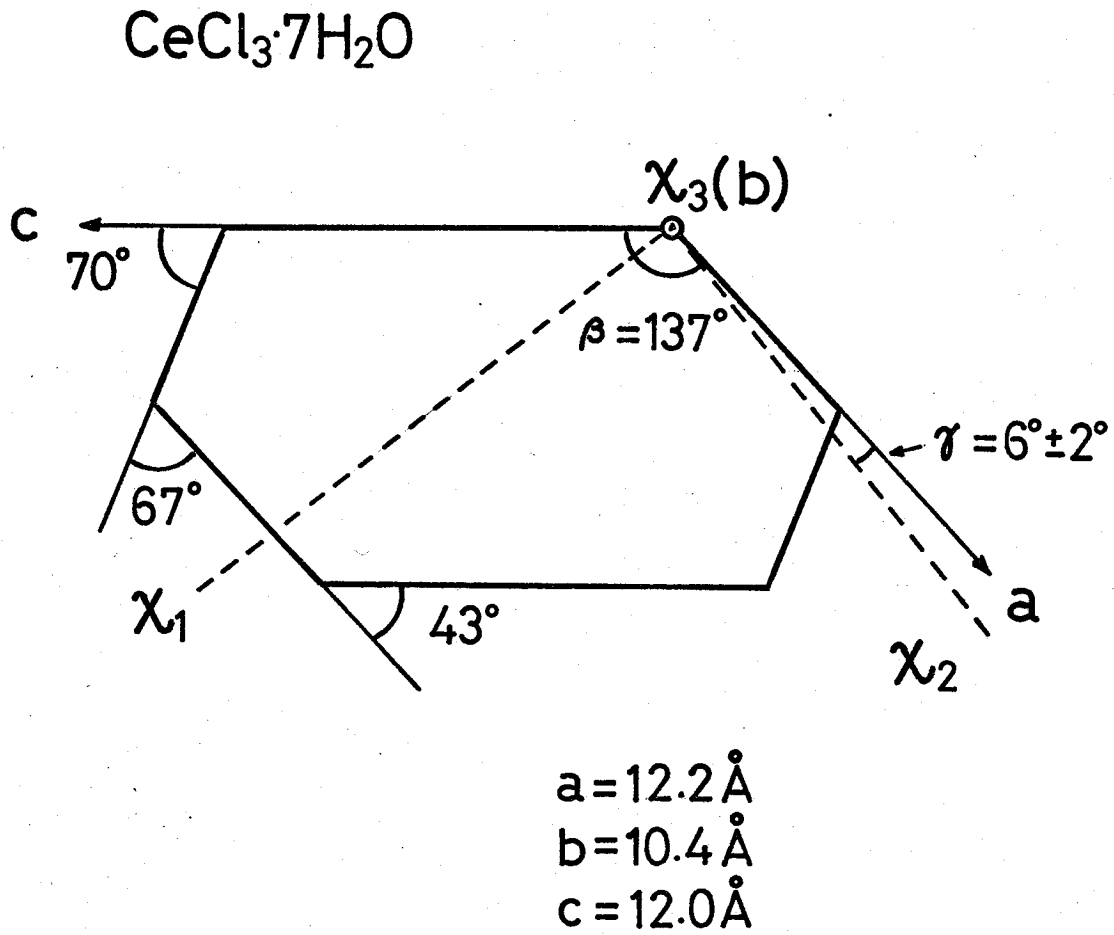

Fig. 5 The cross section of $CeCl_3.7H_2O$ perpendicular to monoclinic b axis.

are performed by using the steady NMR equipement. In most of the measurements, the high frequency (ν = 12 MHz) and the modulation frequency (ν = 40 Hz) are used. The static external field is applied perpendicular to the pick up coil.

The typical result is shown in Fig. 6, where three cross relaxation signals are distinguishable in the harmonic fields, H_4, H_6 and H_7 (see the notation in § 1.1 Fig. 1). The result for the sample which involves definitely the twin structure is shown in Fig. 7, where the cross relaxation signals reveal with the additional fine structure, or splitting across. The samples which give the results as shown in Figs. 8a) and 8b) are frequently obtained. As far as within Fig. 8a), the sample seems to be real single-crystal. However, inclining the external magnetic field as is shown in Fig. 8b), we find it to be twin sample in fact. In this way, we could check the twin samples.

The angular variation of the harmonic fields is shown in Fig. 9, where the external magnetic field is varied in the a-c plane. The angular dependence is approximately expressed as follows:

$$\frac{H_\nu(\theta)}{H_\nu(0)} = \frac{1}{|\cos\theta|} \tag{25}$$

where θ represents the angle between χ_2 axis and the direction of the external magnetic field. In this way, we ascertain the fact that the g-values of other axes are negligibly smaller than the value with χ_2 axis. This method is used also to check the orientation of the specimen.

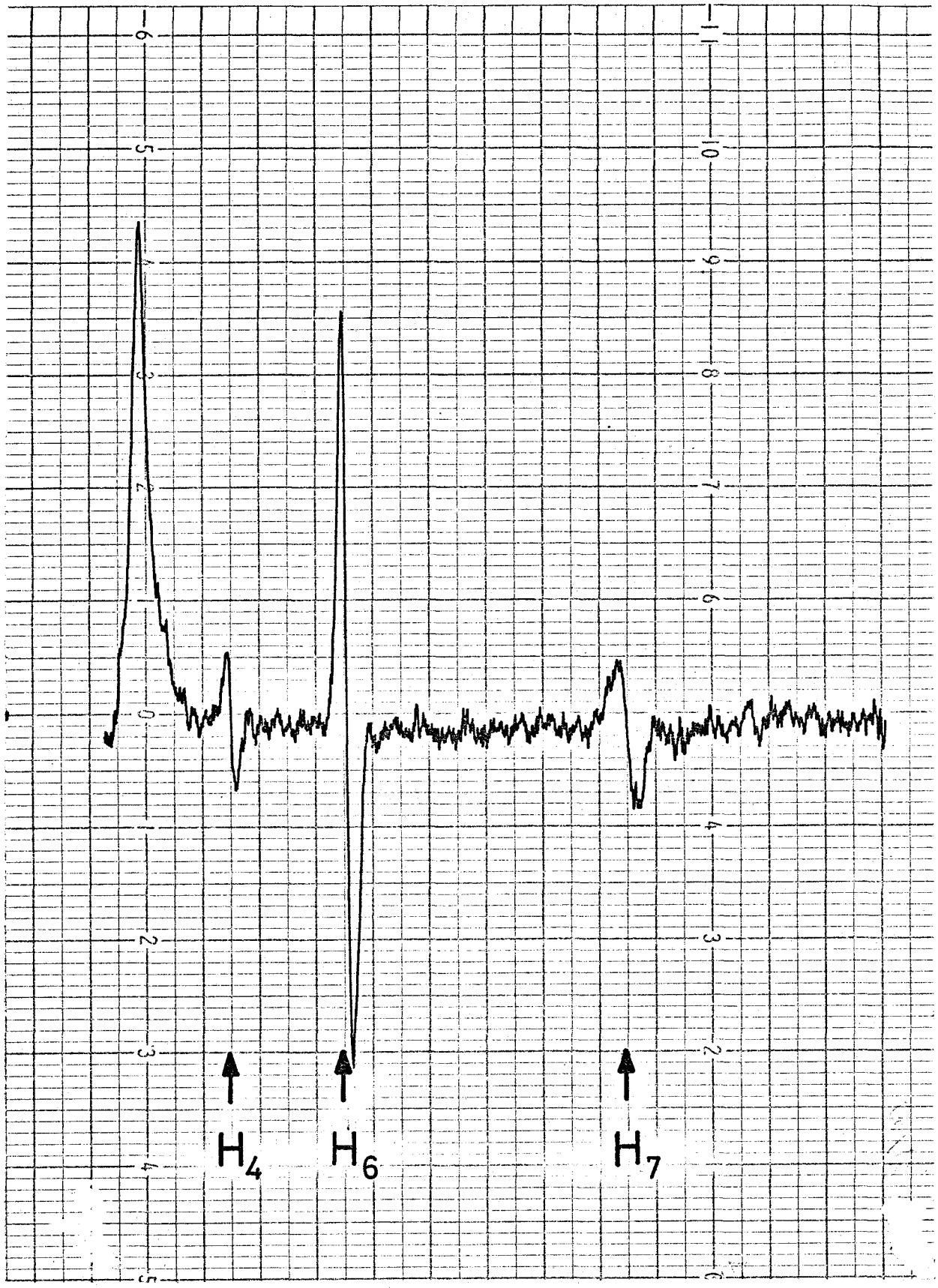

Fig. 6 Typical result of cross relaxation measurement. H_4, H_6 and H_7 represent harmonic fields (see notation in Fig. 1).

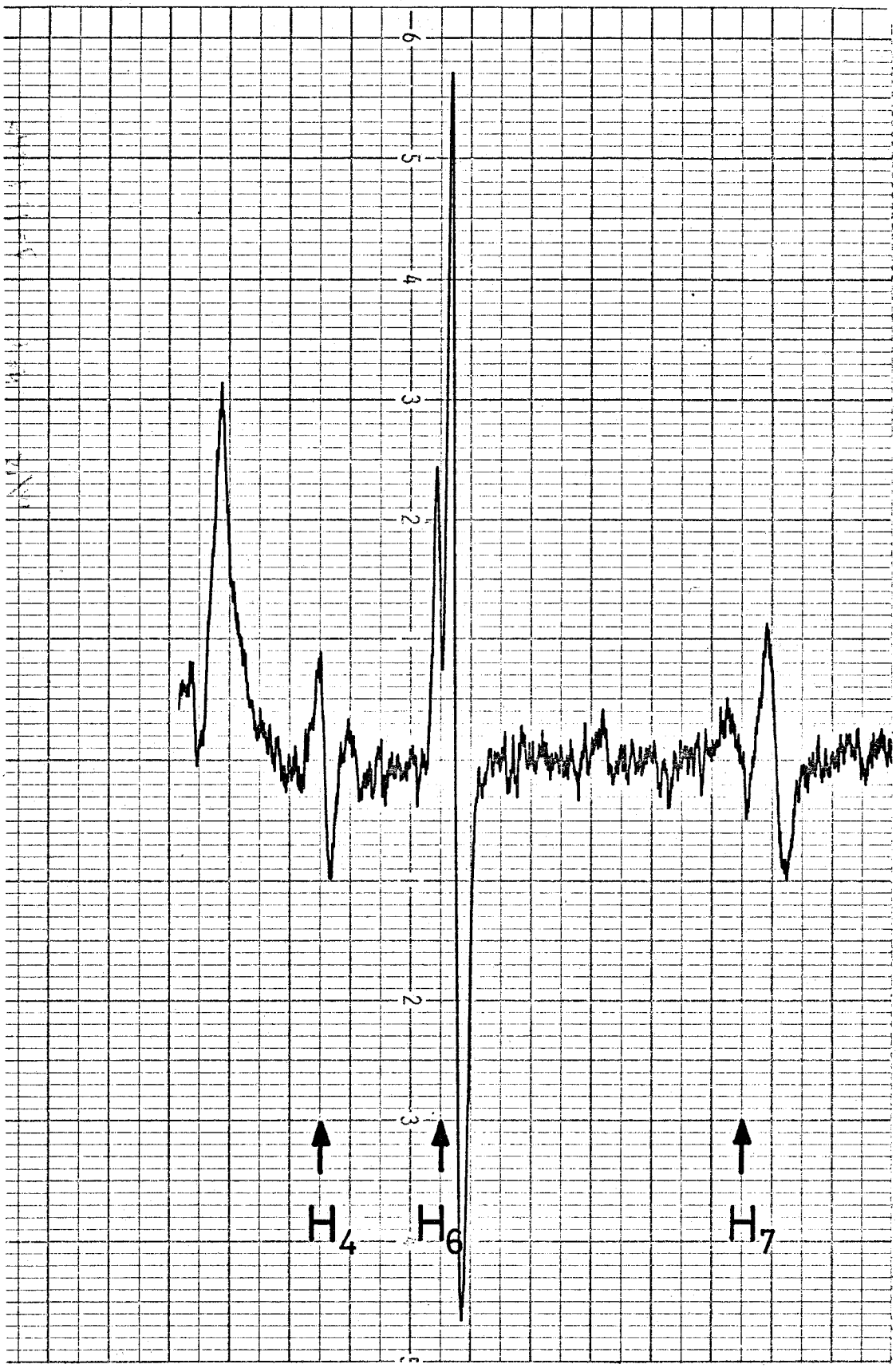

Fig. 7 Cross relaxation signals for sample which involves definitely twin structure.

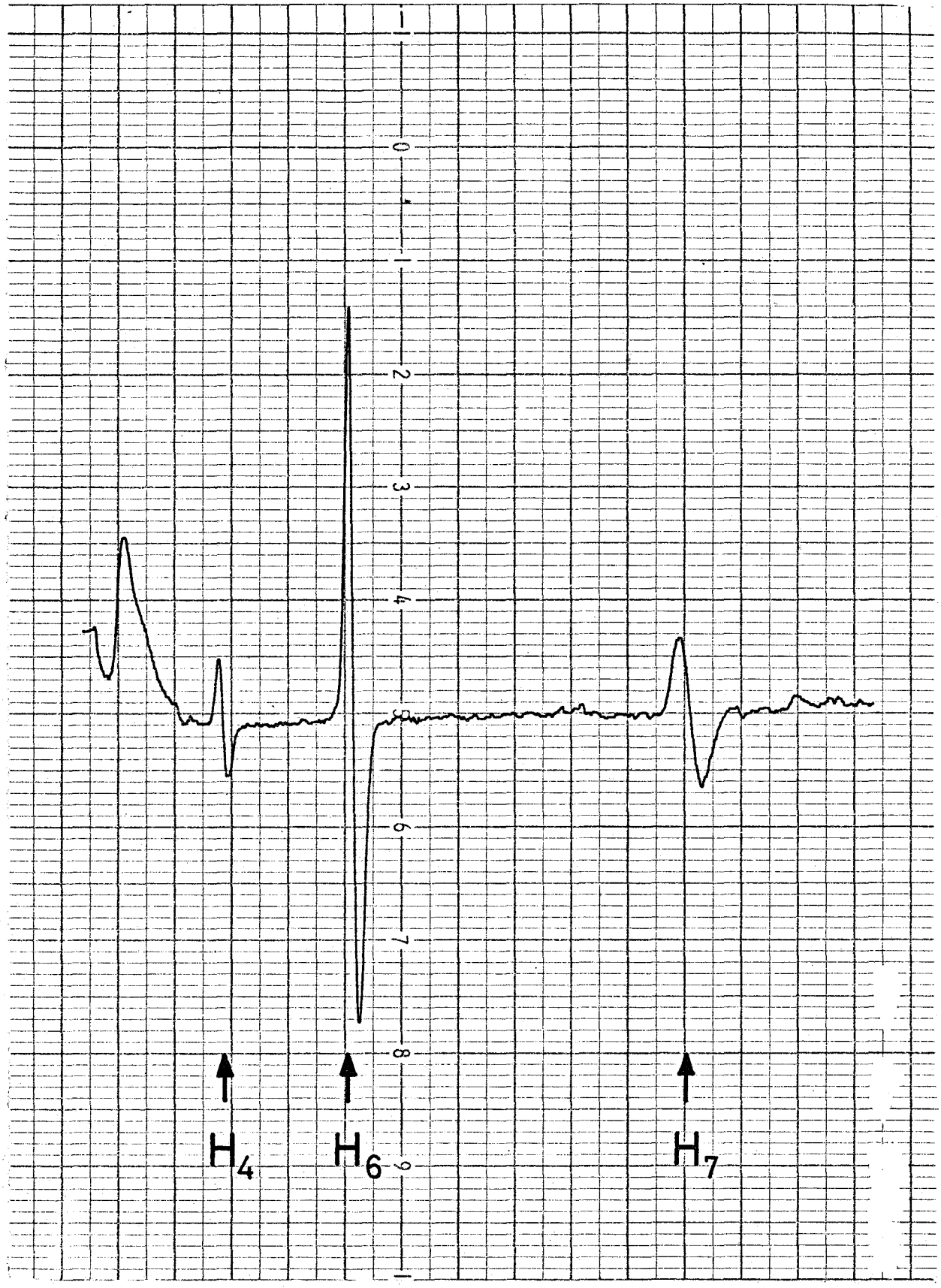

Fig. 8a) Cross relaxation signals for false single-crystal.

($H /\!/ \chi_2$)

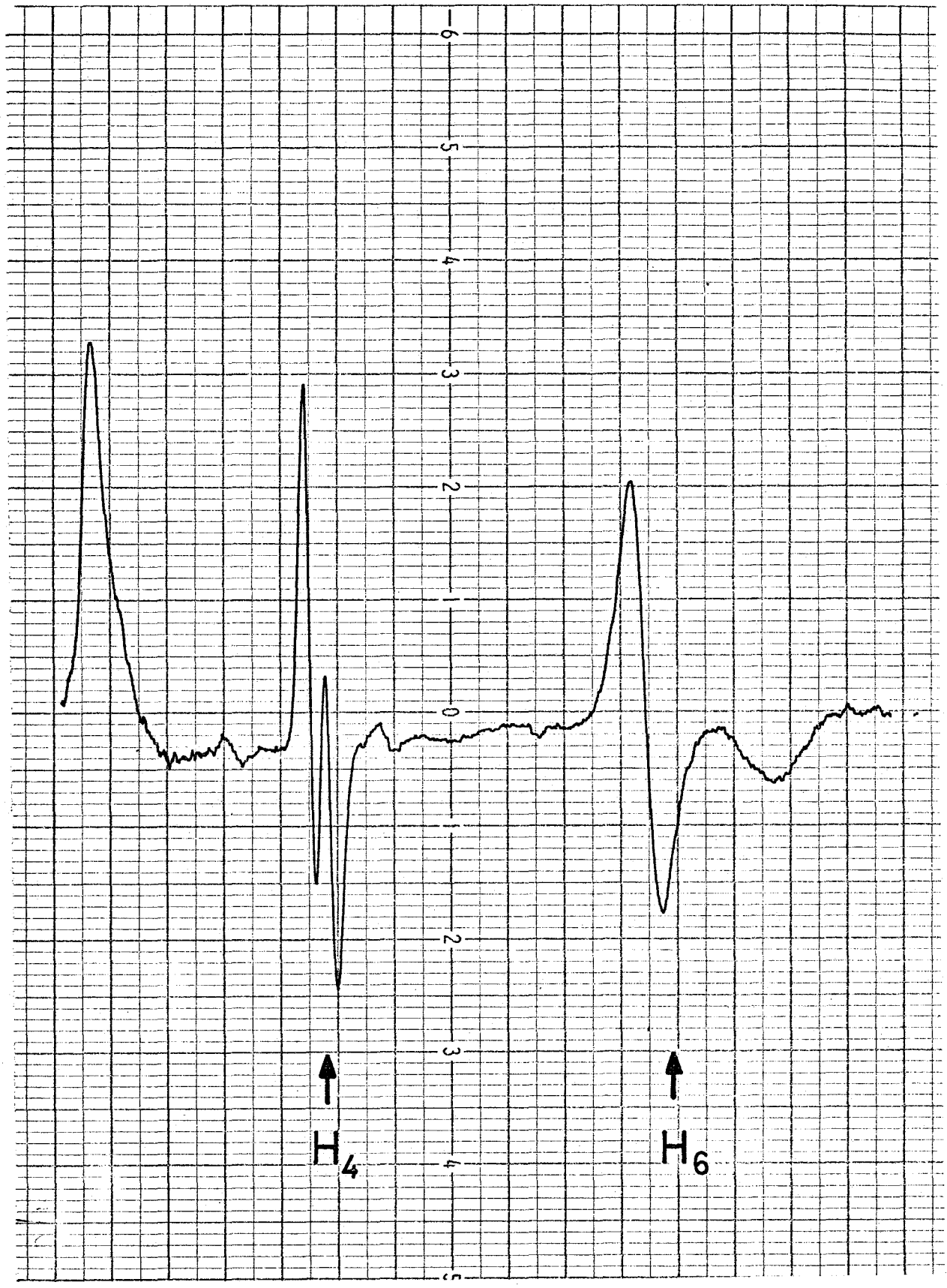

Fig. 8b) Cross relaxation signals for false single-crystal.

($\theta \sim 70^{\circ}$)

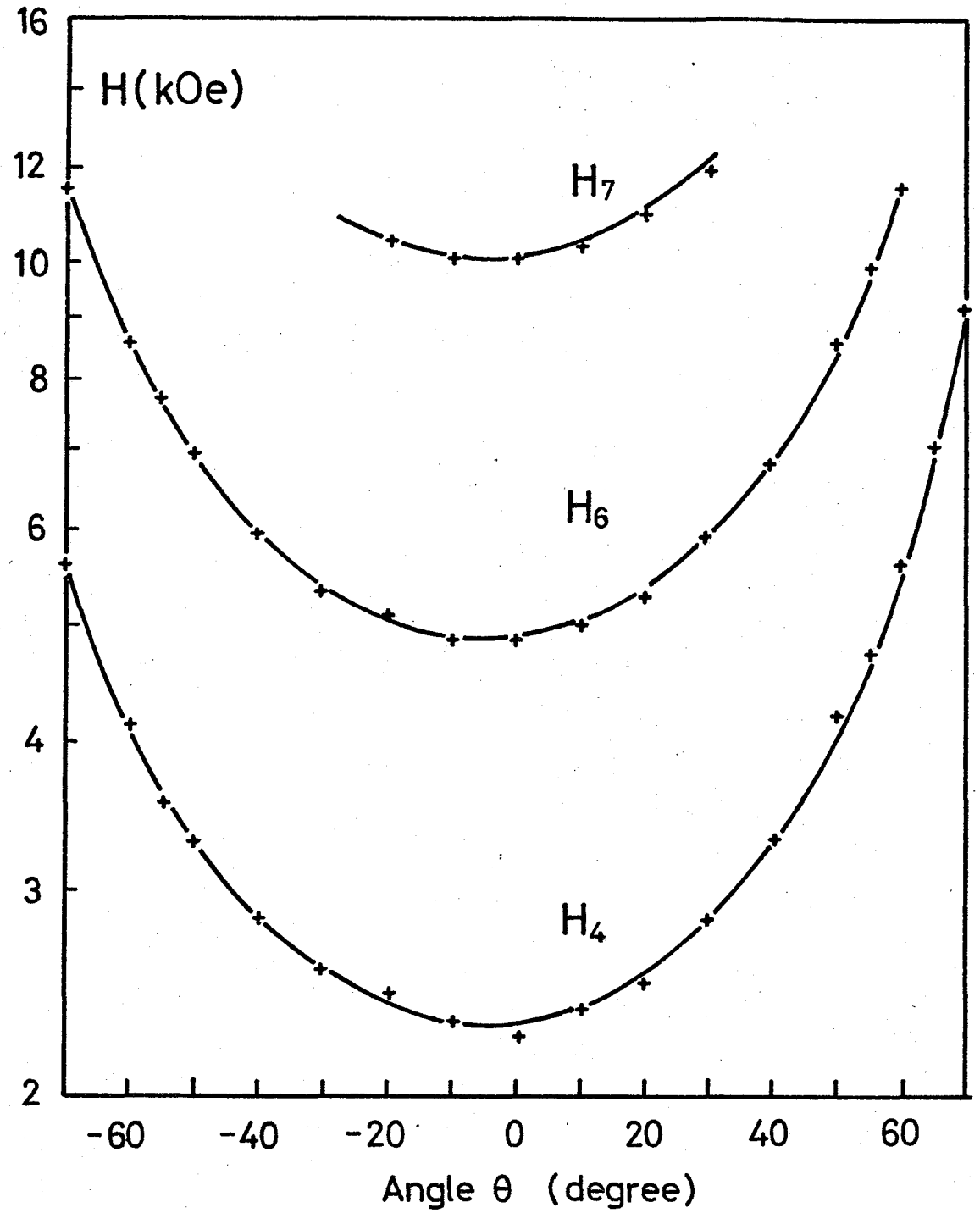

Fig. 9 Angular variation of harmonic fields.(H// a-c plane)
See the notation in Fig. 1.

§2.3 Adiabatic Demagnetization Apparatus

Magnetic cooling experiments are performed by using the adiabatic demagnetization apparatus, which is shown in Fig. 10.

The external magnetic fields up to 45 kOe are applied by using the supperconducting magnet (SCM) of 100 mm length and 25 mm diameter. The SCM power supply line is connected with 1 mΩ standard resistor in series. The current values are recorded on X-Y recorder.

The glass-wall adiabatic cell is used. In order to shut out the radiation, the cell is covered with the black nylon sheets. The cell is connected to the vacuum line with the cobar seal.

The heat guards consist of the Cr-K alum and Apiezon J oil, and they are packed in the bakelite container. The two heat guards are connected each other with the bakelite pipe such that they shield the specimen. The assembly is supported by the bakelite rod and the nylon nails.

The radiation shield is placed inside the vacuum line just at the entrance of the cell. It consists of three sheets of the semi-circular copper plates painted black.

§2.4 Thermometry

As the thermometer favourable to the measurement at low temperature in the magnetic field, we used the carbon resistor, Speer 220 Ω ($\frac{1}{2}$W). The carbon resistor, whose mould was stripped off, was attached to a small gutter in the specimen with Apiezon N grease. In order to obtain much closer thermal

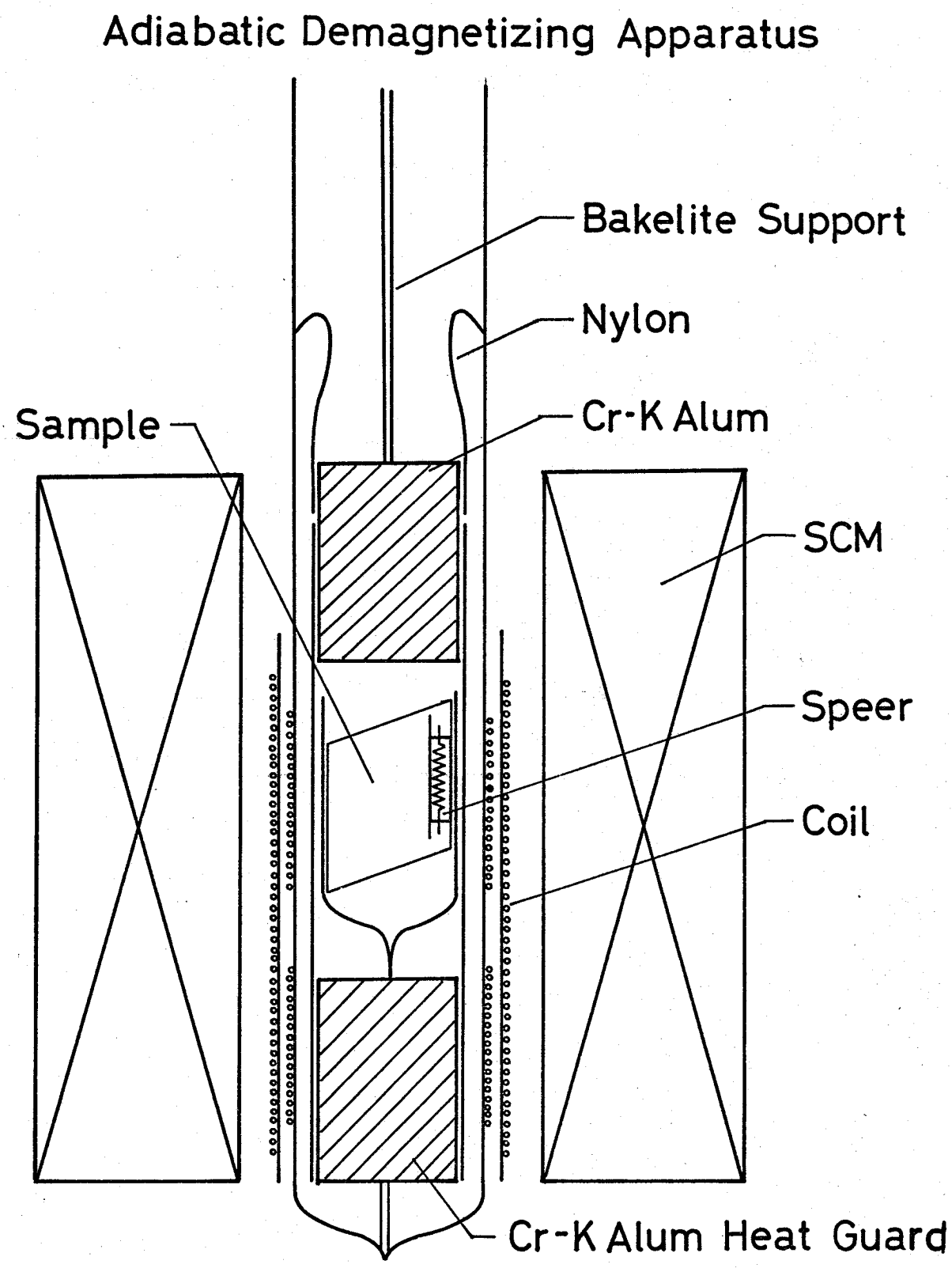

Fig. 10 Adiabatic Demagnetization Apparatus.

contact, the resistor and the specimen were bound up with nylon thread. Resistance was measured by the DC four terminal method. The measuring current was varied from 0.1 μA to 0.01 μA, according to the temperature range, keeping its power dissipation always below 10^{-12} W. In order to prevent thermal leak from 1K bath through lead wires, the manganin wires were used as electric leads inside the adiabatic cell. The lead wires were shielded with Stycast 2850-GT at the outlet from the adiabatic cell. The voltage across the carbon resistor was amplified by the micro-voltmeter and was directly recorded on X-Y recorder.

§2.5 Magnetic Susceptibiltity Measurement Apparatus

The magnetic susceptibilities of the specimen in the isentropic process are observed by using the modified AC Hartshorn bridge, whose block diagram is shown in Fig. 11. In most of the measurements, frequency used was ν = 1 kHz. In order to obtain high sensitivity, the secondary coil is wound directly around the adiabatic cell, and consists of two pieces, each of which is equal turns but in counterweise. The primary coil is wound around the bakelite bobin. The induced voltage across the secondary coil is proportional to the susceptibility of the specimen, if the compensation of the coil is complete. Geometrically unbalanced signal without specimens is usually compensated by electronic way using a phase shifter and a mixer circuit. Under the experimental condition of magnetic cooling, the specimen is fixed inside one of the pieces of the secondary coil and the compensation in

BLOCK DIAGRAM of APPARATUS for SUSCEPTIBILITY MEASUREMENT

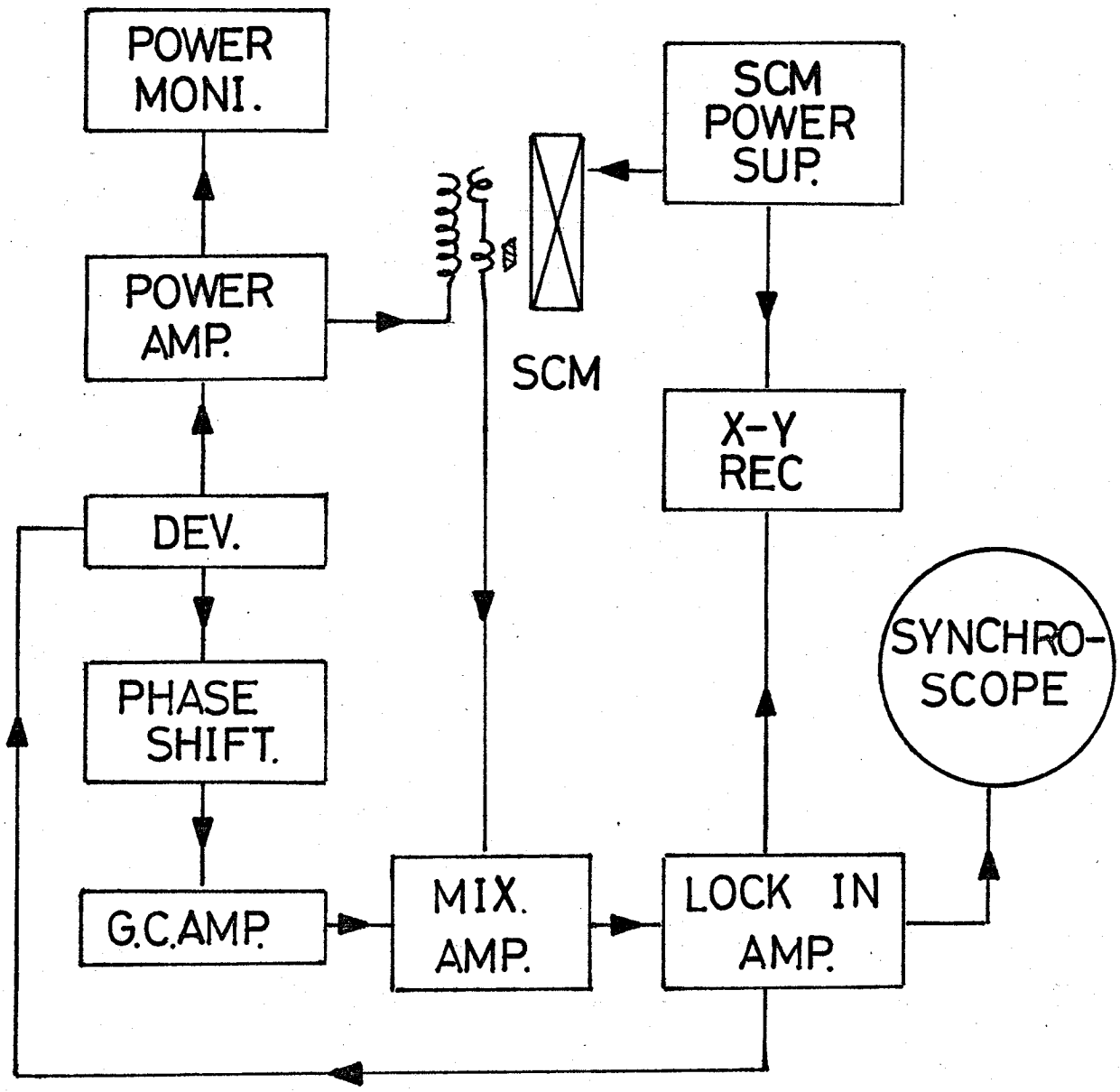

Fig. 11 Block Diagram of Magnetic Susceptibility Measurement Apparatus.

this case is done including the contribution due to the specimen. As the AC susceptibility of $CeCl_3.7H_2O$ at ν = 1 kHz has magnetic field dependence giving sharply non-zero contribution only around the several special values of magnetic field, we compensated all the contributions to the pick up coil except there and then detected the non-zero induced voltage proportional to the susceptibility of the sample at the crossing field.

The compensation signal is amplified by the PAR lock-in amplifier Model 124 with the plug-in preamplifier Model 117. The out put of the lock-in amplifier is recorded on X-Y recorder.

Chapter III EXPERIMENTAL RESULTS

§3.1 Zero Field Susceptibility

In order to establish the spin pair model proposed by Weber et al., we observed the zero field susceptibility of $CeCl_3.7H_2O$, in wide range of temperatures.

In the liq. He^4 temperatures, the susceptibility is measured by using the sigle crystal specimen.

In the lower temperatures, the powdered specimen is used, taking account of the advantage for thermal contact among the coolant, the specimen and the thermometer. The temperature below 1 K is obtained by the adiabatic demagnetization of the CrK alum. About two hundred of copper wires are used as the thermal link between the CrK alum and the sample. The temperature of the specimen is measured by the Speer 220Ω carbon resistor thermometer. The resistor is also linked by about fifty of copper wires. All of the wires have the diameter of 0.1 mm. The susceptibility is measured by using the AC Hartshorn bridge with the frequency ν = 26 Hz. Under this experimental condition, as the specimen is fixed in the coil, the absolute value of the susceptibility is calibrated from that in the liq. He^4 temperatures.

These experimental results are shown in Fig. 12.

On the other hand, from the molecular field theory discussed in §4.1, the zero field susceptibility is expressed as follows,

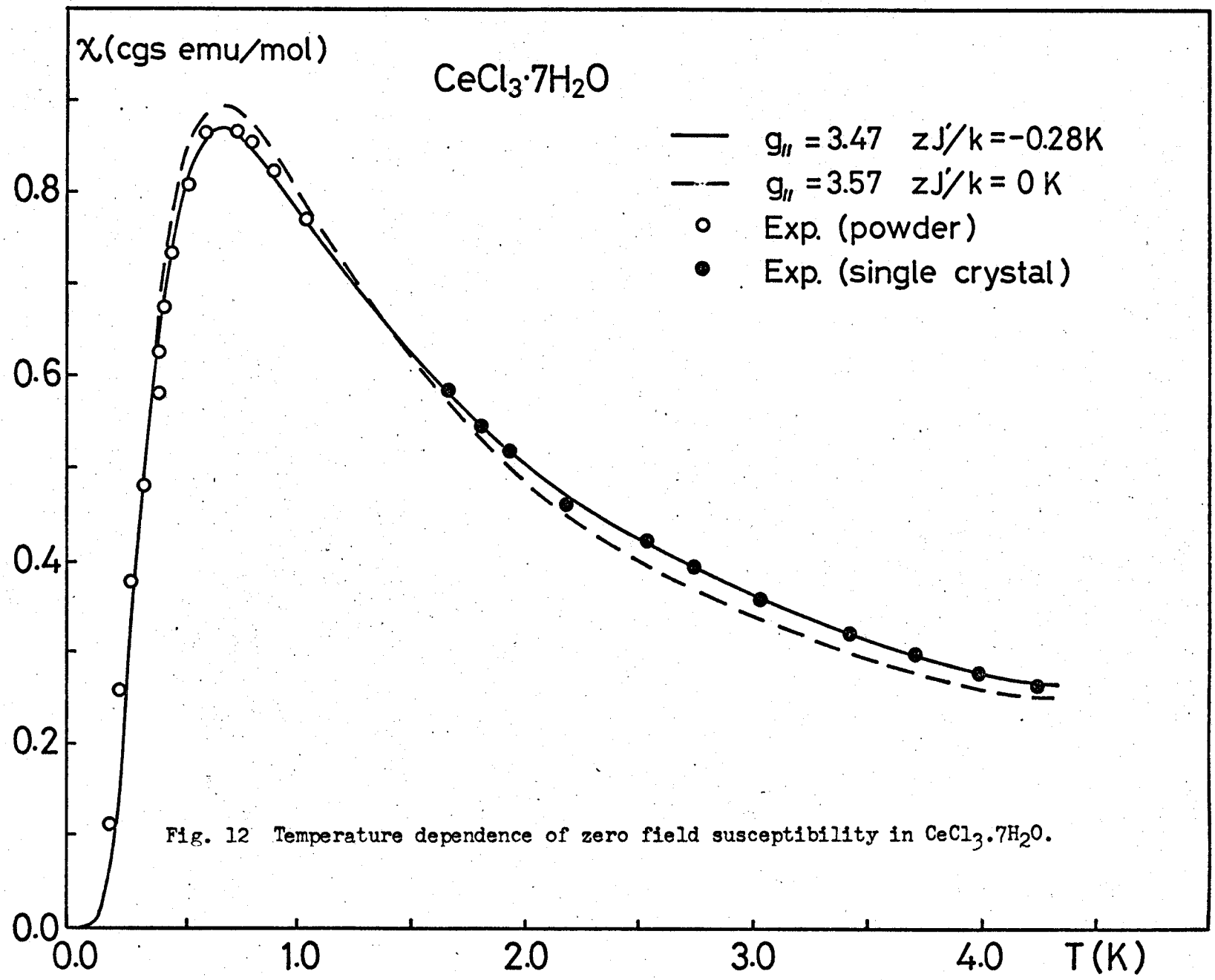

Fig. 12 Temperature dependence of zero field susceptibility in $CeCl_3.7H_2O$.

$$\chi = N g_{//}^2 \mu_B^2 \cdot \frac{2}{k_B T (\exp J/kT + 3) + zJ'} \qquad (26)$$

where J and J' represent, respectively, the intra- and the inter-pair exchange interaction constant and N, z and $g_{//}$ give, respectively, the total number of spin-pair, the number of interacting neighbors and g-value associated with χ_2-axis.

First, assuming J' = 0, we obtained the values J/k = 1.08 K and $g_{//}$ = 3.57 from the fitting the observed susceptibility to above equation. The result is represented by the dotted line in Fig. 12. In this fitting, several systematic deviations were found between the calculated and the experimental result.

It is found that these deviations are almost removed by setting the inter-pair interaction, zJ'/k = - 0.28 K, which corresponds the value obtained from the susceptibility measurements at the crossing point, which are described in §3.2. In this case, we obtain the values J/k = (1.08±0.02) K , (zJ'/k = - 0.28 K) and $g_{//}$ = (3.47 ± 0.02). The result is represented by the solid line in Fig. 12. These values for J/k and $g_{//}$ are slightly smaller than those obtained by Weber et al. They reported the following values,

$g_{//}$ = 3.60 (ESR and Zero Field Susceptibility),[6]

J/k = (1.16 ± 0.05) K (Cross Relaxation)[3]

and J/k = (1.20 ± 0.06) K (Specific Heat).[2]

We remark the following facts. Their experiments are performed in liq. He^4 temperatures and/or above, On the other hand, our experiment is performed in wide range of temperatures including below 1 K. Furthermore, our result is analized by

taking account of the inter-pair interaction. From the consideration mentioned above, the values obtained by us are more reliable than theirs. At the same time, the weakly ferromagnetically interacting spin pair model is demonstrated from our measurements.

§3.2 Susceptibility at the Crossing Point

In order to know the strength of the inter-pair interaction, the temperature dependence of the AC susceptibility at the point of the level crossing was observed using the AC exciting current with the frequency ν = 1 kHz. The plot, $1/\chi$ vesus T is shown in Fig. 13.

For the non interacting spin-pair system, the calculated results of the field dependence of the isothermal and the adiabatic susceptibility are shown in Figs. 14 and 15, respectively, with the various reduced temperatures. Far from the point of the level crossing, the adiabatic susceptibility decreases as the temperature decreases. However, in the vicinity of the point of the level crossing, the adiabatic susceptibility increases as the temperature decreases. Furthermore, in this case, the adiabatic susceptibility becomes nearly equal to the isothermal susceptibility at the sufficiently low tempertures. In Fig, 13. the solid and the dotted line correspond to, respectively, the isothermal and the adiabatic susceptibility at the crossing point. At the temperature lower than T $\sim$0.4 K, these two susceptibilities are represented by the Curie law.

Figure 13 shows the inverse AC susceptibilities whose individual corresponds to the peak value at the crossing point on χ - H curve in the course of the natural warming up of the temperature after the adiabatic demagnetization cooling. To control the temperature of the specimen, the manganin heater is used in some temperature ranges. To cover the wide temperature ranges, the measurements are repeated with overlap for several

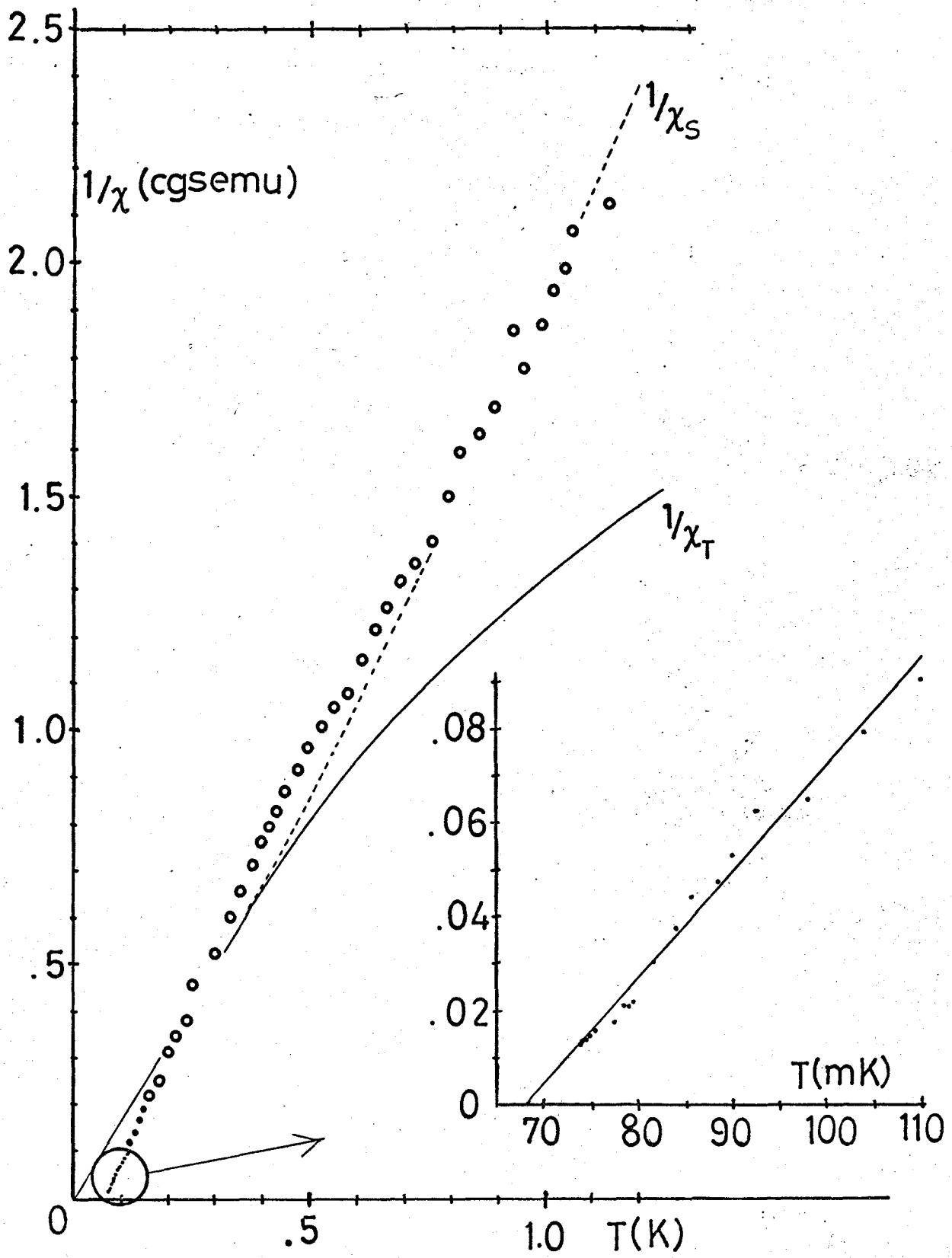

Fig. 13 $1/\chi$ - T plot of $CeCl_3.7H_2O$ at the crossing point.

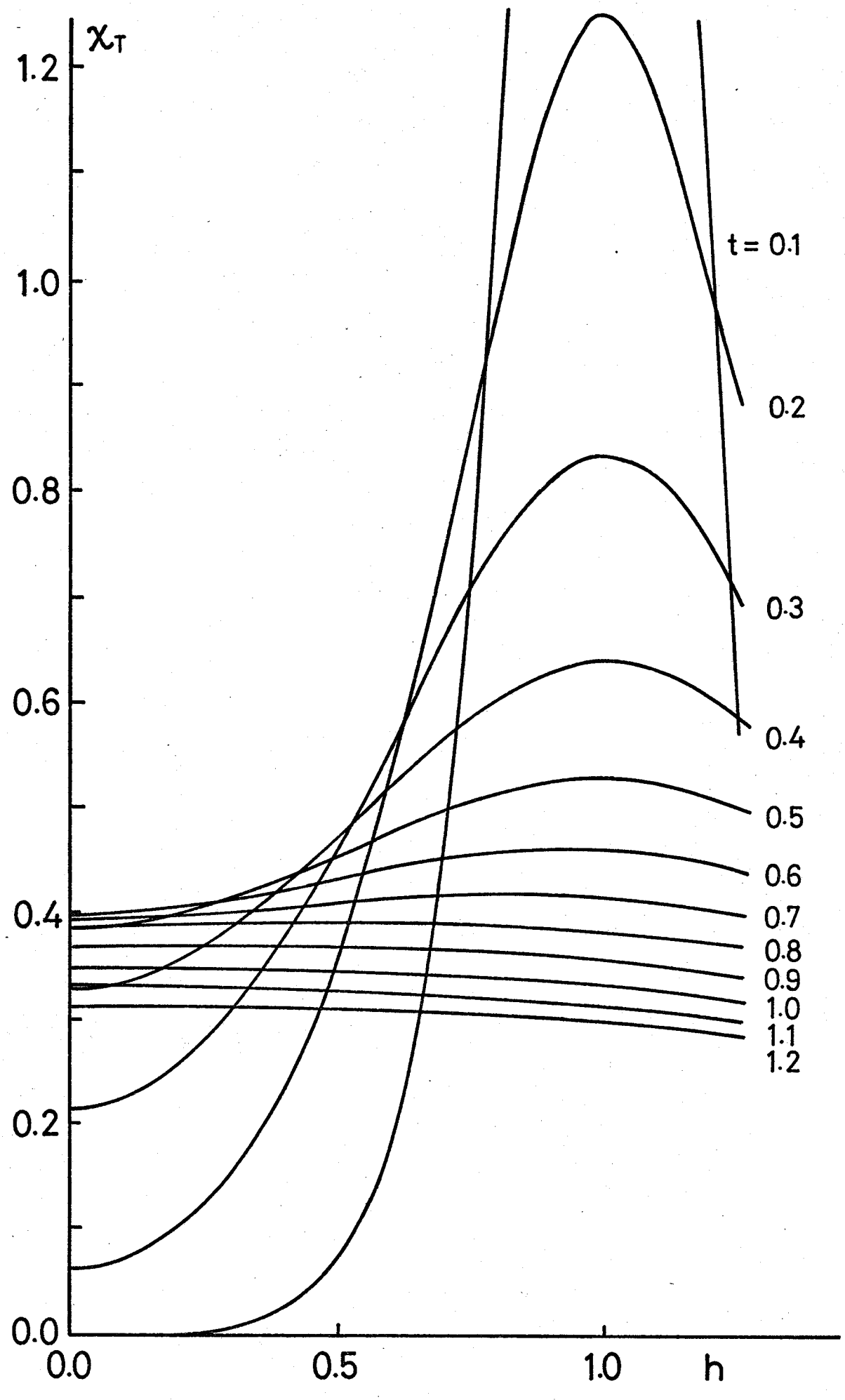

Fig. 14 Field dependence of calculated isothermal susceptibility.

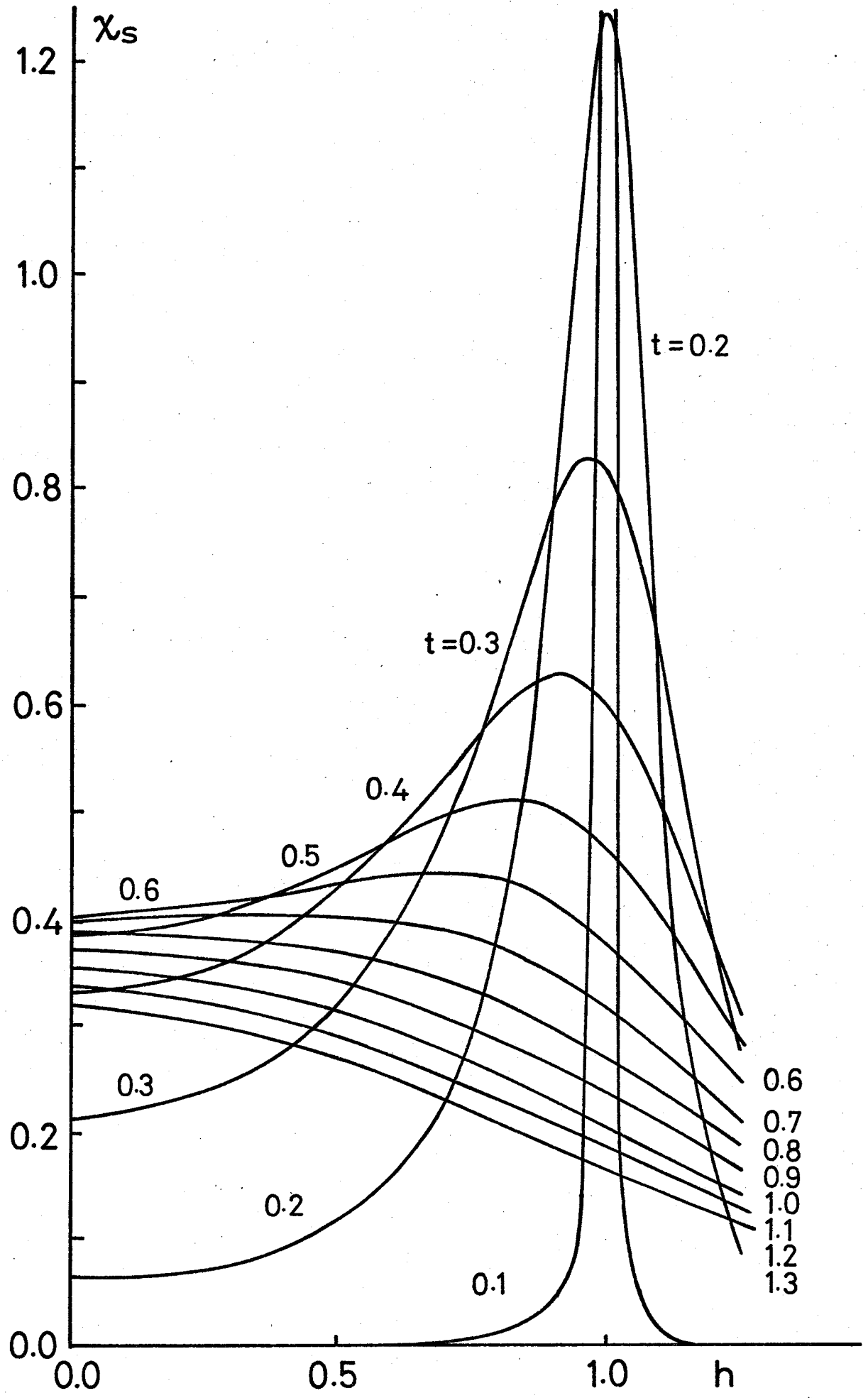

Fig. 15 Field dependence of calculated adiabatic susceptibility.

runs. To reduce the eddy current heating which disturbs the exact temperature measurement, the magnitude of the exciting AC field is depressed to about 0.05 Oe. The magnitude of the susceptibility varies over sixty times within the measuring temperature range. Therefore, it is very difficult that the absolute value of the susceptibility is calibrated in the liq. He temperature ranges.

At low temperatures, the experimental results are represented by the Curie-Weiss law. The Curie-Weiss temperature is ferromagnetic and nearly equal to 68 mK. From the comparison of the result with the Tachiki et al.'s theory, we are possible to conclude that the effective exchange inter-pair interaction α parallel to the field is ferromagnetic and nearly equal to 136 mK.

§3.3 Isentropic Curves

Noting that the zero field energy level splitting of $\Delta E/k = 1.1$ K is rather small, we used the conventional demagnetization method to cool the specimen.

The preliminary result in the powdered $CeCl_3.7H_2O$ is shown in Fig. 16. Although Ce^{3+} ions in the sample have the very large anisotropy in g-tensor, the appreciable cooling is observed. Under the initial condition, $T_i = 1.5$ K and $H_i = 30$ kOe, the cooling curve has a minimum at the field slightly above 5 kOe.

The density of the spin-pairs in $CeCl_3.7H_2O$ is nearly equal to that of Ce^{3+} ions in $Ce_2Mg_3(NO_3)_{12}.24H_2O$ (CMN), which is well known as the most ideal paramagnetic salt to obtain the lowest temperature by adiabatic demagnetization. The magnetic heat capacity of $CeCl_3.7H_2O$ is as small as CMN, because it is proportional to the magnetic ion density of the salt. Therefore, it was necessary to use a proper salt as a heat guard for the present experiment to cool such a magnetically dilute specimen and to maintain the reached low temperature. From this reason, we used the CrK alum heat guards as described in §2.3. For the simplicity of the experimental apparatus, the specimen and its heat guards are demagnetized by using, respectively, the central and the fringing field of the same magnet. The thermal protection of the specimen is most important in the vicinity of the level crossing field of $H \simeq 4.71$ kOe, where the lowest temperature of the specimen is attained. When the adiabatic demagnetization to the crossing field is

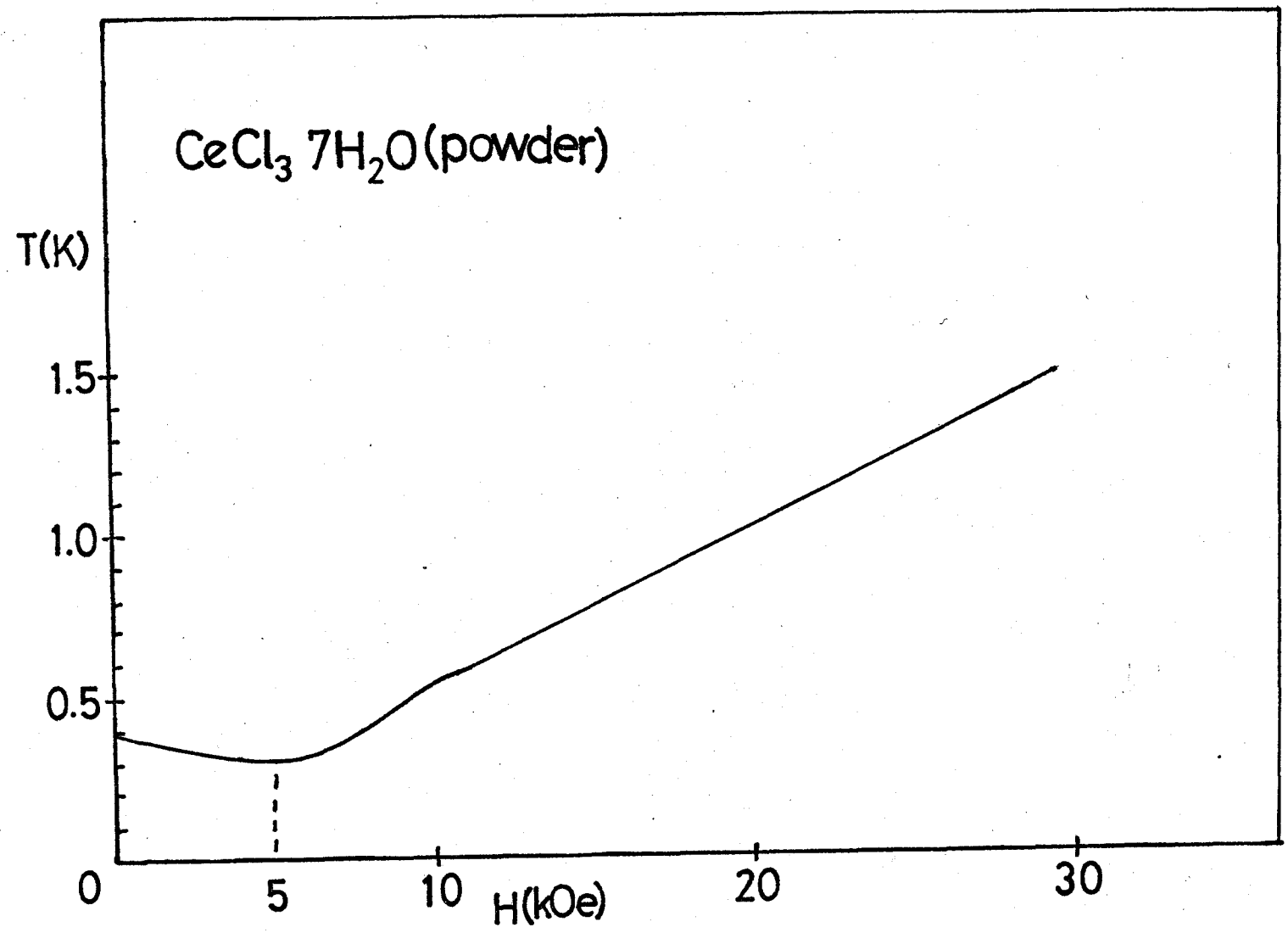

Fig. 16 Experimental adiabatic cooling curves in powdered $CeCl_3.7H_2O$.

performed with the initial condition of H_i = 45 kOe and T_i = 1.2 K, the temperature of the heat guard is expected to be enough low temperature about 0.15 K.**

This remaining fringing field of the order of a few killo oersted has the following advantage from the experimental point of view. First, it keeps the heat capacity of the guard salt large. Second, the susceptibility measurement of $CeCl_3 \cdot 7H_2O$ is not disturbed by the guard salts under the existence of the fringing field.

We perform the adiabatic demagnetization cooling of the single crystal specimen from the initial conditions of T_i = 1.2 K and $H_i \leqq 48$ kOe, by using the heat guard mentioned above. The results under the several initial conditions are shown in Fig. 17. The minimum temperature of about 68 mK is observed. An anomaly that the bottom of the cooling curve becomes flat is found. We can draw the boundary line so as to enclose the flat part of the curves, which is represented by the dotted line in Fig. 17. This indicates that the spin ordering occurs inside the boundary line. The results from the lower initial

---

** This value is estimated from the following approximate relation, $T_f = T_i(H_f/H_i)$. In this equation, H_i and H_f represent, respectively, the initial and the final value of the fringing field. But the ratio of the fringing field to the central field is the geometrical constant. Therefore, it is possible to replace the values of H_i and H_f by those of the central field of the magnet.

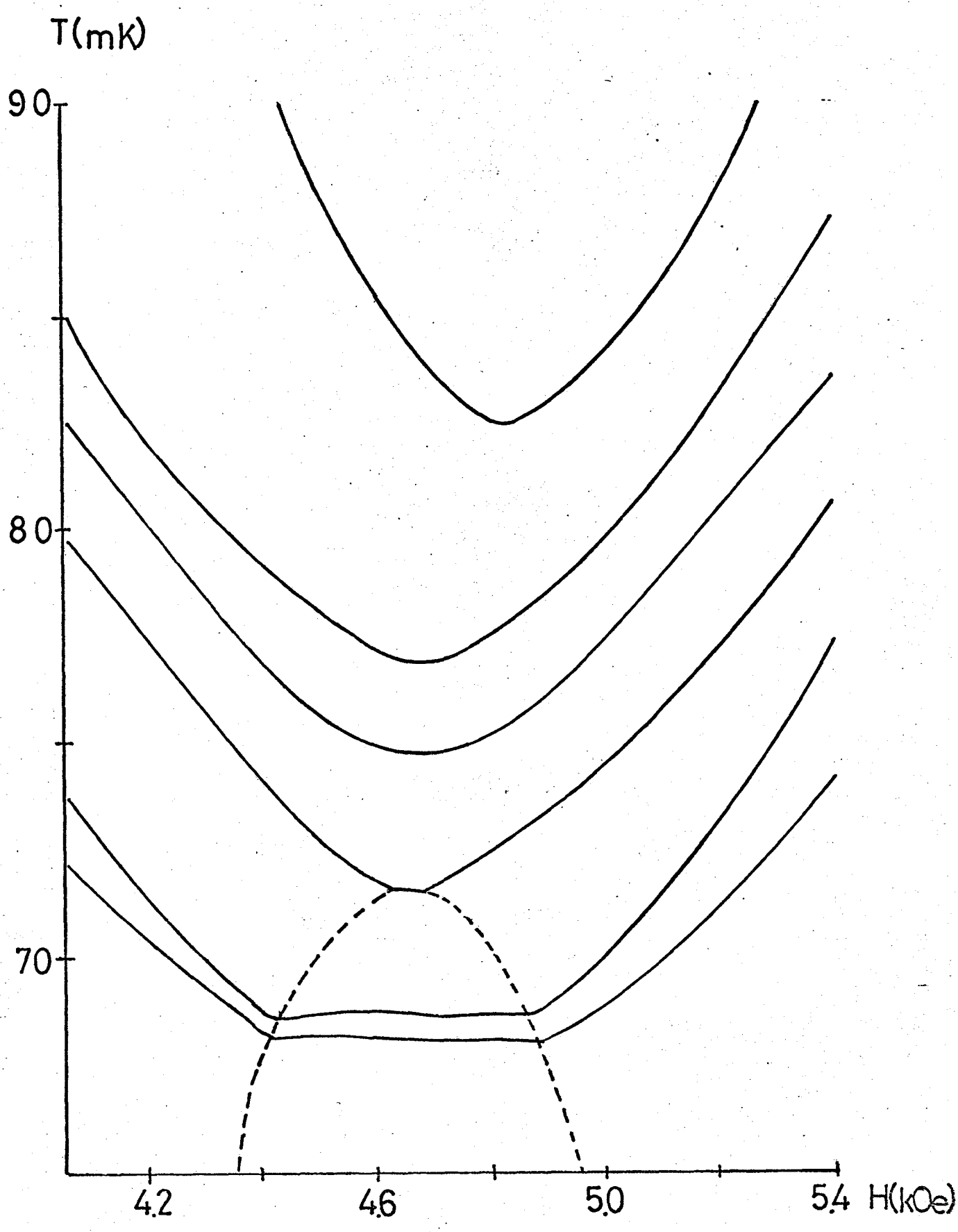

Fig. 17 Experimental adiabatic cooling curves at low temperatures.

magnetic field are shown in Fig. 18, for the purpose of comparing the results with those calculated theoretically.

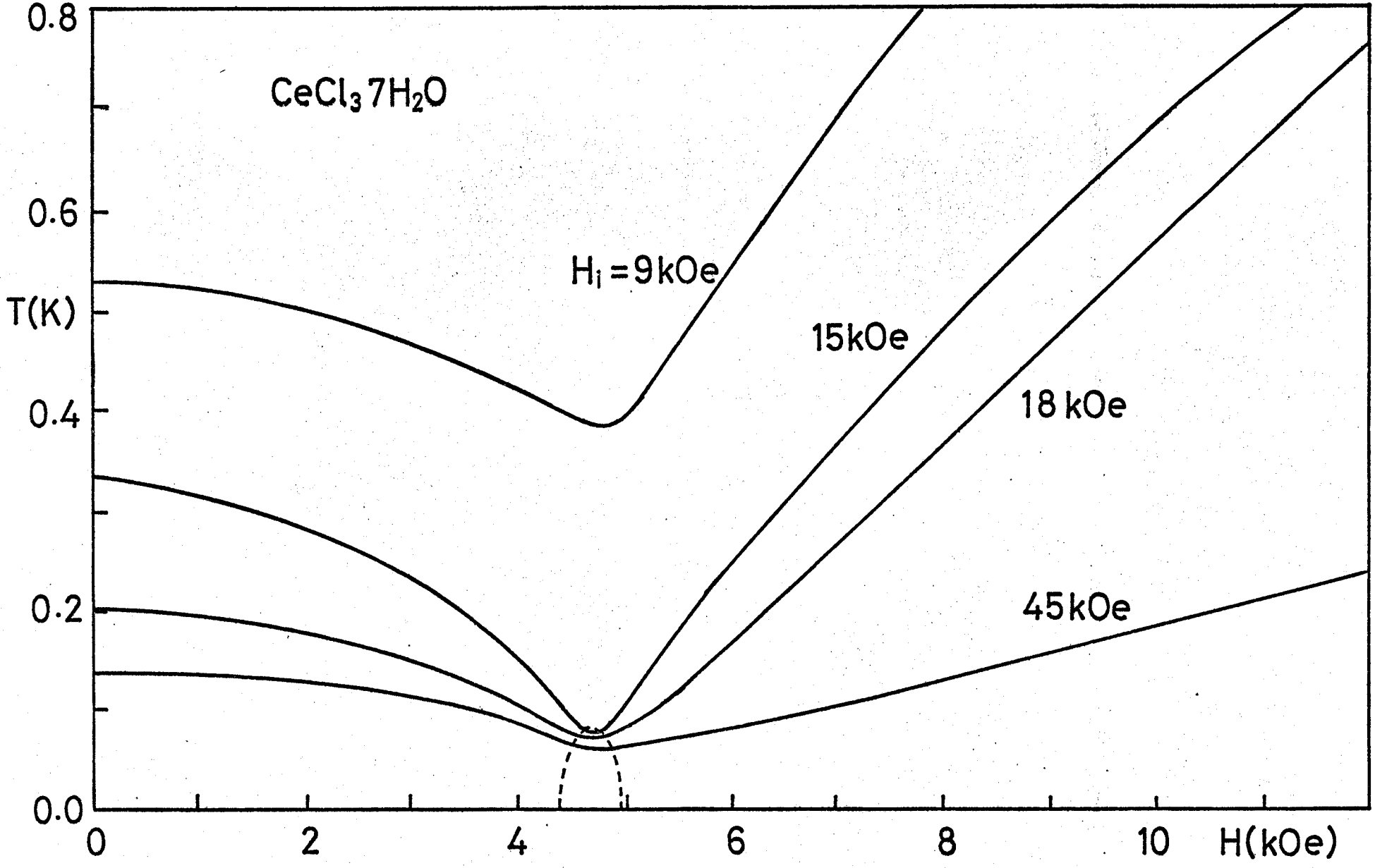

Fig. 18 Experimental adiabatic cooling curves from lower initial magnetic field.

§3.4 AC Susceptibility in Isentropic Process

From the results which are described in the preceding two sections, we can presumally expect the appearance of the ordered state in the system of $CeCl_3.7H_2O$ at the temperatures $T \lesssim 72$ mK, near the level crossing field. For the case of $Cu(NO_3)_2.2.5H_2O$, as described later, drastic change appears in the field dependence of the susceptibility, when the system approaches to the ordered state.

One of the results of AC susceptibility measurements with the frequency $\nu = 1$ kHz is shown in Fig. 19, where the horizontal axis, that is, H-axis is expanded to make clear the shape of the susceptibility, and the minimum temperature $T \cong 68$ mK.

This field dependence is very resemble to those at higher temperatures, except the maximum field value decreases slightly by about 50 Oe from the value at $T = 1.2$ K. In comparison with the cooling curves, the shape of the susceptibility is smooth at the vicinity of the points where the cooling curve bends. We remark the next two points for the reason to this tendency. It may be related with the relaxation effect, although no frequency dependence of the susceptibility has been observed at low temperature in the frequency ranges from 200 Hz to 10 kHz. As other possible reason, it may be due to the character of the inter-pair interaction, such as the ratio to intra-pair one in the strength, the sign, or the measure of low-dimensionality.

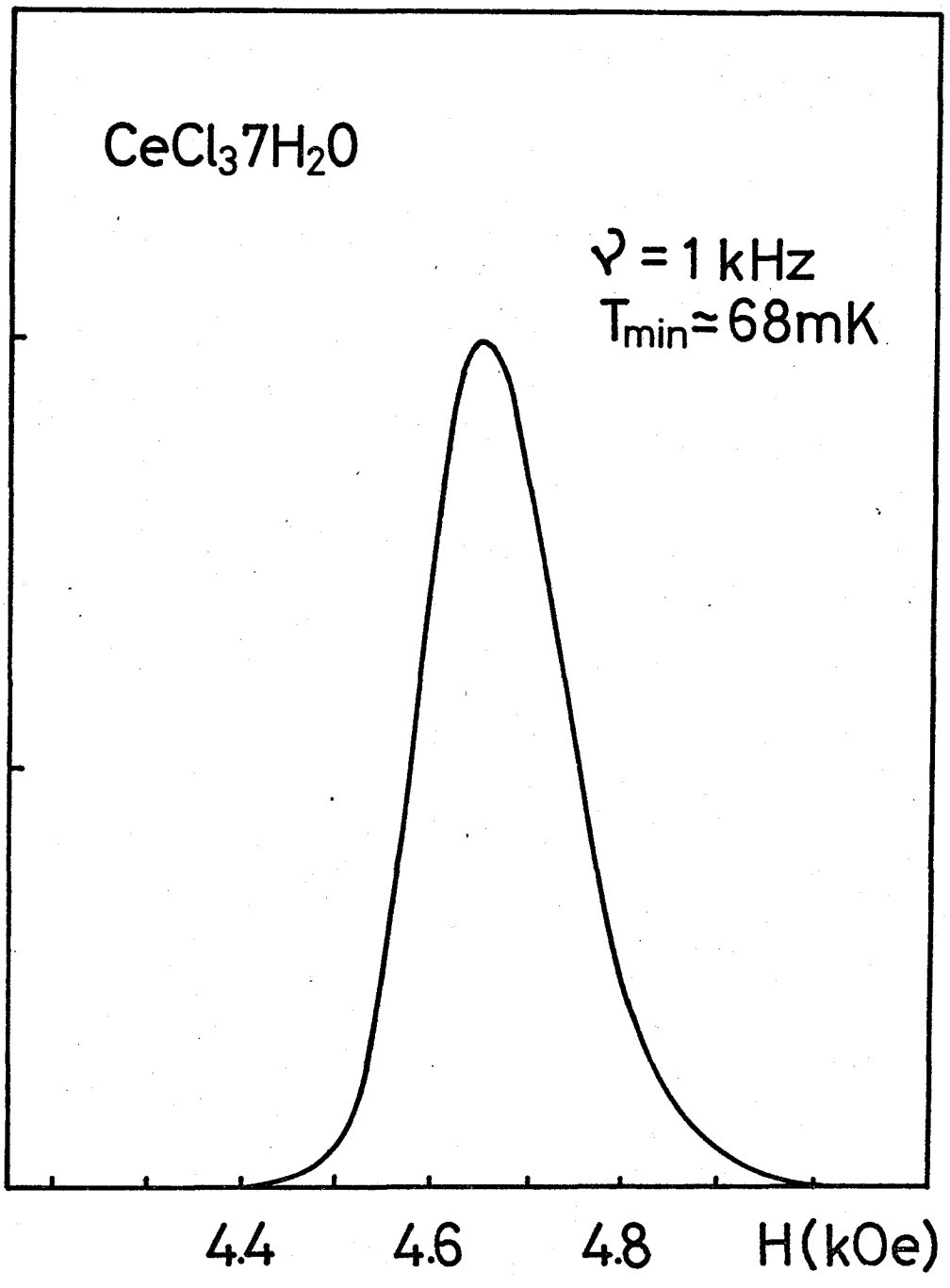

Fig. 19 AC Susceptibility in Isentropic Process.

Chapter IV MOLECULAR FIELD THEORY

§4.1 Several Formulae

For the comparison with the experimental results, including the effect of the upper two levels, we discuss the several thermodynamical properties in the spin pair system. The Hamiltonian for the isolated pair is assumed as follows

$$\mathcal{H}_0 = J\sum_i \Delta_{i1}\cdot\Delta_{i2} + g_{/\!/}\mu_B H\sum_i(\Delta_{zi1}+\Delta_{zi2}). \tag{27}$$

For the inter-pair interaction, again we assume the form

$$\mathcal{H}' = -|J'|\sum_{\langle i,j\rangle}(\Delta_{i1}\cdot\Delta_{j1}+\Delta_{i2}\cdot\Delta_{j2}). \tag{28}$$

In the same way as §1.2, we obtain the following effective Hamiltonian

$$\mathcal{H}_{eff} = J\Delta_{i1}\cdot\Delta_{i2} + g_{/\!/}\mu_B H(\Delta_{z1}+\Delta_{z2})+\frac{1}{2}z|J'|\{m(\Delta_{z1}+\Delta_{z2})-n(\Delta_{x1}-\Delta_{x2})\}, \tag{29}$$

where

$$-m = \langle\Delta_{z1}+\Delta_{z2}\rangle = 2\langle\Delta_{z1}\rangle = 2\langle\Delta_{z2}\rangle, \tag{30}$$

and

$$n = \langle\Delta_{x1}-\Delta_{x2}\rangle = 2\langle\Delta_{x1}\rangle = -2\langle\Delta_{x2}\rangle. \tag{31}$$

Noting the relations,

$$(\Delta_{z1}+\Delta_{z2})\frac{1}{\sqrt{2}}(\alpha_1\beta_2+\beta_1\alpha_2) = 0, \tag{32}$$

and

$$(\Delta_{x1}-\Delta_{x2})\frac{1}{\sqrt{2}}(\alpha_1\beta_2+\beta_1\alpha_2) = 0, \tag{33}$$

and taking the states $\alpha_1\alpha_2$, $\frac{1}{\sqrt{2}}(\alpha_1\beta_2-\beta_1\alpha_2)$, $\beta_1\beta_2$, $\frac{1}{\sqrt{2}}(\alpha_1\beta_2+\beta_1\alpha_2)$, as base vectors, we obtain the following matrix representation for H_{eff}

$$H_{eff} = J \begin{bmatrix} f & g & 0 & \\ g & -1 & -g & \\ 0 & -g & -f & \\ & & & 0 \end{bmatrix}, \tag{34}$$

where $f = h + \lambda m$, $g = \lambda n$, $h = g \mu_B H/J$ and $\lambda = \frac{1}{2} z |J'| /J$. Now, for the simlicity of the description, we assumed that J is equal to unity, in other words, we adopt the exchange constant J as the unit of the energy. Then, the secular equations for H_{eff} are

$$\varepsilon^3 - \varepsilon^2 - (f^2 + g^2)\varepsilon^2 - f^2 = 0 \quad (\varepsilon = \varepsilon_1, \varepsilon_2, \varepsilon_3),$$

and (35)

$$\varepsilon = 0 \quad (\varepsilon = \varepsilon_4).$$

Using these energy eigen values, the free energy per spin pair is expressed as follows,

$$F = -t \left\{ \ln \left(\sum_j e^{-\frac{\varepsilon_j}{t}} \right) \right\} + \frac{1}{2}\lambda (m^2 + n^2), \tag{36}$$

where t represents the reduced temperature kT/J, the last term $\frac{1}{2}\lambda(m^2 + n^2)$ is the compensation term for twice counting of the inter-pair interaction.

The equilibrium values for m and n are determined by minimizing the free energy (36) with respect to them. Thus, the self-consistent equations are obtained as follows,

$$m = \left\langle -\frac{\partial \varepsilon_j}{\partial f} \right\rangle, \tag{37}$$

and

$$n = \left\langle -\frac{\partial \varepsilon_j}{\partial g} \right\rangle, \tag{38}$$

where the bracket $\langle\ \rangle$ represents the following quatity

$$\langle \Phi(\varepsilon_j)\rangle = \sum_j \Phi(\varepsilon_j)\, e^{-\varepsilon_j/t}/Z \tag{39}$$

The derivatives $\frac{\partial \varepsilon_j}{\partial f}$, $\frac{\partial \varepsilon_j}{\partial g}$ are expressed as follows,

$$\left.\begin{aligned} \frac{\partial \varepsilon}{\partial f} &= \frac{2f(\varepsilon+1)}{3\varepsilon^2+2\varepsilon-(f^2+g^2)} \\ \frac{\partial \varepsilon}{\partial g} &= \frac{2g\varepsilon}{3\varepsilon^2+2\varepsilon^2-(f^2+g^2)} \end{aligned}\right\} \quad (\text{for } \varepsilon=\varepsilon_1,\varepsilon_2,\varepsilon_3), \tag{40}$$

and $\frac{\partial \varepsilon}{\partial f} = \frac{\partial \varepsilon}{\partial g} = 0$ $\qquad$ (for $\varepsilon=\varepsilon_4$).

The entropy s is expressed as follows,

$$\mathcal{S} = -\sum_j p_j \ln p_j = \ln Z + \frac{1}{t}\langle \varepsilon_j\rangle , \tag{41}$$

where p_j represents $e^{-\varepsilon_j/t}/Z$.

From the definition of the bracket $\langle\ \rangle$, it is easy to identify the following formulae.

$$\left(\frac{\partial}{\partial t}\right)_{f,g}\langle\Phi(f,g,t)\rangle = \langle\frac{\partial\Phi}{\partial t}\rangle + \frac{1}{t^2}\left\{\langle\Phi\cdot\varepsilon_j\rangle - \langle\Phi\rangle\langle\varepsilon_j\rangle\right\},$$

$$\left(\frac{\partial}{\partial f}\right)_{g,t}\langle\Phi(f,g,t)\rangle = \langle\frac{\partial\Phi}{\partial f}\rangle - \frac{1}{t}\left\{\langle\Phi\frac{\partial\varepsilon_j}{\partial f}\rangle - \langle\Phi\rangle\langle\frac{\partial\varepsilon_j}{\partial f}\rangle\right\}, \tag{42}$$

and $$\left(\frac{\partial}{\partial g}\right)_{f,t}\langle\Phi(f,g,t)\rangle = \langle\frac{\partial\Phi}{\partial g}\rangle - \frac{1}{t}\left\{\langle\Phi\frac{\partial\varepsilon_j}{\partial g}\rangle - \langle\Phi\rangle\langle\frac{\partial\varepsilon_j}{\partial g}\rangle\right\}.$$

Using these formulae, and taking into account the relations (37), (38), (40) and (41), we obtain the following relations,

$$\begin{bmatrix} \left(\frac{\partial m}{\partial t}\right)_h \\ \left(\frac{\partial n}{\partial t}\right)_h \end{bmatrix} = R^{-1} \begin{bmatrix} \left(\frac{\partial m}{\partial t}\right)_{f,g} \\ \left(\frac{\partial n}{\partial t}\right)_{f,g} \end{bmatrix},$$

$$\begin{bmatrix} \left(\frac{\partial m}{\partial h}\right)_t \\ \left(\frac{\partial n}{\partial h}\right)_t \end{bmatrix} = R^{-1} \begin{bmatrix} \left(\frac{\partial m}{\partial f}\right)_{g,t} \\ \left(\frac{\partial n}{\partial g}\right)_{f,t} \end{bmatrix},$$

$$\left(\frac{\partial m}{\partial f}\right)_{g,t} = \left\langle -\frac{\partial^2 \varepsilon_j}{\partial f^2} \right\rangle + \frac{1}{t}\left\{ \left\langle \left(\frac{\partial \varepsilon_j}{\partial f}\right)^2 \right\rangle - \left\langle \frac{\partial \varepsilon_j}{\partial f} \right\rangle^2 \right\},$$

$$\left(\frac{\partial m}{\partial g}\right)_{f,t} = \left(\frac{\partial n}{\partial f}\right)_{g,t} = \left\langle -\frac{\partial^2 \varepsilon_j}{\partial f \partial g} \right\rangle + \frac{1}{t}\left\{ \left\langle \frac{\partial \varepsilon_j}{\partial f} \frac{\partial \varepsilon_j}{\partial g} \right\rangle - \left\langle \frac{\partial \varepsilon_j}{\partial f} \right\rangle \left\langle \frac{\partial \varepsilon_j}{\partial g} \right\rangle \right\},$$

$$\left(\frac{\partial n}{\partial g}\right)_{f,t} = \left\langle -\frac{\partial^2 \varepsilon_j}{\partial g^2} \right\rangle + \frac{1}{t}\left\{ \left\langle \left(\frac{\partial \varepsilon_j}{\partial g}\right)^2 \right\rangle - \left\langle \frac{\partial \varepsilon}{\partial g} \right\rangle^2 \right\}, \qquad (43)$$

$$\left(\frac{\partial m}{\partial t}\right)_{f,g} = \left(\frac{\partial \Delta}{\partial f}\right)_{g,t} = + \frac{1}{t^2}\left\{ \left\langle \varepsilon_j \right\rangle \left\langle \frac{\partial \varepsilon_j}{\partial f} \right\rangle - \left\langle \frac{\partial \varepsilon_j}{\partial f} \cdot \varepsilon_j \right\rangle \right\},$$

$$\left(\frac{\partial n}{\partial t}\right)_{f,g} = \left(\frac{\partial \Delta}{\partial g}\right)_{f,t} = + \frac{1}{t^2}\left\{ \left\langle \varepsilon_j \right\rangle \left\langle \frac{\partial \varepsilon_j}{\partial g} \right\rangle - \left\langle \frac{\partial \varepsilon_j}{\partial g} \cdot \varepsilon_j \right\rangle \right\},$$

$$\left(\frac{\partial \Delta}{\partial t}\right)_{f,g} = + \frac{1}{t^3}\left\{ \left\langle \varepsilon_j^2 \right\rangle - \left\langle \varepsilon_j \right\rangle^2 \right\},$$

and $$\left(\frac{\partial \Delta}{\partial t}\right)_h = \left(\frac{\partial \Delta}{\partial t}\right)_{f,g} + \lambda\left\{ \left(\frac{\partial m}{\partial t}\right)_h \left(\frac{\partial \rho}{\partial f}\right)_{g,t} + \left(\frac{\partial n}{\partial t}\right)_h \left(\frac{\partial \Delta}{\partial g}\right)_{f,t} \right\},$$

where R^{-1} represents the inverse matrix for

$$R = \begin{bmatrix} 1 - \lambda\left(\frac{\partial m}{\partial f}\right)_{g,t}, & -\lambda\left(\frac{\partial m}{\partial g}\right)_{f,t} \\ -\lambda\left(\frac{\partial n}{\partial f}\right)_{g,t}, & 1 - \lambda\left(\frac{\partial n}{\partial g}\right)_{f,t} \end{bmatrix}. \qquad (44)$$

The magnetic susceptibility observed under the adiabatic process is corresponding to the adiabatic susceptibility

$$\left(\frac{\partial m}{\partial h}\right)_\Delta = \left(\frac{\partial m}{\partial h}\right)_t - \left(\frac{\partial m}{\partial t}\right)_h^2 \Big/ \left(\frac{\partial \Delta}{\partial t}\right)_h . \qquad (45)$$

The formulae for the disordered phase, which is characterized by n = 0, are much simpler than those for the ordered phase descibed above. In fact, the following formulae can be obtained easily.

$$\varepsilon_1 = -f, \quad \varepsilon_2 = -1, \quad \varepsilon_3 = f \quad \text{and} \quad \varepsilon_4 = 0.$$

$$m = p_1 - p_3 .$$

$$\left(\frac{\partial m}{\partial t}\right)_h = \left(\frac{\partial m}{\partial t}\right)_f \Big/ \left\{1 - \lambda\left(\frac{\partial m}{\partial f}\right)\right\},$$

$$\left(\frac{\partial m}{\partial h}\right)_t = \left(\frac{\partial m}{\partial f}\right)_t \Big/ \left\{1 - \lambda\left(\frac{\partial m}{\partial f}\right)\right\},$$

$$\left(\frac{\partial m}{\partial f}\right)_t = \frac{1}{t}\left\{p_1 + p_3 - m^2\right\},$$

$$\left(\frac{\partial m}{\partial t}\right)_f = \left(\frac{\partial s}{\partial f}\right)_t = \frac{1}{t^2}\left\{f^2(p_1 + p_3) - \langle\varepsilon_j\rangle m\right\}, \tag{46}$$

$$\left(\frac{\partial s}{\partial t}\right)_f = \frac{1}{t^3}\left\{\langle\varepsilon_j^2\rangle - \langle\varepsilon_j\rangle^2\right\},$$

and $$\left(\frac{\partial s}{\partial t}\right)_h = \left(\frac{\partial s}{\partial t}\right)_f + \lambda\left(\frac{\partial m}{\partial t}\right)_h \left(\frac{\partial s}{\partial f}\right)_t .$$

Especially, zero field susceptibility is expressed as follows,

$$\chi = \frac{\frac{1}{t}\cdot\frac{2}{Z}}{1 - \lambda\frac{1}{t}\cdot\frac{2}{Z}} . \tag{47}$$

Rewriting this with the original units, we obtain the next form, which holds also in the case of antiferromagnetic interaction,

$$\chi = N g_{/\!/}^2 \mu_B^2 \frac{2}{k_B T(3 + \exp J/k_B T) + zJ'} . \tag{48}$$

§ 4.2 Absolute Zero

At the absolute zero temperature, providing $0 < \lambda < \frac{1}{2}$, the next three solutions are possible,

$$\begin{aligned} & m = 0 \quad \text{and} \quad n = 0 && (h < h_{c1}) , \\ & m = 1 \quad \text{and} \quad n = 0 && (h > h_{c2}) , \end{aligned} \tag{49}$$

$$\text{or} \quad m = h\{h^2 - (1 - 2\lambda)\}/(2\lambda)$$

$$\text{and} \quad n^2 = (1 - h^2)(h^2 - 1 + 2\lambda)(h^2 + 1 + 2\lambda)/(2\lambda)^2 \qquad (h_{c1} < h < h_{c2}) , \text{**} \tag{50}$$

where $h_{c1} = \sqrt{1 - 2\lambda}$ and $h_{c2} = 1$.

The former two solutions are disordered phases. The last solution is an ordered phase.

The reduced susceptibility $\chi = \partial m/\partial h$ is described as

$$\begin{aligned} & \chi = 0 && (h < h_{c1} \text{ or } h > h_{c2}) , \\ & \chi = \{3h^2 - (1 - 2\lambda)\}/(2\lambda) && (h_{c1} < h < h_{c2}) . \end{aligned} \tag{51}$$

Thus, the phase transitions which occur at $h = h_{c1}$ and $h = h_{c2}$, are second order with respect to the magnetic field.

In this case, as the entropy of the system is also zero, the adiabatic susceptibility is also expressed by above equation.

** In the limit as $\lambda \to 0$, this solution is expressed as follows,

$$m = h/\lambda \qquad (h_{c1} < h < h_{c2})$$

where $h_{c1} = 1 - \lambda$ and $h_{c2} = 1$.

This corresponds to the result obtained in § 1.3 .

§4.3 Phase Boundary and Isentropic Curves

Assuming that the phase transition is of the second order, we are possible to obtain the phase boundary in the following way. The ordered phase is characterized by $n \neq 0$, and the disordered phase is characterized by $n = 0$. Therefore, the second order phase boundary is obtained by limiting n to zero in the ordered phase. From eq.(34), by using the first order perturbation with respect to n, we obtain the following equation

$$n = \frac{\lambda n}{1+f}(p_2 - p_1) + \frac{\lambda n}{1-f}(p_2 - p_3),$$

or

$$\frac{1}{\lambda} = \frac{1}{1+f}(p_2 - p_1) + \frac{1}{1-f}(p_2 - p_3). \tag{52}$$

In this limit, the quantities p_j are expressed as follows,

$$p_1 = e^{-\beta f}/Z, \quad p_2 = e^{\beta}/Z, \quad p_3 = e^{\beta f}/Z, \quad p_4 = 1/Z, \tag{53}$$

where

$$Z = 1 + e^{\beta f} + e^{-\beta f} + e^{\beta}. \tag{54}$$

Assuming $\lambda = 0.125$, the phase boundary obtained from this equation is shown in Fig. 20 as a dotted line. The curve is nearly symmetric with respect to the line $h = 0.934$, where the transition temperature have a maximum, $t_{c\ max} \simeq 0.0646$.

Again, assuming $\lambda = 0.125$, we obtain the isentropic curves for the several values of the entropy, which are shown in Fig. 20 . The overall feature of the isentropic curves are shown also in Fig. 21. The curve in the ordered phase is expressed by the nearly straight line having small negative slope.

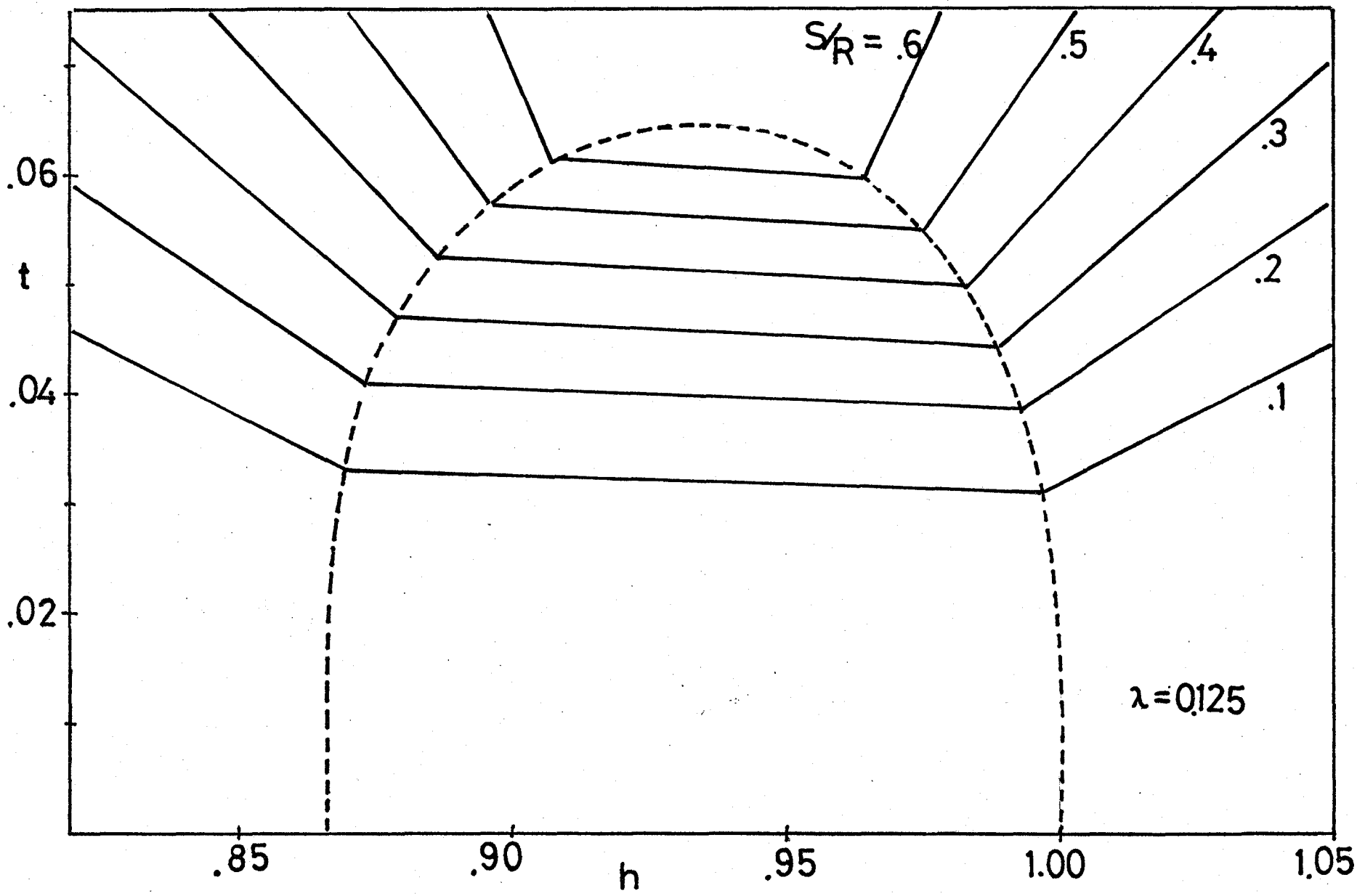

Fig. 20 Phase boundary and isentropic curves for spin pair system calculated by assuming $\lambda = 0.125$.

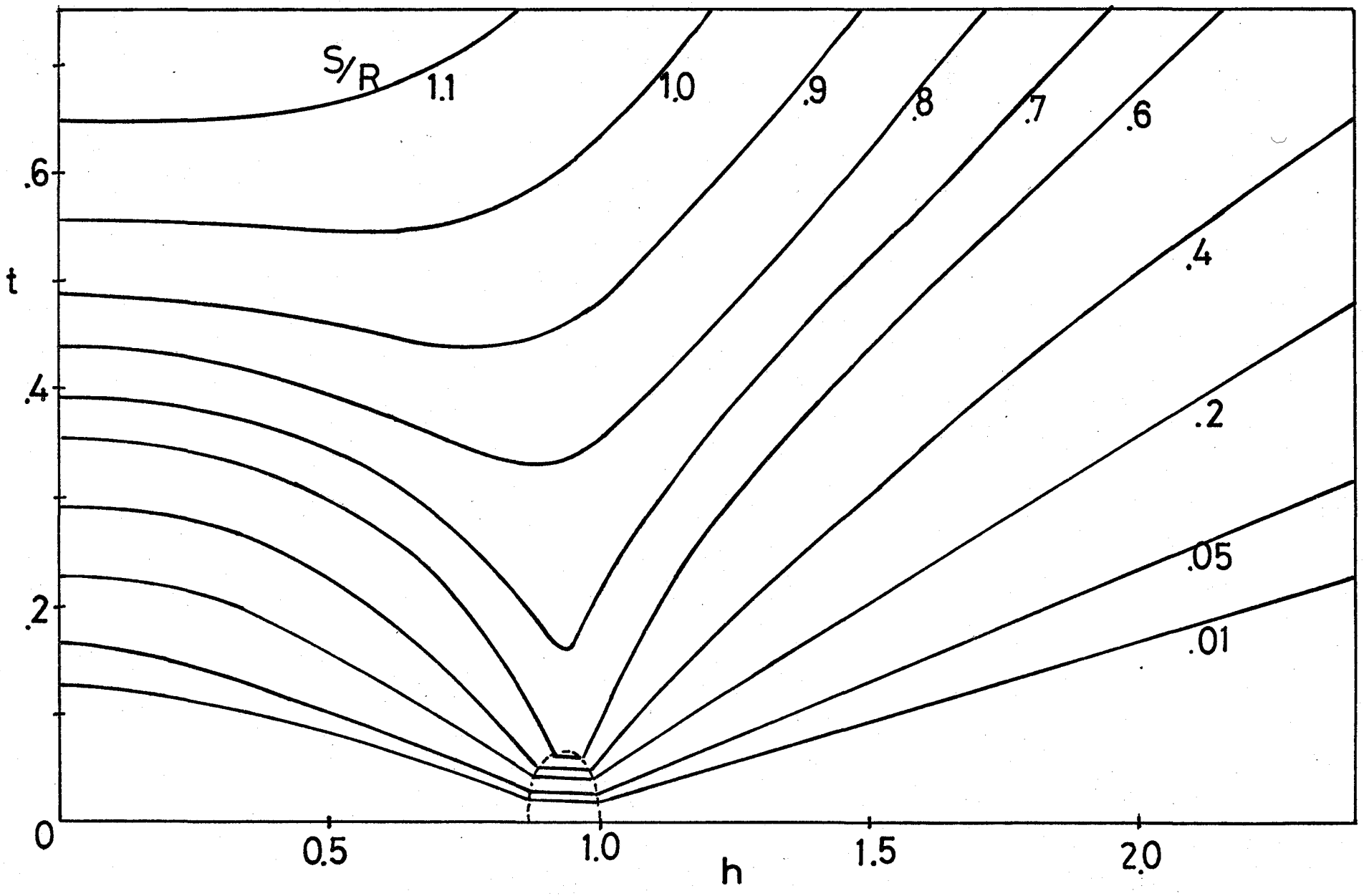

Fig. 21 Overall feature of isentropic curves for spin pair system calculated by assuming $\lambda = 0.125$.

§4.4 Adiabatic Susceptibility

Using the formulae in §4.1, we can obtain the adiabatic susceptibility along the isentropic process. Again assuming $\lambda = 0.125$, we obtain the results shown in Fig. 22.

Also at the finite temperature, the adiabatic susceptibility of the ordered phase is nearly equal to that at the absolute zero. The adiabatic susceptibility in the disordered phase, is strongly dependent on the values of the field and temperature, therefore the temperature variation along the isentropic process is taken into account.

In the case, $S/R \gtrsim 0.693$, the system is not entered into the ordered phase, and the adiabatic susceptibility becomes more sharp as the entropy values becomes lower.

On the other hand, in the case, $S/R \lesssim 0.693$, the system is entered into the ordered phase within a certain range of the field values, where the adiabatic susceptibility is nearly equal to that at the absolute zero temperature as already described. In this case, the adiabatic susceptibility in the disordered phase makes small broad maximum and tends to zero towards the phase boundary.

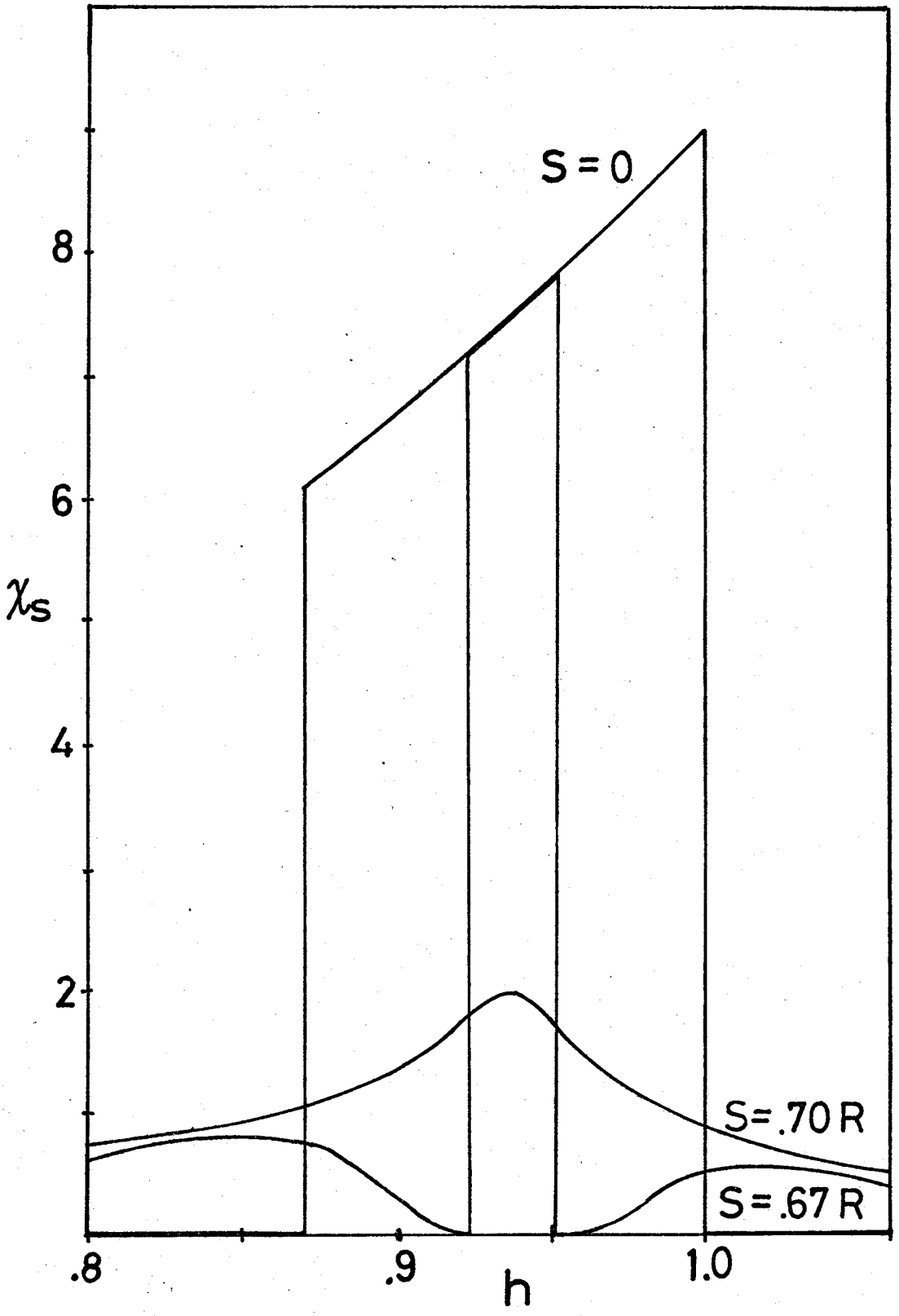

Fig. 22 Field dependence of adiabatic susceptibility along isentropic process calculated by assuming $\lambda = 0.125$.

Conclusion

We study experimentally the magnetic cooling and phase transition in spin pair system with singlet ground state, $CeCl_3.7H_2O$.

We perform successfully the adiabatic demagnetization with the initial condition, H_i = 48 kOe and T_i = 1.2 K. The cooling curve is obtained with the minimum temperature of 68 mK around the energy level crossing field of 4.7 kOe. The susceptibility at the crossing field is represented by the Curie-Weiss law with the ferromagnetic Curie-Weiss temperature of 68 mK in sufficiently low temperature region. This is consistent with the temperature dependence of the zero field susceptibility. It is found that the bottom of the cooling curve becomes flat around the crossing field at the temperature below 72 mK. From this fact, it is concluded that the spin ordering occurs around the crossing field at the temperatures lower than the critical temperature of 72 mK.

The field dependence of the observed AC susceptibility is very resemble to that at higher temperature, except the maximum field value decreases slightly by about 50 Oe from the value at 1.2 K. In comparison with the cooling curves, the shape of the susceptibility is smooth at the vicinity of the points where the cooling curve bends. The possible reasons for this tendency are pointed out.

REFERENCES

1) K.H.Hellwege, R.von Klot and G.Weber : Phys. kondens. Materie 2(1964)397.

2) S.Hüfner, R.v.Klot, F.Küch and G.Weber : Z. Naturforsch. A 22(1967)1999.

3) R.von Klot and G.Weber : Z. Phys. 209(1968)380.

4) M.Tachiki and T.Yamada : J. Phys. Soc. Japan 28(1970)1413; M.Tachiki and T.Yamada : Progr. theor. Phys. 46(1970) Suppl. p291.

5) Weitz (unpublished) See Ref. 1.

6) K.H.Hellwege, R.v.Klot, P.Kronuer, G.Schafer, S.Scheller and G.Weber (unpublished) See Ref. 3.

Part II Pulsed Adiabatic Magnetization in $Cu(NO_3)_2.2.5H_2O$

Chapter I INTRODUCTION

Most of experiments on magnetic cooling such as adiabatic demagnetization have been performed using a conventional electromagnet, or a superconducting solenoid. The sweep speed of the field in a usual case has been chosen slow enough to keep both the cooling salt and other substances being in almost thermal equilibrium and also, from the practical reason, to avoid possible eddy current heating during the adiabatic field passage.

This quasi-static thermodynamical condition in the course of adiabatic cooling is considered to be important so far to cool the total system as low as possible. However, this would not be necessary so long as we are concerned with only the cooling of the salt itself. Further, a usual adiabatic cell may be also unnecessary, if we are interested in the thermodynamics and the magnetism associated with only the spin system of the cooling salt. Because the adiabatic condition between the salt and the thermal bath in usual case would be replaced by that between the spin and the lattice system inside the salt in this case. It is possible to produce such an adiabatic condition experimentally, even if the effective spin lattice relaxation time within a salt itself is short when it is compared with the minimum sweep speed of the conventional magnet stated above.

In this part, we will report the finding of the cooling and the spin ordering which would be expected even under the condition that the spin system is thermally isolated from the lattice and not influenced by phonons.

Apart from the problem of the cooling of the lattice system of a salt or the indirect cooling of other substances via lattice phonons, we can now successfully employ the following two methods for adiabatic cooling which would be realized in only the spin system.

One is the method well known as adiabatic fast passage in nuclear magnetic resonance, with which the spin system is cooled by the fast variation of RF frequency from off-resonant to resonant. The report on detections of a nuclear spin ordering in a rotating reference frame by Abragam et al.[1] is one of the most fascinating and successful example in this field.

The other is the method of adiabatic magnetization using a strong pulsed magnetic field. Several special specimens such as $Cu(NO_3)_2.2.5H_2O$,[2, 3] $CeCl_3.7H_2O$[2] and $NiSnCl_6.6H_2O$[4] have been studied from the viewpoint of adiabatic magnetization cooling under the static condition so far. Above all, $Cu(NO_3)_2.2.5H_2O$ is the most suitable sample for the purpose of the examination of the spin cooling by pulsed adiabatic magnetization[5] because the already reported isentropic curves,[2, 3] the spin ordering[2, 3] and its phase boundaries[3] under "static" condition would be compared with the results of the present "transient" one. Once, the equality between results in both cases of "static" and "transient" is established, the validity

of the latter method would be apparent in the field of the studies of the magnetism at high pulsed magnetic field. At the same time, the mechanism of magnetic ordering will be examined in reference with lattice system as one of the general properties of phase transition.

Chapter II EXPERIMENTALS

§2-1 Sample

Single crystals of $Cu(NO_3)_2.2.5H_2O$ are obtained by slow evaporation of the saturated solution at 50°C. The crystal is monoclinic and elongated along the crystallographic b-axis. The detailed study of the X-ray analysis has been performed by Morosin.[6] Throughout experiments, the external magnetic field was applied parallel to the needle axis of the crystal, which accords with b-axis and hereafter is written as $H /\!/ b$. The crystal is very hygroscopic and it is necessary to be air-tight around the crystal or to coat the surface with some non-magnetic grease such as Apiezon-N or silicon.

Friedberg et al.[7] first pointed out that Cu^{2+} spins in $Cu(NO_3)_2.2.5H_2O$ are coupled in pairs by isotropic antiferromagnetic exchange interaction of $J/k = 5.2$ K. Summing up the magnetic properties studied already in susceptibility,[7] specific heat,[8] magnetization,[9] paramagnetic relaxation,[10] ESR[11] and NMR[12] measurement, we may conclude the evidence of the isolated pair model of Cu^{2+} spins in $Cu(NO_3)_2.2.5H_2O$, although the values of J/k and g-anisotropy differ slightly among several authors.

Thus, we may write down the spin-pair Hamiltonian of Cu^{2+} spin as

$$\mathcal{H}_{spin\text{-}pair} = J\mathcal{S}_1\cdot\mathcal{S}_2 + g_{/\!/}\mu_B H(\mathcal{S}_{z1} + \mathcal{S}_{z2}) \qquad (1)$$

where $g_{/\!/}$ (parallel to b-axis) = 2.31.[13]

From eq.(1), we can expect readily that the ground singlet and the lowest excited triplet cross under the external magnetic field of $H_c = J/g\mu_B$ as shown in Fig. 1.

This energy level crossing was found by the high frequency susceptibility measurement under high magnetic field up to 50 kOe[10, 14] and the detection of the several types of the cross relaxation process in this salt gave a direct verification of the previously stated pair model as well as the very existence of appreciable order of the inter-pair interaction J' . About the pair-links by J', two models of "ladder" and "alternating chain" are proposed by Friedberg[15] as shown in Fig. 2.

Another powerful evidence for the inter-pair interaction was given by the observation of the cooling by adiabatic magnetization[10] analogous to the usual adiabatic demagnetization. A simple expectation to observe a spin ordering at the crossing field was realized[2] immediately after the first successful findings of the cooling. Results are shown schematically in Fig. 3, giving a new type of an order-disorder transition with semi-circular phase boundary in the T-H diagram.

Tsuneto and Murao,[16] and Tachiki et al.[17] examined the spin ordering of the ground state singlet magnetic systems. Especially, Tachiki et al. proceeded their theory in the case of $Cu(NO_3)_2.2.5H_2O$ and obtained qualitatively good agreement with experiment.

M. W. van Tol et al.[3] examined the phase transition by NMR and specific heat measurement around the crossing field and clearly demonstrated the double stages of the structure of

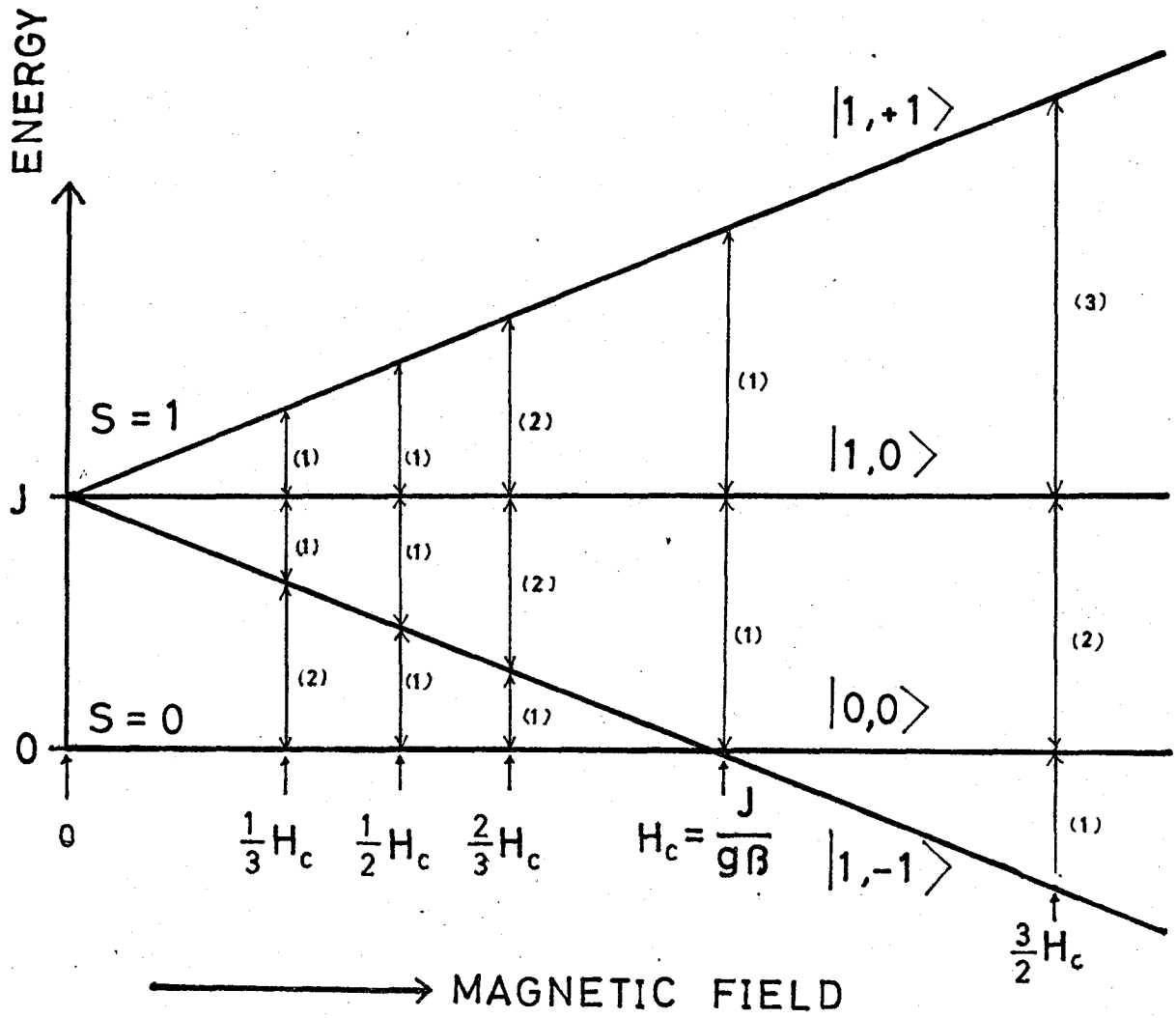

Fig. 1 Diagram of the energy level splitting of the ground spin states of Cu^{2+} spin-pair in $Cu(NO_3)_2.2.5H_2O$ under an external magnetic field.

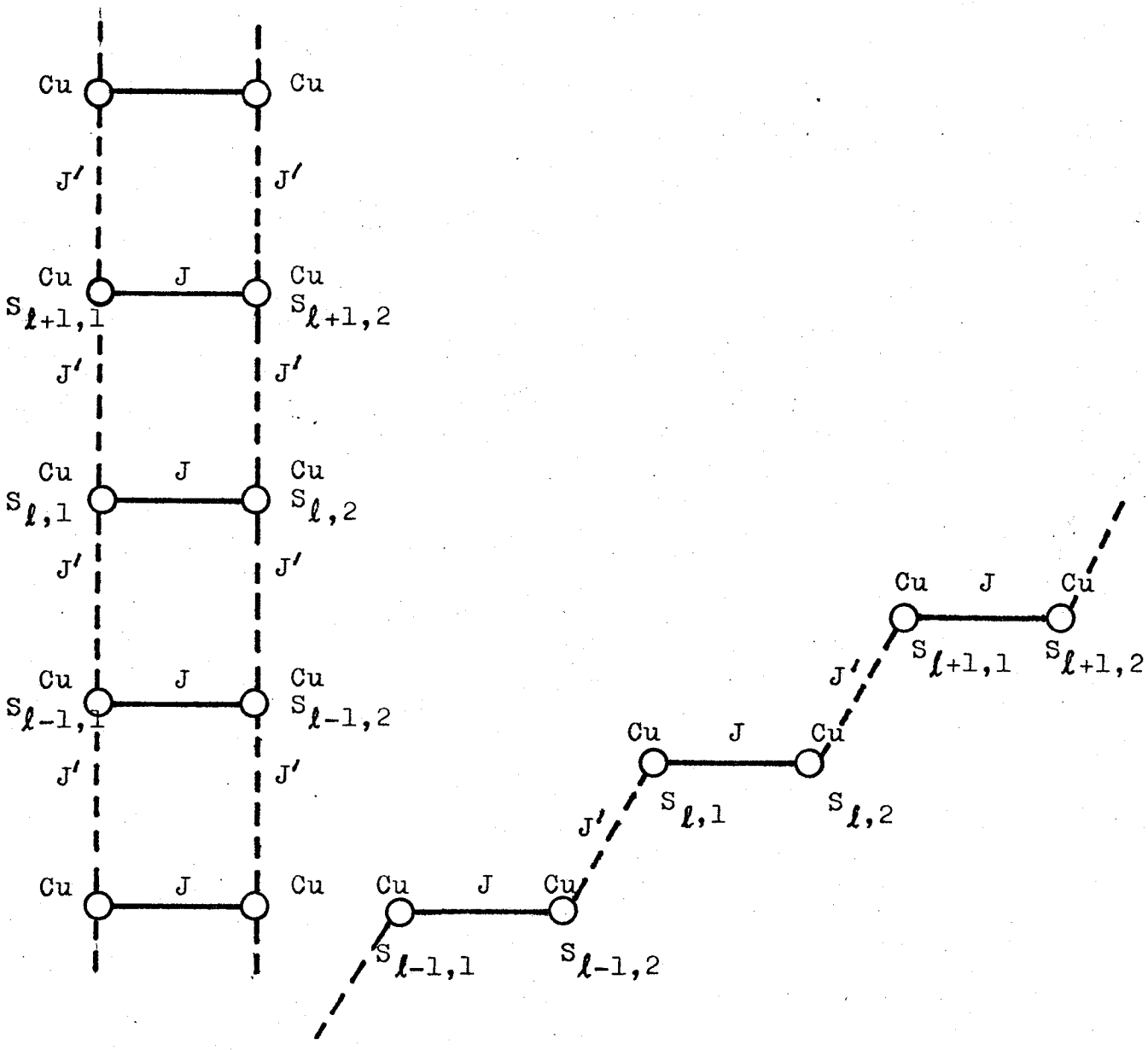

Fig. 2 Diagram of magnetic ladder model (I) and alternating chain (II). The figure refer to possible magnetic exchange paths for the copper nitrate structure. Model I is favored for copper nitrate.

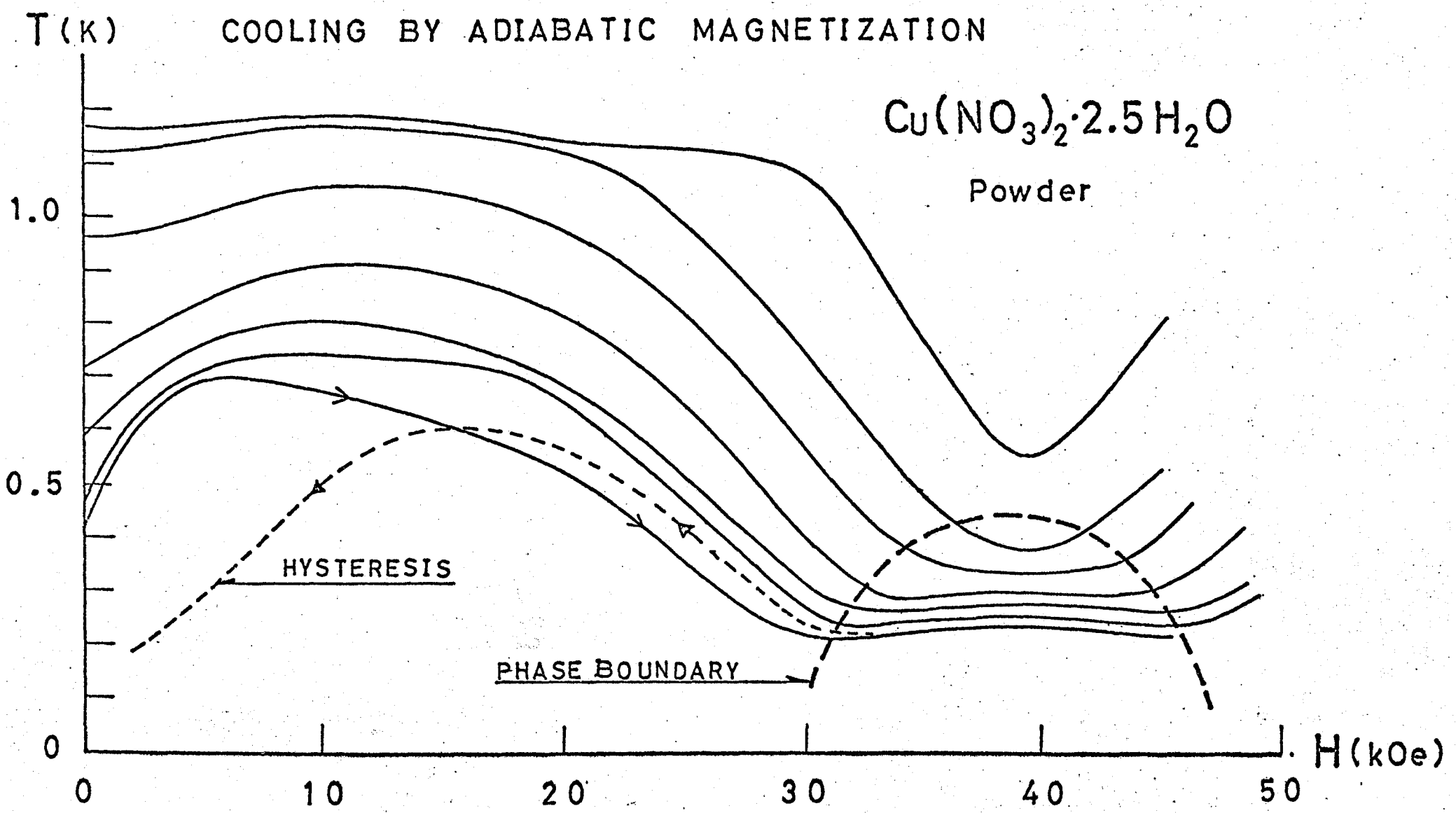

Fig. 3 Experimental isentropes of $Cu(NO_3)_2 \cdot 2.5H_2O$

Starting temperature for each run is given by the value at H = 0.

the phase boundary, one of the short range, the other of the long range as shown in Fig. 4. The appearance of the short range order reflects the low dimensionality of the spin-pairs and successive long range order will be due to either inter-ladder or inter-chain weak interaction.

§2.2 Pulsed Adiabatic Magnetization

In § 2.1, we outlined the reported magnetic properties of $Cu(NO_3)_2.2.5H_2O$ where an external magnetic field had been varied slowly and considered to be thermodynamically almost "static" at the every stage. Now, we apply here a "transient" method to the study of the thermodynamic and the magnetic properties of $Cu(NO_3)_2.2.5H_2O$ under high magnetic field.

In the cooling of a spin system by pulsed adiabatic magnetization, the estimation of the spin temperature is possible only through the susceptibility measurement in place of the indirect "lattice" thermometers.

The most essential point in our transient experiment is to cut off the thermal link between a spin and a lattice system, the measure of which is given by a spin-lattice relaxation time τ_{sl}. According to the relaxation measurements by Duyneveldt et al.,[18] τ_{sl} in low field are expressed by Inverse Orbach Process given by

$$\tau_{sl} = 2.05\times10^{-5}\times(\exp 5.2/T - 1) \quad \text{sec.} \qquad (2)$$

This gives $\tau_{sl} = 4\times10^{-3}$ sec at 1 K and increases rapidly with decrease of temperature. Another measure of the thermodynamical

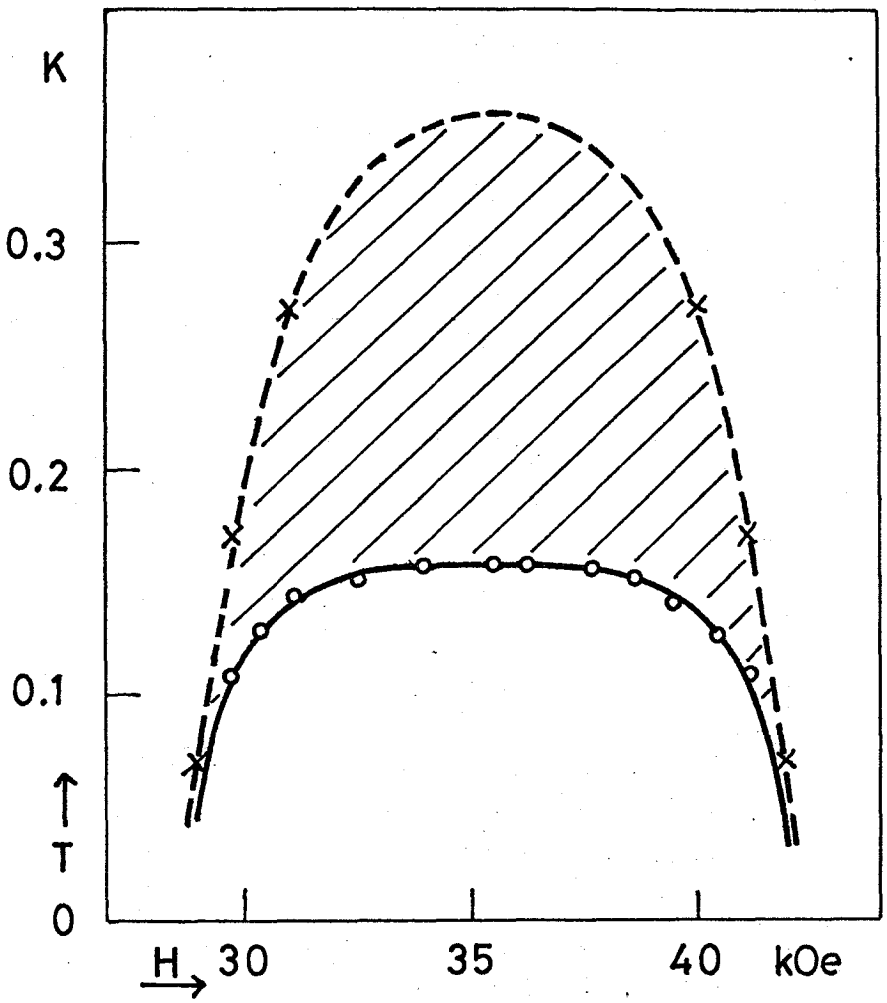

Fig. 4 Experimental transition temperature versus external magnetic field. Shaded area represents large short range order, dashed curve connects minima in the (experimental) isentropes.

quantity is the cross relaxation time τ_{cr} which governs the thermal equilibrium within a spin system. Tokunaga et al.[14] measured high frequency susceptibility under magnetic field up to about 50 kOe and concluded that τ_{cr} at H_c is at least shorter than $5 \cdot 10^{-8}$ sec. The experimental condition $\tau_{cr} < \tau_p < \tau_{sl}$, which is necessary for the cooling of a spin system by a transient method, will be realized by use of a pulsed high magnetic field with the quarter period τ_p less than about 5 msec.

In Fig. 5, the block diagram of the apparatus for pulsed adiabatic magnetization is shown. A number of pulsed coils to satisfy above condition were tested in liq. He^4 bath. After several improvements, we made an 100 kOe magnet, whose dimensions are 50 mm long and 10 mm ϕ inner-diameter. This coil has worked more than a hundred times and the dissipation of liq. He^4 was rather a small amount, giving for example, 0.35 ℓ for one shot. An arc and a corona type discharge do exist in this case but almost disappear by coating an insulating adhesive such as Araldite Rapid for electric lead junctions and fixing pulse coil with some epoxy resin.

Energy bank consists of 120 electrolytic condensers whose individual has the capacity of 100 μF/500 W.V. and the cascade connection of them gives a condenser bank of 50 μF×60/1000 W.V. The ignitor of the sendaitron switch are drived by a TV - flyback transformer. Pulse current is direcly read by a standard resistor (50mV/30A) connected in series with a pulsed coil. As this resistor has leakage inductance of the order of 100 pH, we cannot use it as a

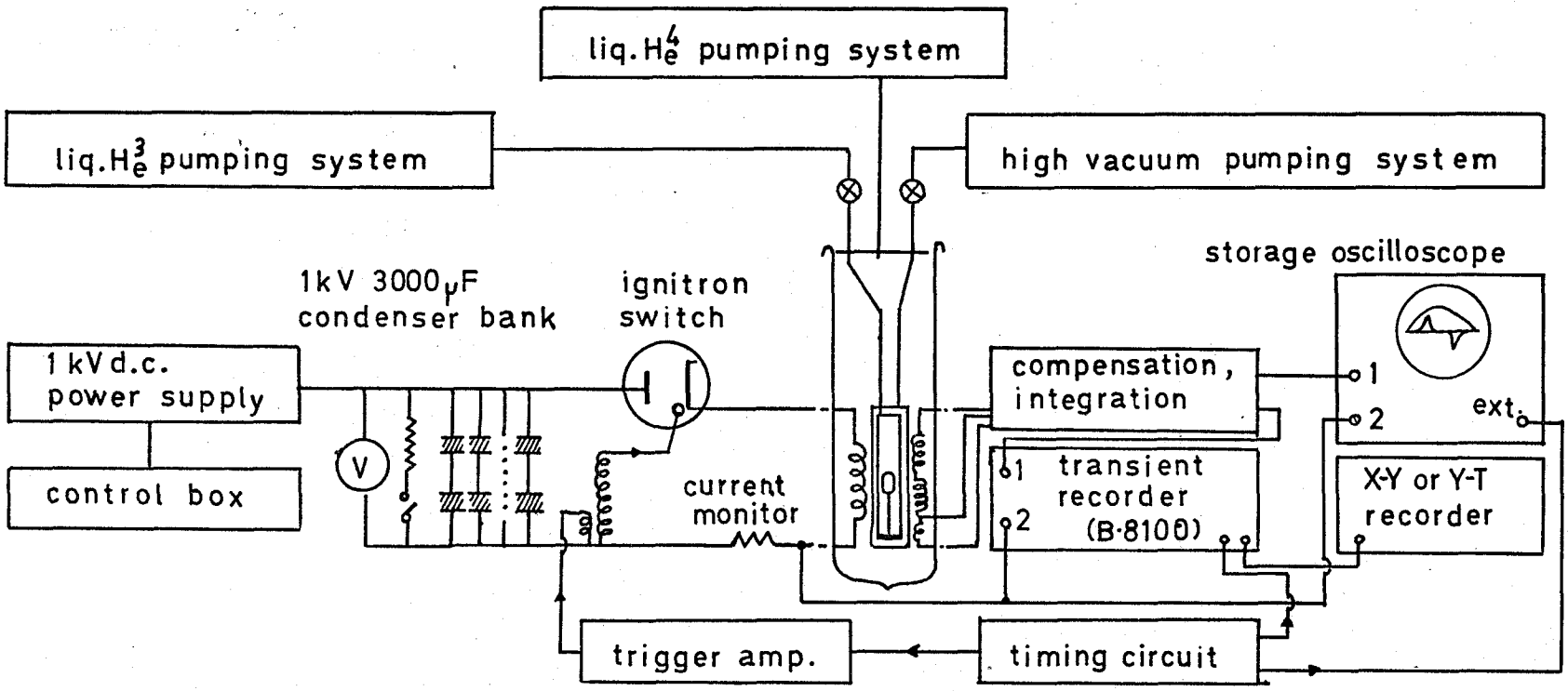

Fig. 5 BLOCK DIAGRAM of PULSED ADIABATIC MAGNETIZATION

current monitor for such a rapid pulse as those with the rise time less than 100 μsec.

Signals of the sample are given in the form of an induced voltage across the pick up coil as

$$v_s \propto \frac{\partial \phi}{\partial t} \tag{3}$$

where ϕ is the magnetic flux. Of course, the flux originated from a pulsed field are almost compensated because of counter-windings of the two pieces of pick up coil and the residual unbalance are resistively compensated. To prevent burning out of the lead wire of the pick up coil, two pieces of them are connected in series from the beginning and the small auxiliary coil is used for compensation.

Induced voltage v_s is roughly proportional to the derivative of the magnetization with respect to magnetic field, which gives susceptibility, so long as the time dependence of the magnetic field is approximately linear. In our case, pulsed magnetic fiels of 80 kOe is strong enough to observe the derivative of the magnetization at 35 kOe $\pm$ 5kkOe with an error of linearity within a few percent.

After compensated, the pick up voltage is put into the digital/analog - memory function. Transient Recorder (Biomation Model 8100) is superior to a storage oscilloscope in some respects, for instance, in time resolution, memory function and flexibility of data analysis. The examples of the recorder trace are shown in the next section.

At the first step of the experiments, the sample, the

pick up coil and the pulsed magnet were immersed together in liq. He^4 bath. An adiabatic cell was used in the next step, where the sample was set in a vacuum cell and the initial condition was given by the contact via exchange gas. The same results were found in these two methods of the experiments of the pulsed adiabatic magnetization using a pulsed magnet of τ_p = 4 msec.

Therefore, in the experiments at liq. He^3 temperature region, the sample was immersed directly in liq. He^3. In these cases, thermal bottle-neck might exist not only in spin-lattice but also in lattice bath. There were no remarkable differences between a short and a long pulse with τ_p of 160 μsec and 4 msec, respectively. Results are summarized in the case of the long pulse.

Some results of our transient method are compared with those of the "static" isothermal experiments. The apparatus for the "static" case are usual He^3 pot system and appeared elsewhere.

Chapter III EXPERIMENTAL RESULTS

§3.1 Susceptibility at Zero Field in "Static" Case

In §1.2 of Part I, we have already mentioned about the absence of the long range ordering of the spin pair system at zero field. $Cu(NO_3)_2.2.5H_2O$ is just the case. The susceptibility is expected to show a broad maximum of the Schottky-type at T = 0.62 zJ/k and below this temperature the system becomes nonmagnetic with decreasing temperature. Figure 6 shows the experimental results of the temperature dependence of the susceptibility at H = 0 with the theoretical curves. The agreement with theory is satisfactory if we add a small inter-pair interaction of $zJ'/k = 1.68$ K[21] in the isolated pair model with $J/k = 5.2$ K. The theoretical expression of the susceptibility is already given by eq.(26) in §3.1 of Part I.

§3.2 Susceptibility under External Field in "Static" Case

Magnetic field dependence of the AC susceptibility is shown in Fig. 7, in which the field is applied parallel to b-axis and the temperature is taken as the parameter for each run. Response of the adiabatic susceptibility is obtained at the measuring frequency of ν = 1 kHz, below T = 1.28 K. The figure shows the tendency of the saturation of the susceptibility around $H = H_c$ and this change of the shape toward lower temperature seems to show a development of a kind of spin ordering. Referring to the already reported phase diagram of $Cu(NO_3)_2.2.5H_2O$, the short range order of spins occurs at

Fig. 6 Susceptibility versus temperature for $Cu(NO_3)_2 2.5H_2O$.
Theoretical results for isolated pair and for interacting pair compared with our data (·).

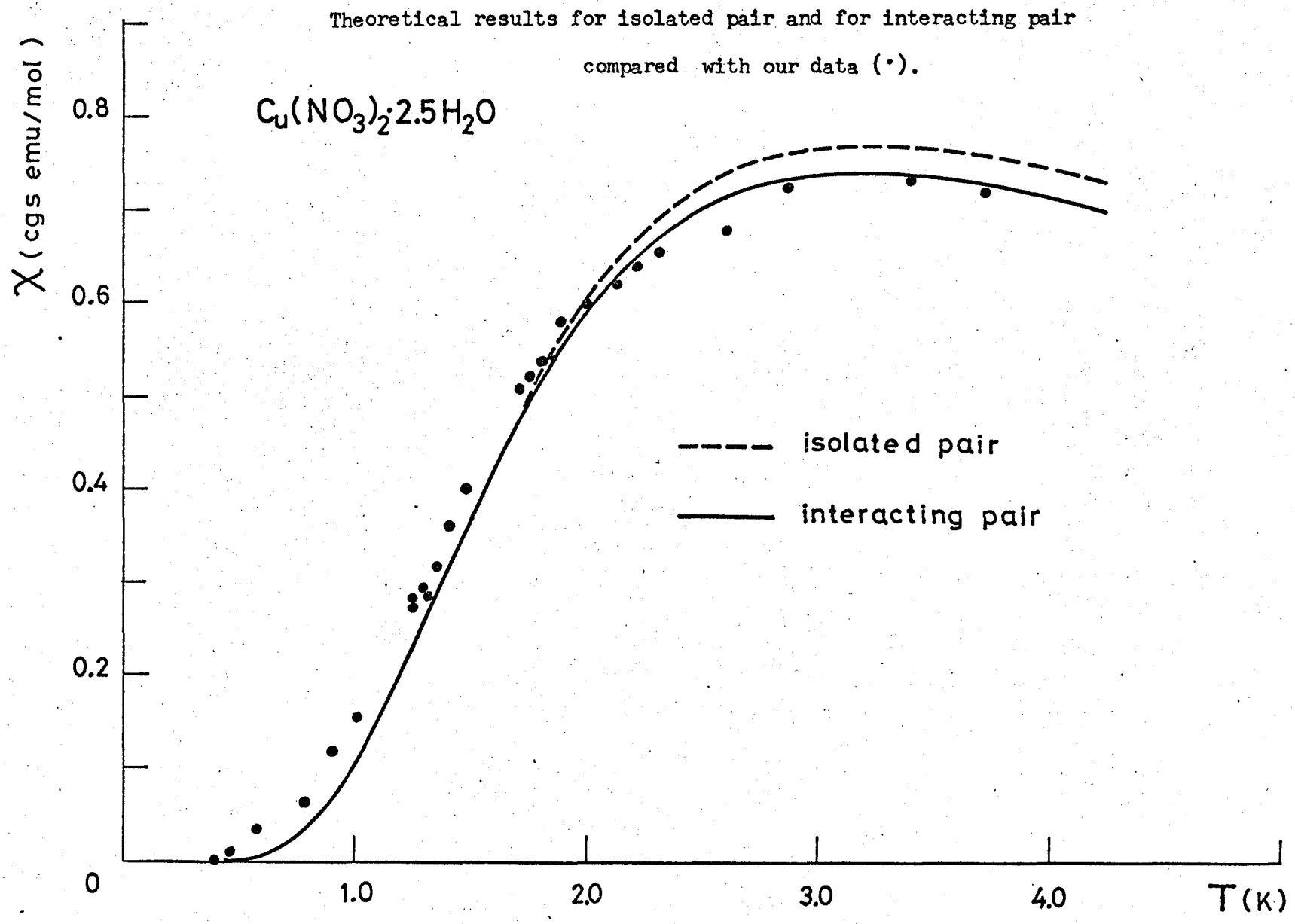

Fig. 7 AC susceptibility versus external magnetic field for $Cu(NO_3)_2 2.5H_2O$.

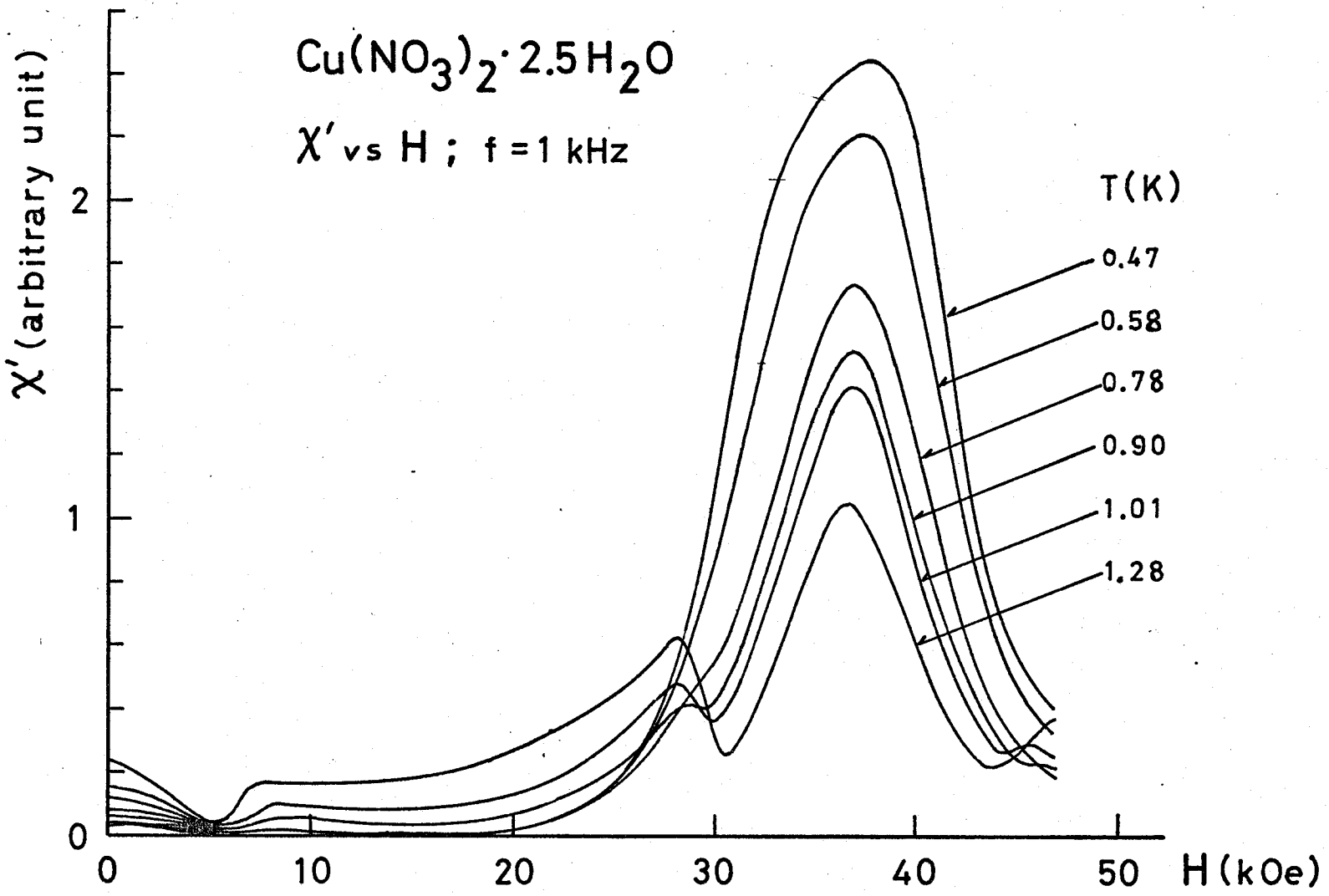

T = 0.35 K.

In § 3.1 and § 3.2, we have obtained an essentially adiabatic susceptibility under isothermal, in other words, "static" field sweep. These results will be compared with the next "transient" results.

§3.3 Results of Transient Method

A series of the field derivative of the magnetization under pulsed magnetic field are obtained for the several values of the starting temperatures as typically shown in photo 1.

In the early stage of experiments, a double channel strage oscilloscope is used and the analysis of the results is performed through these photos of the stored signals. Photos, 1(a), 1(b) and 1(c) show the response at the only first half of the pulsed field and the total response is, of course, antisymmetric as shown in photo 1(d). All the experimental data is summarized with the pulsed field which was set and discharged with almost equal condition. Relative setting errors will be less than a few per cent. The vertical sensitivities are relative for both signals and pulsed field which are calibrated later by pick up coils. The horizontal sensitivity is fixed with a time scale of 500 μsec/div.

The wings corresponding to the cross relaxation[10, 14, 18] are observed at the both side of the susceptibility maximum at $H = H_c$ above $T_i = 1.7$ K.

The estimation of the cooling by the pulsed adiabatic magnetization is possible referring to the static result in §3.2.

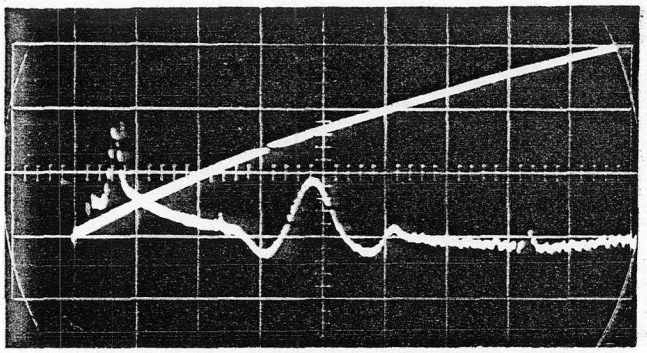

Photo. 1(a)

T_i = 2.50 K

τ = 100 μsec/div.

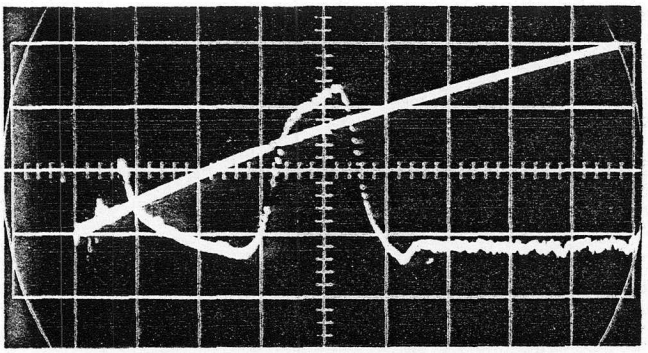

Photo. 1(b)

T_i = 1.56 K

τ = 100 μsec/div.

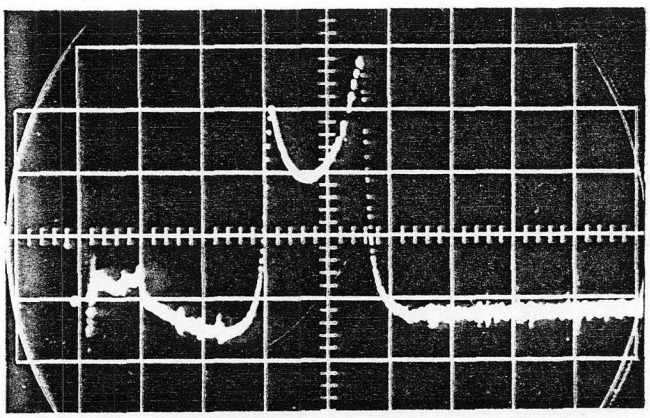

Photo. 1(c)

T_i = 1.11 K

τ = 100 μsec/div.

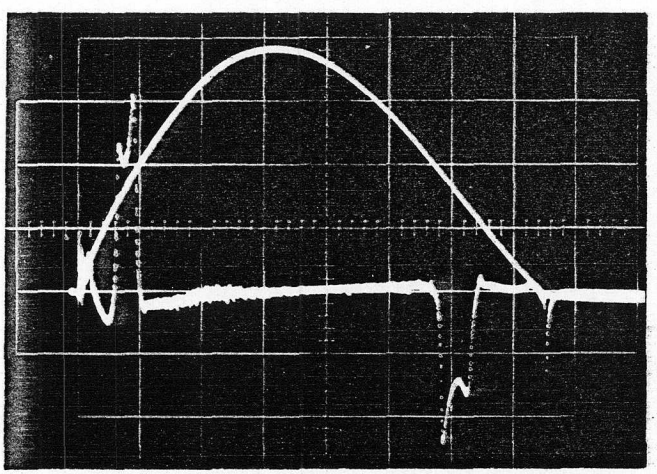

Photo. 1(d)

T_i = 1.28 K

τ = 500 μsec/div.

Photo. 1 Photographs of dM/dt signals in a pulse field. Vertical sensitivities are fixed for (a), (b), (c) and (d). τ is horizontal time scale.

Typical example is given in the case of T_i = 1.56 K, for which the susceptibility around H = H_c is found to corresponds nearly to those of T = 0.47 K in the static isothermal experiment.

The most striking is the appearance of the double peaks of the signal with the starting temperature below 1.5 K. The double peaks with sharp edge are observed at T_i = 1.11 K, for which the phase transition of the second order becomes possible to be observed.

At lower temperature of 0.5 K $\leqq T_i \leqq$ 1 K, the shape of the signal itself is almost the same as that of T_i = 1 K. In Fig. 8, $(\partial M/\partial H)_s$ curves and a pulsed magnetic field are plotted as a function of the sweep time t(μsec). The initial temperature T_i is varied from 4.2 K to 0.4 K as shown in the figure. The pulsed field is applied so as to be approximately equal for each run and shown with a single dotted line. The figure also shows the existence of the critical fields, H_{c1} and H_{c2}, between which the ordered state exists and outside of them, the system is in disordered state giving no contribution to the susceptibility. Since no distinct change in the shapes of signals around T_i = 1 K is observed as shown in the figure, the phase transition from the short range to the long range order cannot be decided from our data. However, we read that the results below T_i = 1 K are undoubtedly of the long range order. Because the static data[3] has shown that the entropy $S/(\frac{1}{2}R)$ corresponding to T_i = 1.1 K is 0.14 for which the isentropic curve already enters the long range order. Moreover, successful finding of the cooling and the short range ordering[5]

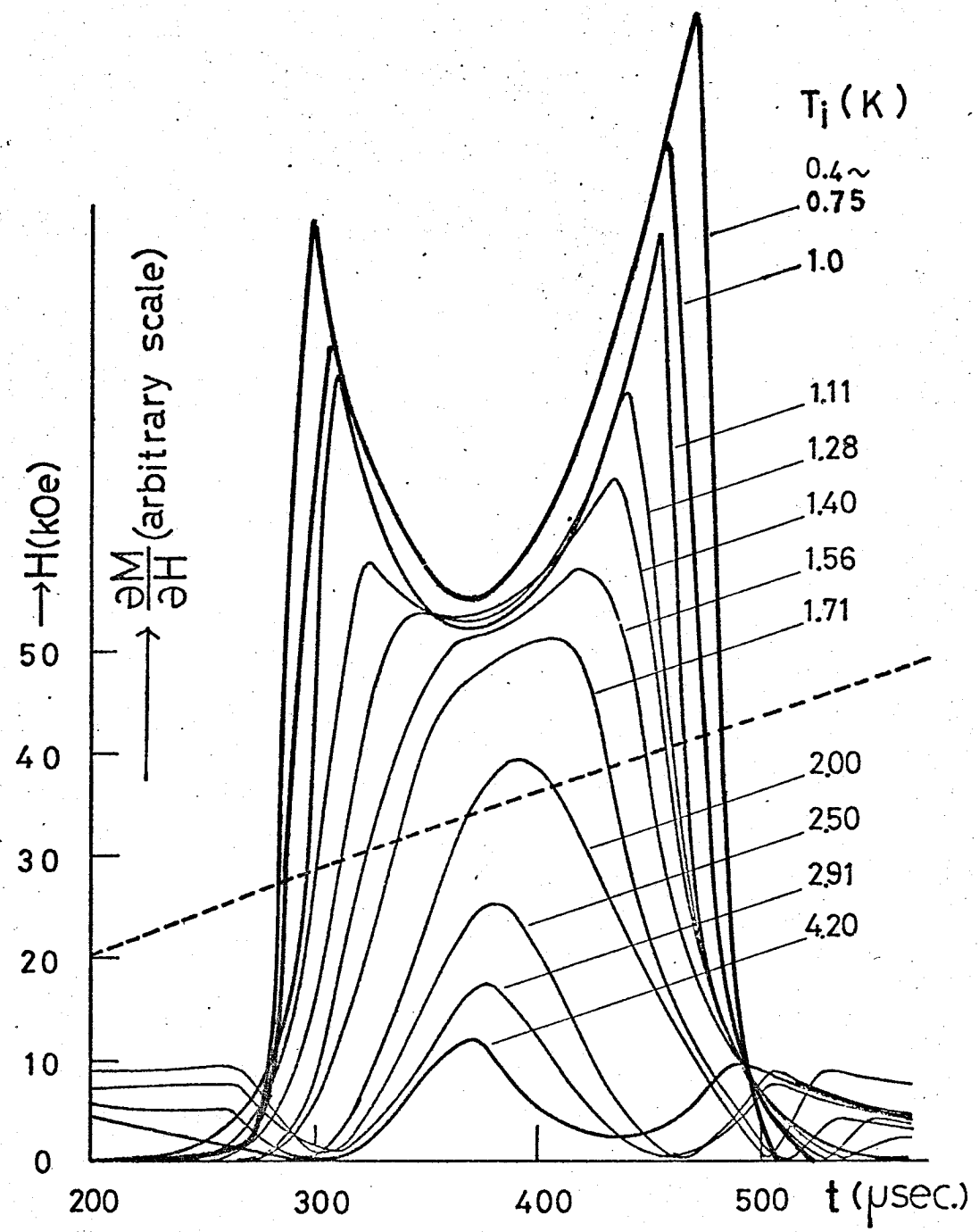

Fig. 8 Observed ∂M/∂H curves (——) and pulsed magnetic field (---) as a function of sweep time t.

above T_i = 1 K seems to show the adiabatic condition between the spin system and the thermal bath is fairly good and is improved further at lower temperature. And also there exists the relatively very short cross relaxation time of the order of 10^{-8} to 10^{-9} sec[14] to compare with our passage time of the pulsed field which is of the order of 10^{-3} sec. We consider above statements give necessary conditions for the establishment of the long range order.

To see the limiting behavior of the ordered state at low temperature, the double channel transient recorder (Biomation 8100) was used together with the monitoring storage oscilloscope. An example at T_i = 0.4 K is shown in Fig. 9.

The obtained traces are best fit for the investigation of the shape of the signal and yet there does not appear distinctly the double structure of the phase boundary, which might be detected in the course of the magnetization.

The magnetization curve for the initial condition of T_i = 0.4 K is obtained by the integration of the derivative of the magnetization, $\partial M/\partial t$, with respect to time. The result of the integration in the magnetic field range from 20 kOe to 45 kOe is plotted in Fig. 10. The magnetic field dependence of the magnetization is expressed not by a linear function[3] of a magnetic field but rather by an inverse sine function which will be given theoretically in the next section.

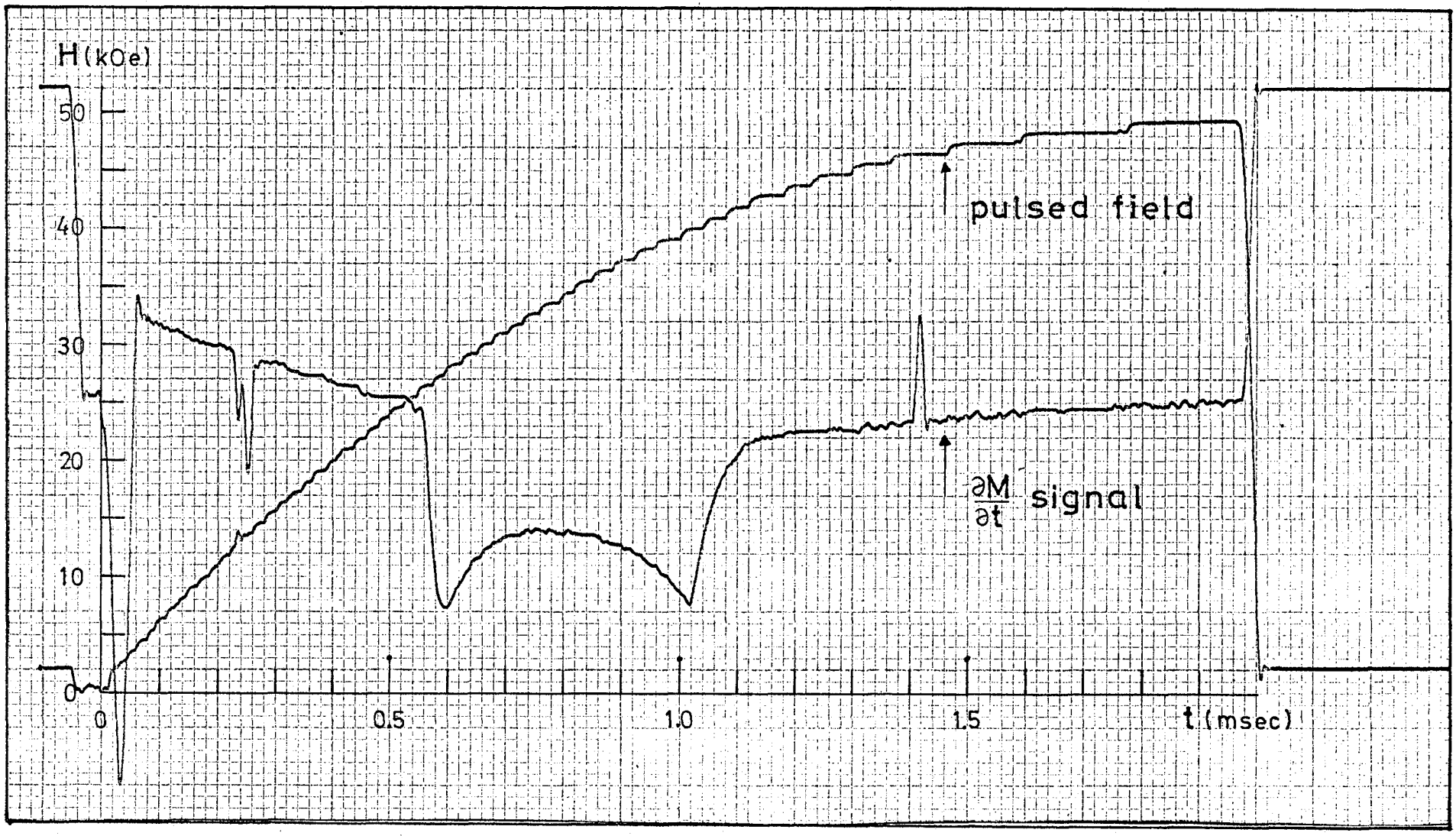

Fig. 9a Recorder trace of dM/dt signal and pulsed field as a function of sweep time t.

The total recording time is 2048 (data words) × 1 μsec (sample interval).

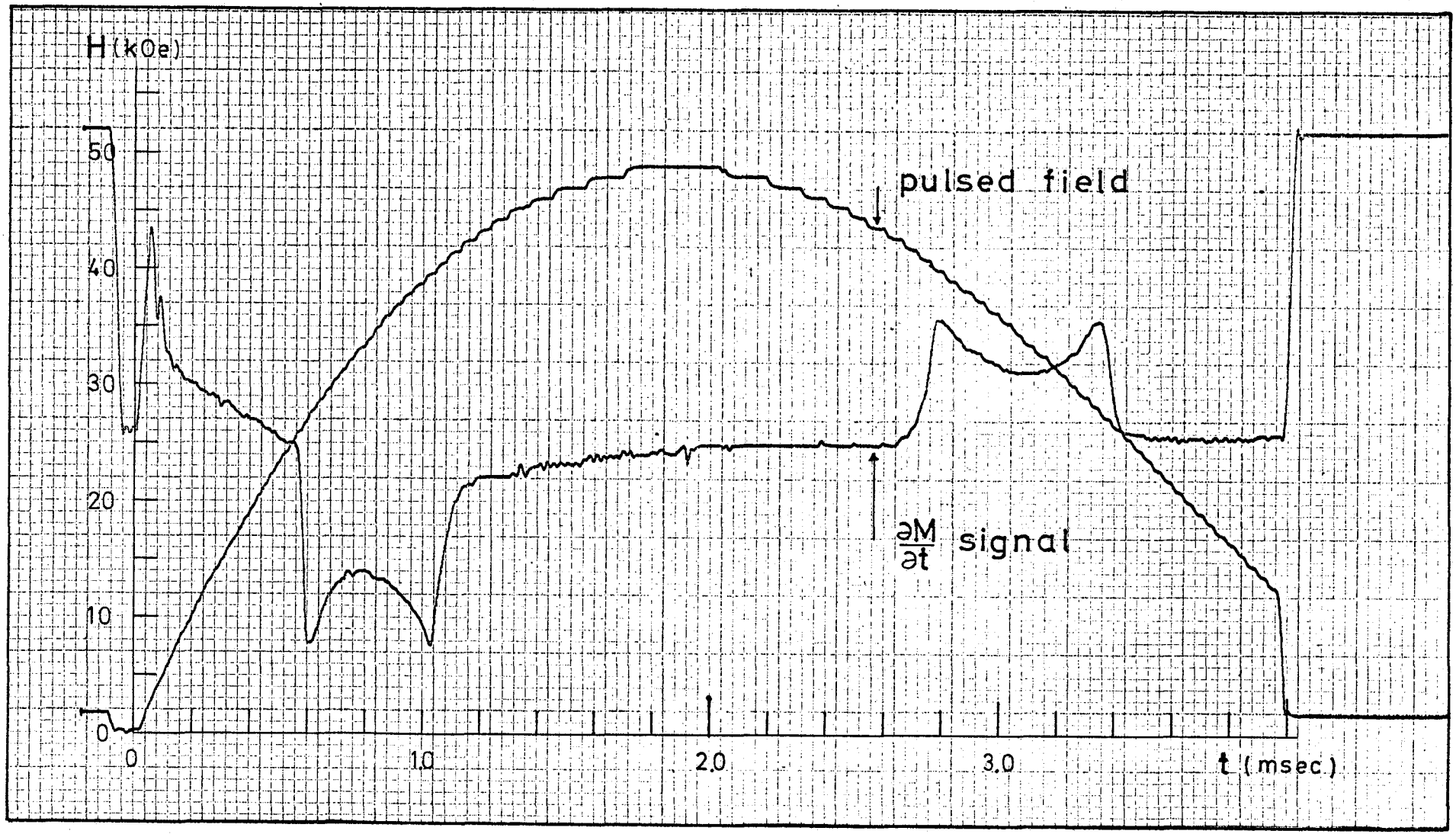

Fig. 9b Recorder trace of dM/dt signal and pulsed field as a function of t.

The total recording time is 2048 (data words) x 2 μsec (sample interval).

Fig. 10 Experimental magnetization isentropes for $Cu(NO_3)_2 2.5H_2O$

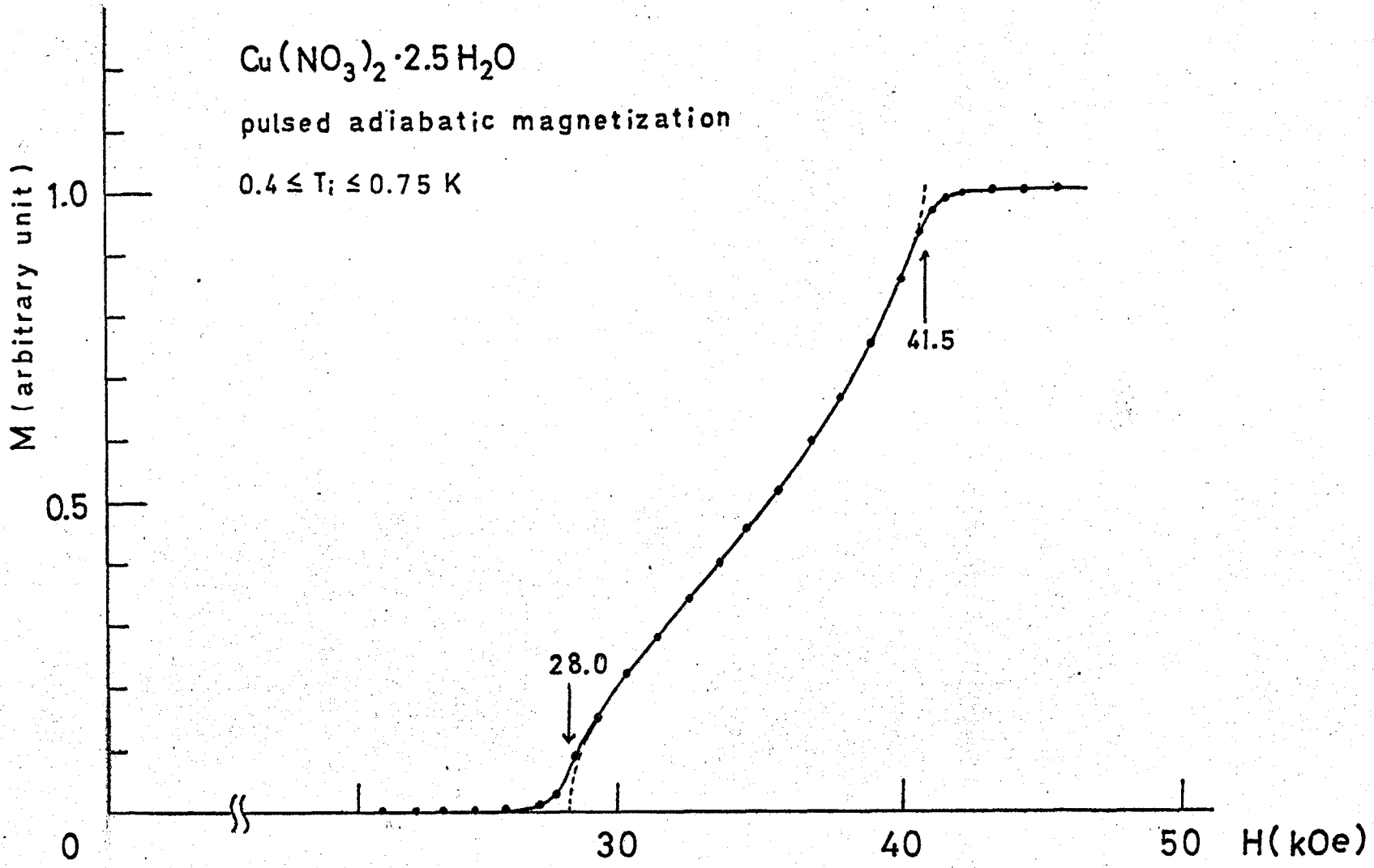

Chapter IV DISCUSSIONS

§4.1 Theory of Short Range Order

According to Tachiki et al.,[19] the spin-pair Hamiltonian for $Cu(NO_3)_2.2.5H_2O$ in the short range ordering region is written, apart from the constant term independent of the spin states, as

$$\mathcal{H} = f\sum_{\ell}\sigma_{\ell}^{z} + \frac{1}{2}K\sum_{\ell}\left[2(\sigma_{\ell}^{x}\sigma_{\ell+1}^{x} + \sigma_{\ell}^{y}\sigma_{\ell+1}^{y}) \pm \sigma_{\ell}^{z}\sigma_{\ell+1}^{z}\right] \quad (4)$$

where σ_{ℓ} is Pauli spin in the ℓ-th pair and f and K stand for the following quantities

$$f = \frac{1}{2}(g\mu_B H - J) - \frac{1}{16}J'(3 \pm 1) \quad (5)$$

$$K = \frac{1}{16}J'(1 \pm 3) \quad (6)$$

where J and J' is the intra- and the inter-pair interaction and either sign + or - are taken corresponding to the two models of the pair links, ladder and alternating chain model, respectively, as shown in Fig. 2.

Exact expressions for various thermodynamical quantities in the case of vanishing longitudinal component, i.e. those in the case of the X-Y model, for one-dimensional lattice under magnetic fields, have been obtained by Katsura.[20] From his theory, the free energy is given by

$$F = -\frac{Nk_BT}{\pi}\int_0^{\pi} \ln\left[2\cosh\left(\frac{f - 2K\cos\omega}{k_BT}\right)\right]d\omega \quad (7)$$

Tachiki et al.[19] examined the qualitative nature of the short range order of spins in $Cu(NO_3)_2.2.5H_2O$ using the above free energy and obtained qualitatively good agreement with "static" experiments on adiabatic magnetization.

To compare the theory with transient experiments, we calculated the adiabatic susceptibility $(\partial M/\partial H)_S$ along the isentropic process from eq.(7). The results are plotted against the reduced field $h = f/2K$ in the vertical unit of $Ng^2\mu_B{}^2/8K$ for several values of entropy, which are shown in Fig. 11. The intra-pair exchange constant $J/k = 5.2$ K is used for the correspondence between entropy and starting temperature T_i which is also shown in the figure.

The theory predicts that the double peaks of $(\partial M/\partial H)_S$ appear symmetrically with respect to $h = 0$ if T_i is less than 1.4 K and that $(\partial M/\partial H)_S$ at $h = 0$ has the maximum value when $T_i \simeq 1.4$K, where $h = 0$ corresponds to the real field of $H = J/g\mu_B + zJ'/4g\mu_B$. This is qualitatively in good agreement with experiment except the asymmetry observed. The theory also explains the experimental values of the boundary fields of $H_{c1} = 29.3$ kOe and $H_{c2} = 40.4$ kOe for each of the double peaks observed with $T_i = 1.11$ K. Taking the reported values of $J/k = 5.2$ K,[7] $g = 2.31$ $(H/\!/b)$[13] and $zJ'/k = 1.68$ K,[21] the theory predicts $H_{c1} = 31.4$ kOe and $H_{c2} = 41.3$ kOe with $T_i = 1.1$ K. Taking account of a possible error of a few percent about the experimental values of magnetic field, agreement with the theory is fairly good. Thus, inter-pair interaction J' is confirmed also from the present experiment to be $J'/k = 0.84$ K (ladder)

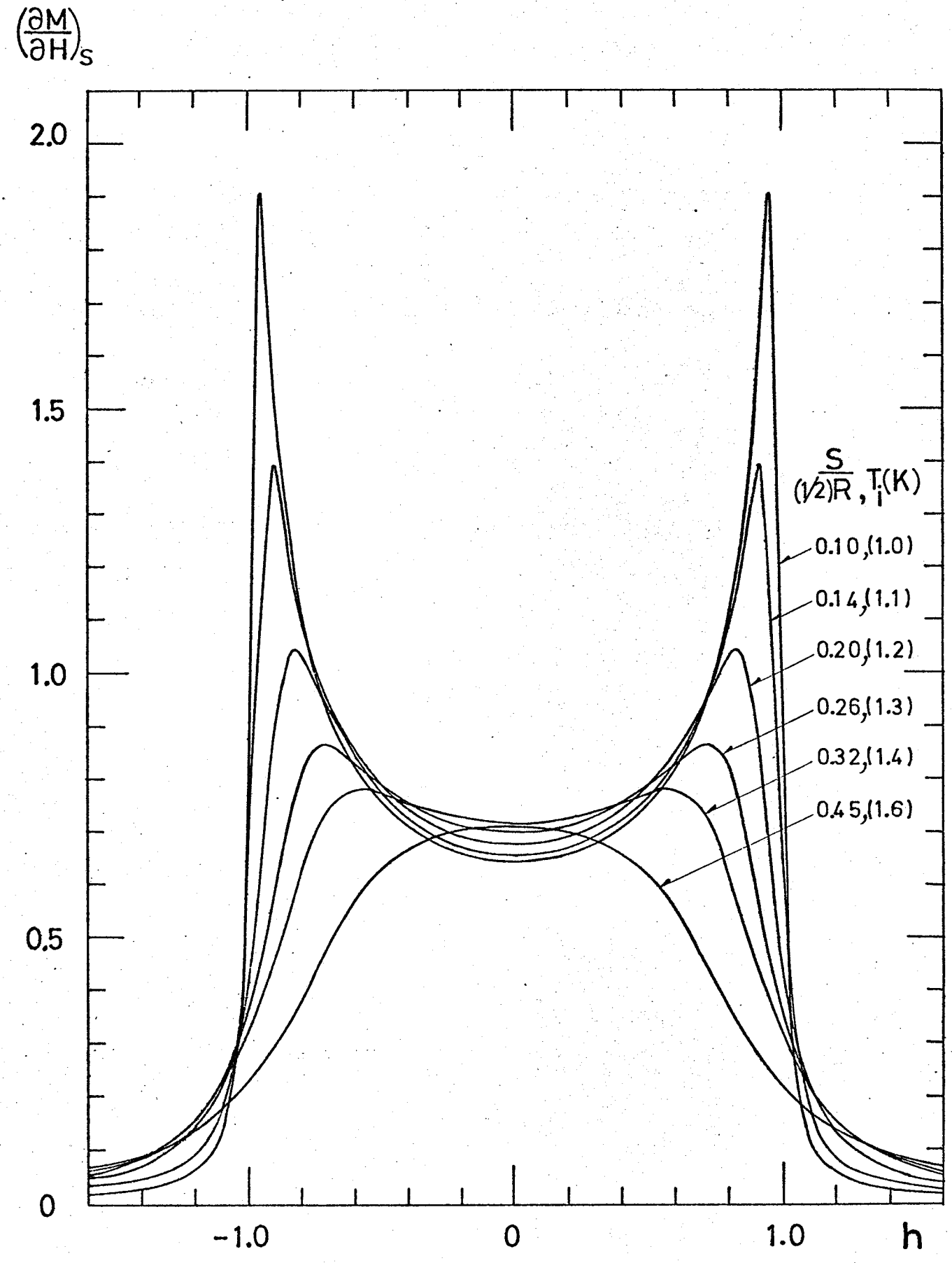

Fig. 11 Variation of $(\partial M/\partial H)_s$ curves as a function of reduced field h. J/k = 5.2 K is used for the correspondence between entropy S and starting temperature $T_i(K)$.

or 1.68 K (alternating chain). The theory also predicts that the magnetization in the limiting case of T = 0 has the form

$$M = \frac{2}{\pi} N g \mu_B \cdot \sin^{-1}\left(\frac{g\mu_B H - J - zJ'/4}{J}\right) ; \left|g\mu_B H - J - \frac{zJ'}{4}\right| < \frac{zJ'}{2} \quad (8)$$

which are shown in Fig. 12.

This is already assured experimentally in Fig. 10 and the slight deviation from eq.(8) is again due to the asymmetry of the experimental $\partial M/\partial t$ curves.

Above discussions are based on the theory of the short range order of spins in the case of the X-Y model for one dimensional lattice under magnetic field. Also the theory treats for simplicity only the lower two levels, resulting a symmetric behavior for the field dependence of susceptibility around the reduced field h = 0.

Van Tol et al.[3, 18] introduced an anisotropy of the intra-pair exchange interaction to explain the observed asymmetry of the isentropes which are closely related with the present asymmetry of the susceptibility. In the next section, however, we show the asymmetry is explained quantitatively by taking all the four levels into account in place of the previous two level approximation. At present, there are no decisive experimental evidence for the four level approach to be preferred to the introduction of anisotropic interaction J. But we employ the former because we consider it being more straightforward than the latter. In fact, the choice of anisotropy parameters and inter-pair interaction J' seems to be still rather arbitrary even if the observed isentropes are

Fig. 12 Magnetization versus magnetic field at absolute zero for XY model for one dimensional lattice.

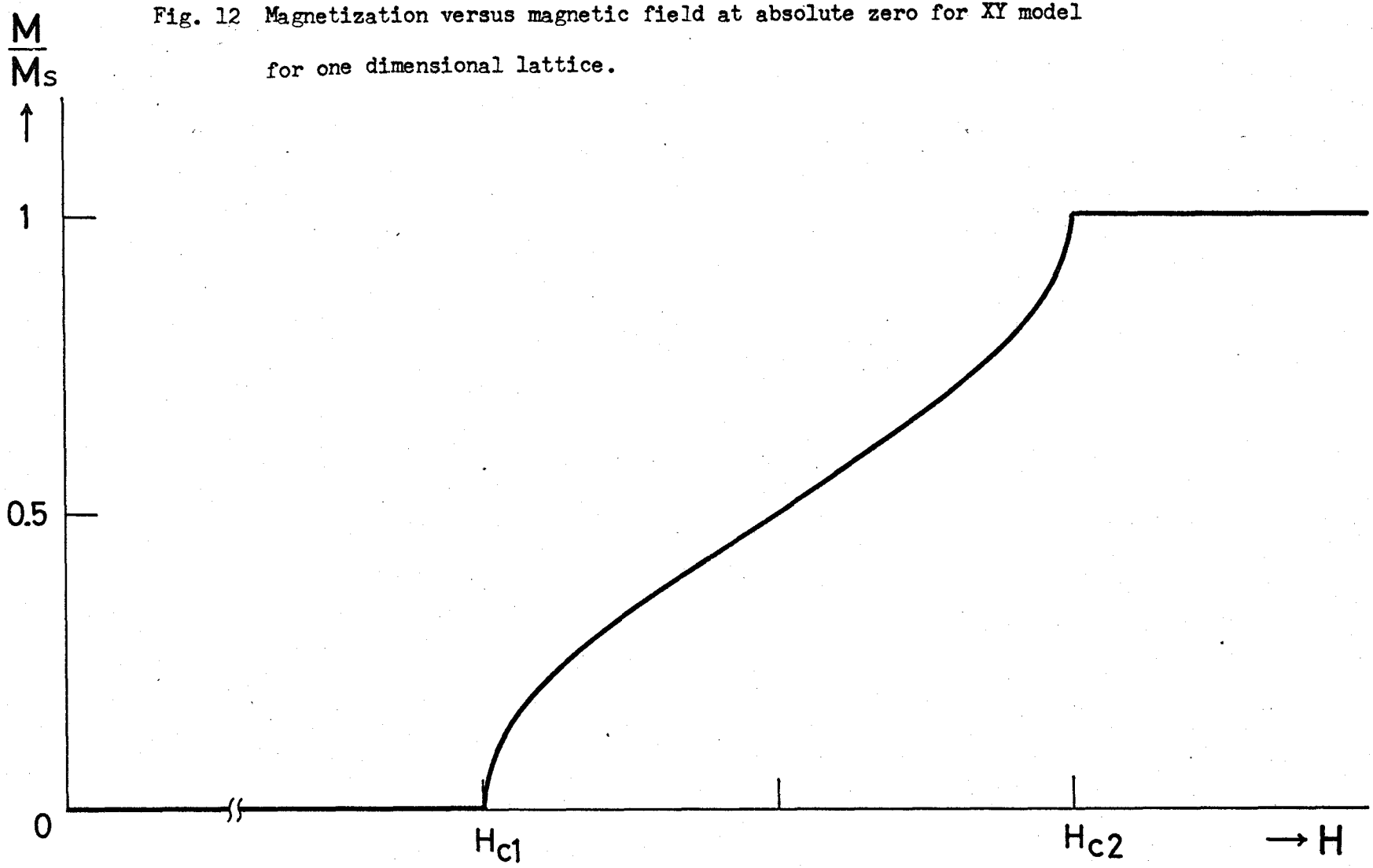

explained qualitatively. Electron spin resonance among the triplet states of Cu^{2+} spin pair has not yet shown any structure due to the existence of anisotropic interaction J.

§4.2 Asymmetry in the Susceptibility $(\partial M/\partial H)_S$ Curves

Now, we discuss the susceptibility of the Cu^{2+} spin pair system in the ordered phase taking account of the effect of the upper two levels. In this case, we adopt two sublattice model because the main inter-pair interaction J' is antiferromagnetic. Using a molecular field approximation for the inter-pair interaction in a similar way as Part I §4.2, we obtain the following effective Hamiltonian for either of the sublattices,

$$\mathcal{H}_{eff}^{(+)} = J\mathbf{S}_{i1}\cdot\mathbf{S}_{i2} + (h-\lambda m')(S_{i1}^z + S_{i2}^z) + \lambda n'(S_{i1}^x - S_{i2}^x) \quad (9)$$

where λ expresses the quantity zJ'/2J, and m' and n' represent the total (parallel) and stagger (perpendicular) magnetization of the other sublattice, respectively. Assuming m = m' and n = -n', $H_{eff}^{(+)}$ is rewritten in the following matrix representation form,

$$\mathcal{H}_{eff}^{(+)} = J\begin{bmatrix} h-\lambda m & \lambda n/\sqrt{2} & 0 \\ \lambda n/\sqrt{2} & -1 & -\lambda n/\sqrt{2} \\ 0 & -\lambda n/\sqrt{2} & -(h-\lambda m) \end{bmatrix} \oplus 0 \quad (10)$$

Although this equation appears in the similar form as in the case of the ferromagnetic inter-pair interaction, the solution is rather complicated. Here, we consider the case at absolute

zero temperature. We take the ground state wave vector as follows,

$$\begin{pmatrix} \sin\theta/2\ \sin\phi/2 \\ \cos\theta/2 \\ \sin\theta/2\ \cos\phi/2 \\ 0 \end{pmatrix} . \tag{11}$$

Providing $0 < \lambda < \frac{1}{2}$, we obtain,

$$m = -\langle s_1^x + s_2^x \rangle = \sin^2\tfrac{1}{2}\theta \cos\phi , \tag{12}$$

$$n = 2 \sin\tfrac{1}{2}\theta \cos\tfrac{1}{2}\theta \,(\cos\phi/2 - \sin\phi/2). \tag{13}$$

After straightforward but rather long calculation, we finally obtain an ordered state, in which the field dependence of the magnetization is described by a variable ϕ as,

$$m = \frac{\cos\phi[\lambda(1-\sin\phi) + \sin\phi]}{\lambda(1-\sin\phi)^2} , \text{ and} \tag{14}$$

$$h = \frac{\cos\phi[2\lambda(1-\sin\phi) + (1+\sin\phi)]}{(1-\sin\phi)^2} , \tag{15}$$

in the field range $h_{c1} < h < h_{c2}$, where $h_{c1} = \sqrt{1 - 2\lambda}$, $h_{c2} = 1 + 2\lambda$ and $\sin\phi$ is varied from 0 to $-\lambda/(1-\lambda)$.
Thus, the susceptibility in the ordered phase is expresssed as,

$$\chi \equiv \frac{\partial m}{\partial h} = \frac{(1+\lambda) + (2-\lambda)\sin\phi}{\lambda[(3+2\lambda) + (3-2\lambda)\sin\phi]} . \tag{16}$$

Especially, on the phase boundaries, it is expressed as follows,

$$\chi = \frac{1-2\lambda}{\lambda(3-4\lambda)} \quad ; \quad (h = h_{c1}), \text{ and} \tag{17}$$

$$\chi = \frac{1+\lambda}{\lambda(3+2\lambda)} \quad ; \quad (h = h_{c2}). \tag{18}$$

Assuming $zJ'/k = 1.68$ K and $J/k = 5.2$ K, that is, $\lambda = 0.16$, the field dependence of this susceptibility is represented in Fig. 13. The calculated asymmetry of the susceptibility amounts to about 20 %, which is very well agreement with the present experimental results in the transient method at the lowest initial temperatures represented in Fig. 8. Temperature independence of the asymmetric $\partial M/\partial t$ curves observed below $T_i = 0.75$ K reflect the finite asymmetry predicted by the theory at absolute zero.

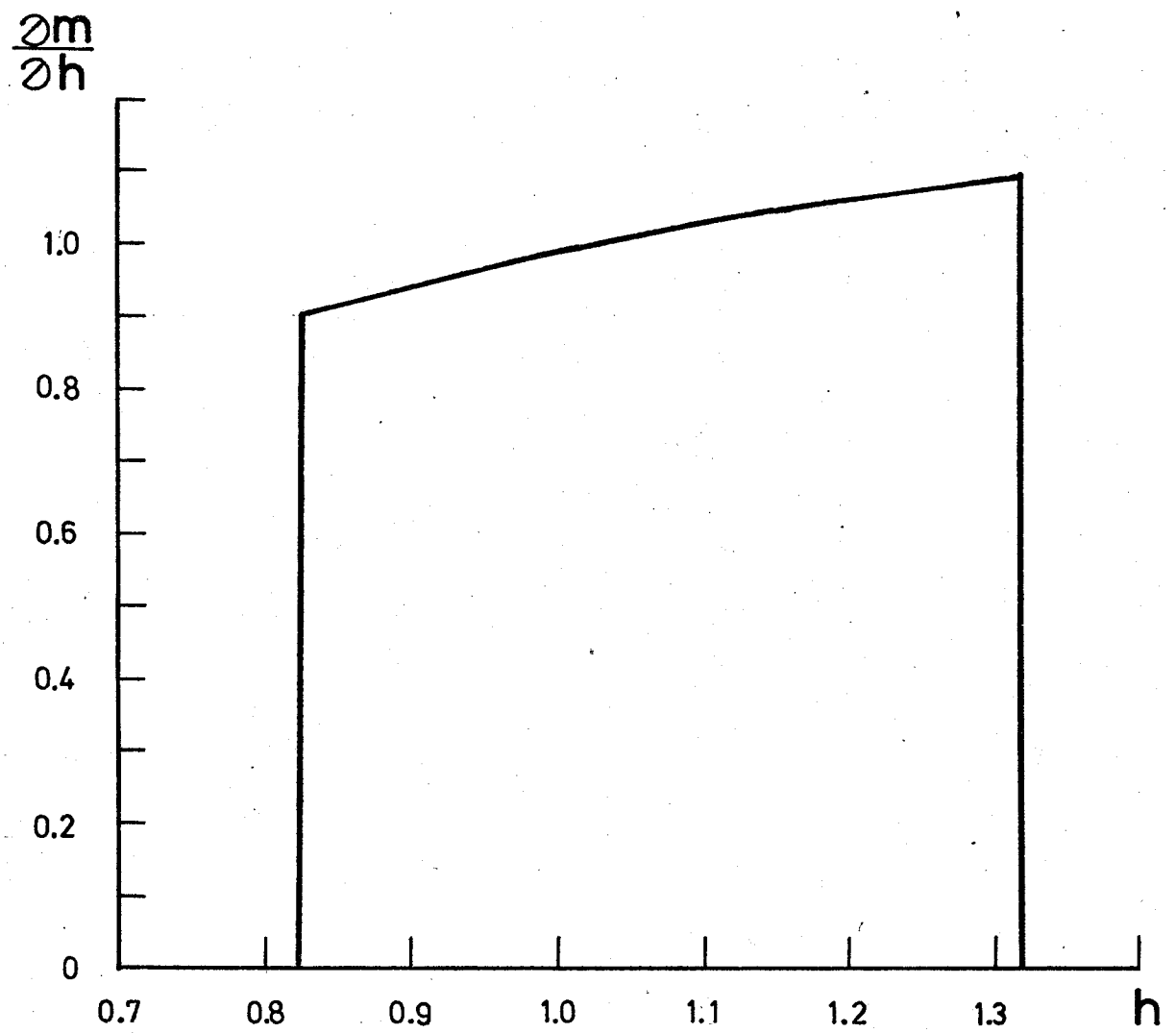

Fig. 13 Field dependence of susceptibility at absolute zero calculated under molecular field approximation.

Conclusion

We succeed in finding of the effective cooling and the spin ordering phenomenon by the susceptibility measurements under the pulsed magnetization process of $Cu(NO_3)_2.2.5H_2O$.

If we start with $T_i \geq 2.0$ K, the spin system behaves like a paramagnet showing the almost symmetric peak. With T_i lower than 1.5 K, asymmetric double peaks are observed with the round minimum around 34 kOe, This phenomenon corresponds to the spin short range order caused by the adiabatic demagnetization cooling.

We calculate the adiabatic susceptibility along the isentropic process from the X-Y model for one dimensional lattice. These calculations are qualitatively in good agreement with the experimental results except the asymmetry observed. This asymmetry is explained qualitatively with the molecular field theory taking account of the effect of the total four levels of the spin-pairs.

The validity of this transient method is established from the above comparison between the observed and the calculated susceptibility. Much more varieties of the studies of the magnetism in high pulsed magnetic field are expected!

REFERENCES

1) M.Chapellier, M.Goldman, Vu Hoang Chan and A.Abragam : J. appl. Phys. 41(1970)849.

2) T.Haseda, Y.Tokunaga, R.Yamada, Y.Kuramitsu, S.Sakatsume and K.Amaya : Proc. 12th Intern. Conf. on Low Temp. Phys., Kyoto, 1970 p685.

3) M.W.van Tol, K.M.Diederix and N.J.Poulis : Physica 64(1973) 363.

4) B.E.Myers, L.G.Polgar and S.A.Friedberg : Phys. Rev. B 6 (1972)3488.

5) K.Amaya, N.Yamashita, M.Matsuura and T.Haseda : J. Phys. Soc. Japan 37(1974)1173.

6) B.Morosin : Acta cryst. B 26(1970)1203.

7) L.Berger, S.A.Friedberg and J.T.Schriempf : Phys. Rev. 132 (1963)1057.

8) S.A.Friedberg and C.A.Raquet : J. appl. Phys. 39(1968)1132.

9) B.E.Myers, L.Berger and S.A.Friedberg : J. appl. Phys. 40 (1969)1149.

10) K.Amaya, Y.Tokunaga, R.Yamada, Y.Ajiro and T.Haseda : Phys. Letters A 28(1969)732.

11) N.S.VanderVen (unpublished).

12) S.Wittekoek and N.J.Poulis : J. appl. Phys. 39(1968)1017.

13) K.Amaya and I.Fukuda (unpublished).

14) Y.Tokunaga, S.Ikeda, J.Watanabe and T.Haseda : J. Phys. Soc. Japan 32(1972)429.

15) J.C.Bonner, S.A.Friedberg, H.Kobayashi and B.E.Myers : Proc. 12th Intern. Conf. on Low Temp. Phys., Kyoto, 1970 p691.

16) T.Tsuneto and T.Murao : Physica 51(1971)186.

17) M.Tachiki and T.Yamada : J. Phys. Soc. Japan 28(1970)1413; M.Tachiki and T.Yamada : Progr. theor. Phys. 46(1970)Suppl. p.291; M.Tachiki, T.Yamada and S.Maekawa : J. Phys. Soc. Japan 29(1970)663.

18) M.W.van Tol, H.M.C.Eijkelhof and A.J.Van Duyneveldt : Physica 60(1972)223.

19) M.Tachiki, T.Yamada and S.Maekawa : J. Phys. Soc. Japan 29 (1970)663.

20) S.Katsura : Phys. Rev. 127(1962)1508; 129(1963)2835.

21) Y.Ajiro, N.S.VanderVen and S.A.Friedberg : Proc. 13th Intern. Conf. on Low Temp. Phys., Colorado, 1972 p380.

Acknowledgements

I wish to express my deep appreciation to Professor J. Itoh for introducing me to the study of low-temperature magnetism. I would like to express my sincere gratitude to Professor T. Haseda for promoting this study and for many stimulating discussions throughout the work. I am very much indebted to Dr. K. Amaya for suggesting the present problem and for indispensable contributions to this work. I would like to express my sincere thanks to Assistant Professor M. Mastuura for his stimulating discussions and continuous interest. I am very grateful to Assistant Professor H. Kiriyama of Institute of Scientific and Industrial Research, Osaka University, for her valuable suggestion about the preparation of the single crystal of $CeCl_3.7H_2O$.

I am very obliged to Assistant Professor K. Asayama for his hearty encouragement. Thanks are due to Mr. S. Ikeda for his helpful comments and for various convenience in carrying out the experiments. I wish to thank the members of our laboratory, Mr. Y. Yamakawa for his help in high frequency susceptibility measurements, and Mr. H. Kobayashi for his technical assistance in preparation of the adiabatic cell. I have benefited much of the enthusiastic co-operation with Dr. S. Kohzuki, Dr. Y. Aoki, Mr. T. Ooi and Mr. M. Tsuziuchi in the earlier stage of the study of $CeCl_3.7H_2O$.

Finally, I acknowledge to Mr. O. Asai and other members at Low-Temperature Center, Toyonaka, Osaka University, who make much efforts to supply me with the liq. He.